INFORMATION PROCESSING IN NEURAL SYSTEMS: OSCILLATIONS, NETWORK TOPOLOGIES AND OPTIMAL REPRESENTATIONS

A DISSERTATION SUBMITTED
IN PARTIAL FULFILLMENT OF THE REQUIREMENTS
FOR THE DOCTORAL DEGREE

Departamento de Ingeniería Informática
Escuela Politécnica Superior

UAM

UNIVERSIDAD AUTÓNOMA DE MADRID

Luis Fernando Lago Fernández
May 2003

Adviser: Fernando J. Corbacho Abelaira

Agradecimientos

Deseo dar mi más sincero agradecimiento a todas las personas que me han ayudado, tanto directa como indirectamente, en la realización de esta tesis doctoral.

En primer lugar a los más cercanos, que siempre han estado ahí apoyándome, muchas veces sin entender demasiado por qué dedicar tanto tiempo y esfuerzo a un proyecto así. Espero que esta sea vuestra respuesta. Gracias a mi madre, a mi hermano y a mis abuelos. Gracias, mamá, por darme la vida y dejarme, casi siempre, dirigirla. Parte del mérito es tuyo. Gracias, abuelo, por haberme enseñado tantas cosas. Sé que estás muy orgulloso. Gracias, abuela, por tanto cariño. Sé que te va a hacer mucha ilusión oir que por fin he acabado la tesis. Ojalá pudieras venir a verme. Gracias, Andrés, por haberme aguantado tanto. Son muchos años durmiendo en la misma habitación.

Gracias Eva, por tu ayuda, por tus ánimos, por tu ilusión y, sobre todo, por tu sonrisa. Esta tesis no habría sido lo mismo sin todas esas cosas.

Gracias a mis amigos. Juan, Diego, Ato, Inés, hemos compartido buenos momentos durante estos cinco últimos años, y espero que sigamos haciéndolo durante unas cuantas tesis más.

Gracias a mis compañeros del laboratorio, los presentes y los que han pasado por aquí. Todos habéis contribuido a hacer más agradable el viaje. Gracias a Manuel, Naza, Marta, Philip, Jaime, Víctor, Antonio, David y Roberto.

Gracias, como no, a Fernando. Me has ayudado en mucho más que en la mera elaboración de esta tesis. Gracias por estar ahí, escucharme y guiarme en esta dura empresa.

Gracias al resto de compañeros y profesores del departamento: Ramón, Paco, Pablo y todos los demás.

Gracias también a Juana por tanta paciencia.

Por último, quiero agradecer la ayuda económica de la Universidad Autónoma de Madrid y la Comunidad de Madrid.

Muchas gracias a todos.

Resumen

Esta tesis está relacionada con el estudio del procesamiento de la información en los sistemas neuronales mediante modelos computacionales. Este enfoque consiste en el desarrollo de modelos matemáticos que reproducen el funcionamiento de las neuronas y las redes neuronales reales. Los modelos se plantean normalmente en términos de ecuaciones diferenciales que han de resolverse numéricamente con la ayuda del ordenador. El objetivo de la elaboración de modelos tiene dos vertientes. Por un lado, extraer la esencia de los procesos biológicos implicados en el funcionamiento neuronal, y obtener una descripción realista que permita generar hipótesis. Por otro lado, entender los principios organizativos que gobiernan el funcionamiento del cerebro, los cuales pueden ayudar en la contrucción de máquinas más inteligentes.

Los sistemas neuronales son capaces de procesar grandes cantidades de información en muy poco tiempo. Por ejemplo, el análisis de una imagen involucra el procesamiento de millones de bits en tiempos que en algunos casos no superan los 200 ms. A pesar de la aparente dificultad, el cerebro resuelve este problema sin apenas esfuerzo.

Sin embargo, los intentos por crear sistemas artificiales capaces de ver han topado con numerosos obstáculos. Las tecnologías aplicadas al desarrollo de ordenadores han experimentado una impresionante evolución en los últimos años. A pesar de ello, problemas como la segmentación de imágenes o el reconocimiento de objetos siguen siendo extremadamente difíciles de resolver. El estudio de las soluciones que proporciona la biología para estos problemas podría conducir al desarrollo de mejores algoritmos.

Una estrategia que el cerebro usa con frecuencia, es el procesamiento en paralelo.

Los distintos aspectos de un problema particular se procesan de forma simultánea en diferentes áreas cerebrales. Descomponiendo el problema en subproblemas más pequeños, resulta más fácil encontrar una solución. Este enfoque que en principio parece adecuado, presenta otro tipo de dificultades, como la integración de toda la información que está distribuida por distintas áreas cerebrales. Las teorías actuales, respaldadas por evidencias experimentales [42, 82], suponen que la presencia de oscilaciones coherentes en la actividad neuronal podría jugar un papel fundamental en este proceso de integración.

En base a esta suposición, la primera parte de la tesis aborda el estudio del tipo de topologías que permiten la rápida aparición de oscilaciones coherentes en la actividad de una red neuronal tras ser estimulada. Distintos tipos de topologías, entre el orden y el desorden, han sido generadas usando un procedimiento introducido recientemente para la generación de topologías de tipo "small-world" [128]. Se han considerado dos modelos neuronales distintos, cada uno de ellos característico de un tipo de excitabilidad neuronal. Las propiedades de respuesta de la red para cada uno de estos modelos han sido estudiadas en relación a la topología. Los resultados demuestran que, en muchos casos, topologías situadas entre el orden y el desorden proporcionan las mejores soluciones desde el punto de vista de las oscilaciones y la velocidad de respuesta.

Los mecanismos que producen oscilaciones y sincronización entre neuronas también se han estudiado, y se han propuesto aplicaciones prácticas para los problemas de "binding", rivalidad binocular y segmentación de imágenes.

El problema del "binding" está relacionado con la asociación de las distintas características de un objeto que se procesan de forma simultánea a través de distintos canales. Las soluciones que se han explorado en esta tesis están basadas en la hipótesis de la correlación temporal [83, 42]. Se introduce un modelo de neuronas que disparan que, basado en la generación ruidosa de potenciales de acción y en la existencia de conexiones excitadoras, es capaz de reproducir las correlaciones medidas entre neuronas corticales [41, 62].

La rivalidad binocular es un fenómeno que se da cuando cada ojo percibe una imagen distinta y no es posible combinar ambas en una única percepción coherente.

En estos casos, el cerebro percibe una alternancia entre ambas imágenes, que puede ser entendida como el resultado de una competición entre diferentes grupos de neuronas que responden a cada una de las dos imágenes. Se propone un modelo de poblaciones descritas por ecuaciones de campo medio en el que la adaptación de la frecuencia de disparo es capaz de producir la alternancia entre percepciones, y reproduce los histogramas de duración de fase medidos en los experimentos.

Como aplicación práctica de las ideas anteriores acerca de la sincronización neuronal, se introduce una red neuronal que segmenta imágenes binarias. La red está compuesta por un conjunto de osciladores acoplados por impulsos, con conexiones locales excitadoras e inhibición global. En respuesta a una imagen binaria, los osciladores que responden a cada una de las componentes conexas en la imagen se sincronizan entre sí.

Finalmente, la última parte de la tesis está dedicada al estudio de otro tipo de problema que debe ser resuelto por el cerebro y por cualquier otro sistema de procesamiento de la información: el desarrollo de representaciones internas que permitan una codificación óptima del espacio de entrada. Dicha representación óptima significa (i) conservar toda la información que es relevante, y (ii) expresarla de una forma más conveniente que facilite el análisis en subsiguientes etapas del procesamiento. Restringiendo el estudio a espacios de entrada discretos y factoriales, se introduce una nueva medida de la "calidad" de un código, cuya maximización da lugar a una codificación óptima (máxima discriminabilidad y factorialidad) en ausencia de ruido.

Abstract

This thesis is concerned with the study of information processing in neural systems form a computational modeling point of view. This approach consists on developing mathematical models that approximate the behavior of real neurons and neural networks. The models are usually expressed in terms of differential equations that must be numerically solved using computers. The aim of modeling is twofold. On the one hand, to extract the essentials of the biological processes involved in the neural functioning, in order to provide a good description of the reality and generate hypotheses that can be confirmed in the laboratory. On the other hand, to understand the principles of organization that govern the brain operation, which may allow for the construction of more intelligent machines.

Neural systems show a remarkable ability to deal with big amounts of information in very small amounts of time. The problem of vision, for example, involves processing the millions of bits of information contained in the visual images in times that in some cases do not exceed 200ms. In spite of the apparent difficulty, the brain performs with quite little effort.

However, when trying to construct machines that are able to see, engineering has usually encountered many obstacles. Despite the enormous development of computers during the last years, which makes them considerably faster than the brain for many applications, problems such as image segmentation or object recognition remain unsolved. Looking at the solutions provided by biology may lead to the development of algorithms that perform better in this kind of tasks.

A principle of organization widely used by the brain is parallel processing. Different aspects of any specific problem are simultaneously processed by different brain

areas. By breaking the problem into smaller subproblems, the solution is more easily achieved. This approach, that a priori seems convenient, sets other philosophical problems such as the integration of all the information that is spread over different brain areas. Current theories, supported by experimental evidence [42, 82], assume that coherent oscillations of neural activity, reflecting a synchronous firing of large neuron assemblies, may play a fundamental role in the integration process.

Based on this assumption, the first part of this thesis deals with the study of neural network topologies that can provide a fast onset of oscillatory activity when the network is stimulated. Different network topologies, ranging from order to disorder, are generated using a recently introduced procedure for the generation of the so-called small-world topologies [128]. For two different neuron models, each one characteristic of a different class of neural excitability, the network response properties are studied in terms of the topology and the connection strength. The results show that, in many cases, a network topology that lies between order and disorder provides the most plausible solution in terms of oscillations and response speed.

The mechanisms that produce oscillatory activity and spike synchronization in neural systems are also studied. Practical applications of oscillations to problems of binding, binocular rivalry and image segmentation are proposed.

The binding problem is related to the association of different features that are processed in parallel by different brain channels. Solutions based on the temporal correlation hypothesis [83, 42] are explored. A simple model of spiking neurons based on a noisy generation of the action potential and excitatory connections between neurons is introduced. It is able to reproduce the experimental correlations measured in experiments with cortical neurons [41, 62].

Binocular rivalry is a visual illusion that appears when each eye is perceiving a different image and they can not be fused into a single coherent perception. In that case the brain perceives an alternation of both images that can be explained based on competition mechanisms that lead to oscillatory activation of the neurons representing the two perceptions. A model based on firing rate equations with spiking frequency adaptation is introduced. It successfully reproduces the mean perception duration measured in experiments.

As a practical application of the ideas of synchronization and binding, a neural network that performs image segmentation is introduced and applied to the segmentation of binary images. The network is composed of pulse coupled oscillators, with local excitatory coupling and global inhibition. When the network is applied to a binary image, the oscillators responding to each of the connected regions reach a synchronized state.

Finally, the last part of this thesis is concerned with another kind of problem that must be solved by the brain or any system that deals with information processing. Namely, the development of internal representations that provide an optimal codification of the input space. Such an optimal representation means (i) conserving all the relevant information, and (ii) expressing it in a more suitable way for processing in further steps. Constraining the study to discrete and factorial input spaces, a new measure of the quality of a code is introduced, whose maximization leads to optimal codification (maximum discriminability and factoriality) in the absence of noise.

Contents

Agradecimientos iii

Resumen v

Abstract viii

1 Introduction 1

1.1 The problem of perception 1

1.2 The solution given by the brain 3

1.3 The binding problem 4

1.4 Entropy, information, optimal representations and factorial codes . . 5

1.5 Objectives of this thesis 6

2 Temporal coding and binding
A biological perspective 11

2.1 Oscillations in the brain: experimental evidence 12

2.2 Spikes vs rates. Processing speed 15

2.3 Concluding remarks 17

3 Optimal network topologies for information processing 18

3.1 Introduction 18

3.2 Neuron models and synaptic dynamics 20

3.2.1 Hodgkin-Huxley model, class 1 excitability 21

3.2.2 FitzHugh-Nagumo model, class 2 excitability 23
3.2.3 Synaptic transmission 25
3.2.4 Numerical integration 26
3.3 Network topologies and graphs 26
3.3.1 Random graphs 30
3.3.2 Regular graphs and lattices 31
3.3.3 Small-world graphs 33
3.3.4 Some real life examples 35
3.4 Effects of the topology on the network response 37
3.4.1 Low characteristic path length produces a fast response 41
3.4.2 High clustering produces coherent activity 42
3.4.3 Optimal topologies 45
3.4.4 Partial conclusions 51
3.5 Dependence on the neuron model and coupling strength 54
3.5.1 Class 1 excitability. Hodgkin-Huxley model 55
3.5.2 Class 2 excitability. FitzHugh-Nagumo model 60
3.5.3 Partial conclusions 67
3.6 Discussion 68

4 Neural synchronization and applications **70**
4.1 Introduction 70
4.2 How to achieve synchronization
Neural mechanisms 72
4.3 Binding of objects and positions in the visual system 75
4.3.1 The mean field approach 79
4.3.2 Model architecture 80
4.3.3 Equations and parameters 81
4.3.4 Results 85
4.3.5 Partial conclusions 86
4.3.6 A simple model of spiking neurons 88
4.3.7 Back to the binding problem 92

4.4 Applications to binocular rivalry 96
4.4.1 The model 97
4.4.2 Results and discussion 102
4.5 Image segmentation 104
4.5.1 The Peskin oscillator 106
4.5.2 A network of spiking oscillators for binary image segmentation 108
4.5.3 Final considerations 114
4.6 Conclusions of the chapter 116

5 Optimal internal representations **118**
5.1 A simple problem of cause extraction 120
5.2 New measure of independence and discriminability 122
5.3 Results 123
5.4 Discussion 126

6 Conclusions **129**

A Introducción **132**
A.0.1 El problema de la percepción 132
A.0.2 La solución del cerebro 133
A.0.3 El problema del "binding" 134
A.0.4 Entropía, información, representaciones óptimas y códigos factoriales 134
A.0.5 Objetivos de la tesis 135

B Conclusiones **140**

Bibliography **143**

List of Tables

3.1 Parameters for the HH model. 22
3.2 Synaptic parameters. 27
3.3 Statistics of three real graphs (network of collaborations between movie actors; electrical network of the western United States; and neural network of the worm *C. Elegans*) and comparison with the statistics of random and regular graphs of the same n and k. Results taken from [129]. 37

4.1 Parameter values for equations (4.3)-(4.5). 83
4.2 Parameter values for equations (4.6)-(4.8). 83
4.3 Parameter values for equations (4.9) and (4.10). 84
4.4 Pair correlations between the pools in V4, IT and PP responding to each of the two objects presented as input to the network. 87
4.5 Parameter values for the simplified SRM model. 93
4.6 Parameter values for the model of binocular rivalry. 101

List of Figures

3.1 A. Frequency of oscillation versus external current for the Hodgkin-Huxley model. The presence of an oscillatory phase at arbitrarily low frequencies is a characteristic of class 1 excitability. B. Frequency of oscillation versus external current for the FitzHugh-Nagumo model. Class 2 excitable neurons present oscillations only in a limited frequency band. 23

3.2 A random graph with $n = 10$ and $k = 4$. 30

3.3 A regular lattice with $n = 10$ and $k = 4$. 32

3.4 A small-world graph with $n = 10$ and $k = 4$. 34

3.5 Characteristic path length L and clustering coefficient for different values of the probability p in a graph of $N = 797$ vertices and a mean connectivity $k = 30$. The results are normalized by the values of the regular graph $L(0)$ and $C(0)$, and are averages over 10 different simulations. 35

3.6 First spike of every neuron in a network of HH units with parameters $n = 797$ and $k = 30$, for different rewiring probabilities. A. $p = 0.000$, $L = 12.36$. B. $p = 0.001$, $L = 6.78$. C. $p = 0.032$, $L = 3.10$. D. $p = 1.000$, $L = 2.26$. The input stimulus consisted of a current pulse of amplitude $I_{ext} = 1.5\mu A/cm^2$, injected at $t = 0ms$ to a subset of 80 contiguous neurons. 40

3.7 A. Normalized characteristic path length, L, and response time, T_r, versus rewiring probability, p, for a network of 797 HH neurons and $k = 30$. The normalization values are those for the regular network ($p = 0$): $L(0) = 12.36$ and $T_r(0) = 119.13ms$. B. T_r versus L for the same network showing the expected linear relation. The points have been fitted using linear regression, giving a slope $\alpha = 5.16$. 42

3.8 A. Normalized characteristic path length ($L(n)/L(600)$, filled diamonds) and response time ($T_r(n)/T_r(600)$, open diamonds) versus network size for regular networks with $k = 30$. The normalization values are those for $n = 600$: $L(600) = 10.47$ and $T_r(600) = 52.33ms$. B. T_r versus L. The points have been fitted using linear regression, giving a slope $m = 5.01$. 43

3.9 Spike rasters for different values of the rewiring probability p in a network of HH neurons with $n = 797$ and $k = 30$. A. $p = 0.000$, $C = 0.74$. B. $p = 0.001$, $C = 0.74$. C. $p = 0.032$, $C = 0.68$. D. $p = 1.000$, $C = 0.07$. A clear dependence of the correlation properties of the network activity on the clustering level is observed. We have coherent activity for highly clustered networks (A, B, C), and incoherent activity for low clustering (D). 44

3.10 Number of spikes versus simulation time for networks of HH neurons with $n = 797$ and $k = 30$. A. $p = 0.000$, $C = 0.74$. B. $p = 0.001$, $C = 0.74$. C. $p = 0.032$, $C = 0.68$. D. $p = 1.000$, $C = 0.07$. A clear dependence of the correlation properties of the network activity on the clustering level is observed. We have coherent activity for highly clustered networks (A, B, C), and incoherent activity for low clustering (D). 45

3.11 Average activity, $V(t)$, in networks of HH neurons with $n = 797$, $k = 30$ and different rewiring probabilities. A. $p = 0.000$, $L = 13.57$, $C = 0.47$, regular network. B. $p = 0.032$, $L = 3.09$, $C = 0.68$, this network falls into the small-world range. C. $p = 1.000$, $L = 2.26$, $C = 0.07$, random network. Stimulus onset at $t = 50ms$. 48

3.12 Average activity oscillation amplitude, $\sigma(p)$, versus the rewiring probability in a network of $n = 797$ HH neurons with connectivity $k = 30$. 49
3.13 Power spectra for the time series of figure 3.11. A. $p = 0.000$, $L = 13.57$, $C = 0.47$. B. $p = 0.032$, $L = 3.09$, $C = 0.68$. C. $p = 1.000$, $L = 2.26$, $C = 0.07$. 50
3.14 Degree of coherence, β, versus rewiring probability, p, for networks of HH neurons with parameters $n = 797$ and $k = 30$. 51
3.15 Different properties of the network versus rewiring probability. A. Characteristic path length and clustering coefficient. B. Response time. C. Average activity oscillation amplitude. D. Degree of coherence. The small-world (high C and low L) has been marked, and shows a coexistence of low response times with oscillatory activity. 53
3.16 Average activity oscillation amplitude, σ, versus connectivity, k, and rewiring probability, p, in networks of HH neurons. Network size is $n = 797$. 54
3.17 Spike rasters for the HH model and different network topologies ranging from regularity to randomness. Synaptic conductance $g = 0.02mS/cm^2$. 57
3.18 Spike rasters for the HH model and different network topologies ranging from regularity to randomness. Synaptic conductance $g = 0.05mS/cm^2$. 58
3.19 Response time $T_r(p)$ (open circles) and local correlation $b(p)$ (filled circles) as a function of the rewiring probability p for the Hodgkin-Huxley network and two different synaptic conductances: A. $g = 0.02mS/cm^2$, B. $g = 0.05mS/cm^2$. Note the absence of points for $p = 1$ in figure A; the lack of global activity in the random network does not allow to calculate the quantities $T_r(p)$ and $b(p)$. 60
3.20 Spike cross-correlograms between neighbor neurons, averaged to all pairs of neighbor neurons. $g = 0.05mS/cm^2$. 61
3.21 Spike rasters for the FN model and different network topologies ranging from regularity to randomness. Synaptic conductance $g = 0.003mS/cm^2$. 63
3.22 Spike rasters for the FN model and different network topologies ranging from regularity to randomness. Synaptic conductance $g = 0.006mS/cm^2$. 64

3.23 Spike rasters for the FN model and different network topologies ranging from regularity to randomness. Synaptic conductance $g = 0.009mS/cm^2$. 65

3.24 Response time $T_r(p)$ (open circles) and local correlation $b(p)$ (filled circles) as a function of the rewiring probability p for the FitzHugh-Nagumo network. A. $g = 0.003mS/cm^2$, B. $g = 0.006mS/cm^2$. C. $g = 0.009mS/cm^2$. The absence of global activity in the network does not allow to calculate the response time $T_r(p)$ for the two highest probabilities in figure A. 66

4.1 Schematics of the flow of visual information in the brain. Information coming from the retina and the LGN reaches the primary visual areas (V1) in the occipital lobe. From there, two different pathways depart. The ventral stream reaches the inferior temporal cortex (IT), and it is involved in the processing of object properties (what). The dorsal stream reaches the posterior parietal cortex (PP), and it is mainly concerned with the processing of spatial information (where). 76

4.2 Schematics of the network architecture. Arrows indicate excitatory connections between the different layers. 78

4.3 Activation function, F, versus input current, I, for the mean field approach. Parameters $\tau = 10$ and $T_r = 5$. 80

4.4 Structure of the network showing the connections reaching the IT layer. Non-directed lines represent connections in both ways. 81

4.5 Structure of the network showing the connections reaching the PP layer. Non-directed lines represent connections in both ways. 82

4.6 Input currents in IT, PP and V4 when two different objects are presented simultaneously to the network. Solid lines: object "X"; dashed lines: object "O". A. IT excitatory pools responding to each object. B. PP excitatory pools responding to each active position. C. V4 active pools. A clear correlation is observed between pools responding to a single object. 86

4.7 Spiking probability P_s versus membrane potential h for the spike response model (SRM) of equation (4.13). The spiking threshold is $h_0 = 0.12$ and the noise parameter is $\beta = 40$. 89

4.8 Spiking probability P_s versus membrane potential h for the simplified model of equation (4.19). The maximum spiking probability is $P_{max} = 0.5$, the spiking threshold is $h_0 = 0$, and the noise parameter is $\beta = 5$. 91

4.9 Response of the SRM (top) and the simplified model (bottom) to a very strong stimulation. 92

4.10 Network architecture for the model of spiking neurons. The V1 layer is not explicitly modeled. Instead, an external stimulation h_{ext} is assumed for V4 neurons that respond to the stimuli. All connections are excitatory. 93

4.11 Spike cross-correlograms between different neuron pairs for the simplified SRM model, showing correlations (left) between neurons responding to a common stimulus, and absence of correlations (right) between neurons responding to different stimuli. The neuron numbers correspond to those of figure 4.10. 94

4.12 A. Binocular rivalry: When two incompatible stimuli are presented one to each eye, the resulting perception is an alternation of them. B. Necker cube illusion: This cube has two possible spatial representations, and both of them are perceived alternatively. It is believed that both effects are produced by the same cerebral mechanisms. 98

4.13 The Diaz-Caneja phenomenon. Sometimes during perceptual rivalry the brain mixes information coming from both eyes to form more coherent perceptions. This effect contradicts the theories based on monocular channel competition and places binocular rivalry closer to other visual illusions. 98

4.14 Network architecture for the binocular rivalry model. Solid connections are excitatory, dashed connections are inhibitory. 99

4.15 Firing rate adaptation dynamics. Left, frequency-current curves for different values of the adaptation parameter a. Right, solution of equations (4.22-4.24) when the pool is being stimulated by a constant current pulse. Blue line corresponds to a simulation with no adaptation; red line corresponds to a simulation in which adaptation is fully effective. 101

4.16 (a) Input current for IT pools when both stimuli are presented. The two pools compete for dominance and an alternation of the winning perception is observed. (b) Input current for V4 modulated pools. Note the correlation with pools in IT, achieved through the top-down connections. (c) Distribution of relative phase durations (dominant phase durations as a fraction of the mean phase duration). It has been fitted with a gamma function ($f(x) = \lambda^r/\Gamma(r)x^{r-1}exp(-\lambda x)$) with parameters $r = 4.60$ and $\lambda = 4.70$. 103

4.17 An example of binary image. 105

4.18 Synchronization of two Peskin oscillators. After the first spike of the two oscillators, the phase difference between them decreases form ϕ to ϕ'. Repetition of this process will lead to a synchronized state. 108

4.19 Network of Peskin oscillators for binary image segmentation. A. The binary image serves as input to the network. The resolution of the original image is reduced to 40×40 to match the network dimensions. B. Network of 40×40 oscillators, connected one to one to the image pixels. Only those connected to a white pixel (shown as red circles) will display oscillatory activity. C. Connection scheme. Each oscillator is connected to its 8 nearest neighbors. 109

4.20 A. Initial condition for the network. All the oscillators start with a random potential uniformly distributed between 0 and $V_{max}^{ini} = 0.9$. The phase difference between the first and the last oscillators is marked as ϕ. B. After the first spike of all the network oscillators, the phase difference has decreased to ϕ'. 111

4.21 Network activity in response to the input image of figure 4.17. A. The activity of all the oscillators responding to the object on the left of the image synchronizes after a few oscillations. B. Idem for the oscillators responding to the object on the right. C. Spike raster of all the 1600 oscillators showing intra-group synchronization and inter-group desynchronization. 112

4.22 A. The same experimental conditions as in figure 4.21, but a different initial condition, may lead to a globally synchronized solution due to the lack of desynchronization mechanisms. B. When the number of connected components in the input image increases, this effect is more evident. 113

4.23 Response of the model to a binary image with four connected components. A-D: Activity of all the oscillators responding to each of the four objects. E: Spike raster showing the firing times of all network oscillators. Four different clusters are formed, each one responding to one of the connected components in the input. 114

5.1 Subset of the input patterns. All of them are generated as a random combination of 5 vertical and 5 horizontal bars that appear independently with a probability $p = 0.15$. 120

5.2 Given an input space X, the objective of the code is to provide a good representation Y that conserves all the information while minimizing the statistical dependence between the representational units. 121

5.3 Neural network structure. Each of the hidden units responds to a subregion of the input space (its receptive field) determined by a 5×5 binary matrix. The figure shows the receptive fields (only connections with value 1 are drawn) and the corresponding states of two neurons for a given input pattern. 124

5.4 $H(Y)$ (solid thick), $M(Y)$ (solid), and $S(Y)$ (dotted) versus iteration number of the genetic algorithm for $H(Y)$ maximization (A) and $M(Y)$ maximization (B). In both cases we used a neural network with $N = 20$ hidden units. 125

5.5 A. Receptive fields after maximization of $H(Y)$. B. Receptive fields after maximization of $M(Y)$. The gray level indicates the probability of activation of a neuron with such a receptive field. Neurons with a dark receptive field are stimulated more often than neurons with a brighter one. 126

Chapter 1

Introduction

1.1 The problem of perception

One of the most difficult problems the brain has to deal with is the perception of the environment. We are constantly perceiving and identifying millions of images, sounds, odors, etc., and we do it with apparently little effort. The analysis of an image, or the recognition of a face, are easy problems for our brain. The real dimension of the problem arises when one tries to build machines that can see, hear or smell with the same precision, reliability and robustness as the brain does, and in the same amount of time the brain does. To see the difficulties that perception involves, let us imagine one of the most typical situations our brain has to tackle. Imagine you are looking for a friend among many other people. In the process, millions of bits of visual information are reaching your brain coming from the retina, and it has the non simple task of organizing all this information before giving an answer: your friend is late again. From the "photographic" representation of the world that is formed in the retina to the most elaborated cortical representation of the world that provides knowledge, the brain has to go through many problems that have been puzzling researchers since the beginnings of neuroscience.

First, there is a problem of *representation*, that has to do with coding internally the external world. This coding must be efficient, otherwise there would be no room for all the amount of data coming from the eyes, and must represent all the relevant

information about the world. This implies noise filtering and elimination of redundancies, that is, cleaning the data so that only effective information is conserved. This should be done at different levels depending on the specific situation the brain is dealing with.

Second, there is a problem of *segmentation*, that is, breaking the perceived scene into the different elements it is composed of. In the example case, you perceive each of the people in the scene as an independent element. Your brain has been able to extract the information referring to each one separately. Again, different segmentations can be performed as different goals are pursued. In this particular situation what you need is information about the faces; but if you knew your friend is wearing a red shirt maybe your brain's strategy would change.

Then there is the problem of *recognition*. The brain has cleaned the image, expressed it in a more suitable way for further processing, segmented the different components and filtered the information that is not relevant for the current objective. Now it has to analyze the different faces and see if one of them matches that of your friend. Object and face recognition are really difficult problems, mainly because of the variability with which objects appear in the world. In different circumstances your friend's face must be identified under different conditions of light, position, scale, angle, etc. Imagine only the differences that may appear just due to rotation in a three dimensional world.

What comes before and what comes after in the list above is quite difficult to say. Obviously a segmentation process helps in the task of recognition, but also recognition may help segmentation. It is easier to segment the different people in the image once you know there is people in the image, for example. Also some knowledge about what we are perceiving may be useful to determine what is relevant and what is not, and to eliminate redundant information. So the process of perception must be seen as a complex task that involves all of the mentioned points, and maybe more, as a whole. Some of the processes may influence the others in a mutual way, and recognition may arise as the result of a conjoint actuation of all of them, rather than one after the other.

Finally, to add more complexity to the problem, the brain has limited time to compute. Typically, recognition tasks are solved by the brain in a few tens of milliseconds, which is much less than the time required for any machine to perform the recognition of the simplest objects. Longer times could imply catastrophic consequences for survival.

In this thesis I will deal with some issues concerning how the brain processes information and achieves object recognition. Some of the questions that will be considered in the different chapters are:

- How does the brain code and process the information about the world?
- If the brain uses, as it seems to be the case, parallel processing, how does it solve the binding problem?
- How does the brain select the representational units to code information? In other words, which kind of coding is most convenient to obtain an adequate internal representation of the world?

1.2 The solution given by the brain

Relative to the first question, let us see how the brain is organized to deal with the processing of visual information. The visual cortex of mammalians is one of the most studied areas across the brain. I will remark the following aspects of its organization as essential for the task of vision:

- *Layered structure and hierarchy:* The visual cortex is known to be organized into different layers which respond to stimuli of gradually increasing complexity. For example, neurons in the primary visual cortex (V1) respond to very simple stimuli as edges or oriented bars, neurons in V4 respond to simple objects, and neurons in inferior temporal cortex respond to very complex stimuli, such as faces. Also the neurons' receptive fields are of increasing size as we go up through the visual path.

- *Parallel processing:* The cerebral cortex processes visual information through different channels that simultaneously code different features of the stimuli. The best known example is the existence of two visual pathways that independently process information about objects (*what*) and about spatial properties (*where*).

- *Feedback and lateral connections:* Most of the connections among the different cortical areas are reciprocal, and additionally there are many lateral connections between neurons in a given area.

- *Learning:* Neurons are able to change their connection strengths in order to adapt to the different situations. These adaptation mechanisms allow for the development of optimal internal representations.

Given these aspects of cortical organization, we could infer that the brain is exploiting two main facts when dealing with visual processing. On the one hand, it is performing a decomposition of the visual information into simple components that are easier to process, and then a gradual recomposition of the scene through neurons that gradually respond to more complex features. This is a divide and conquer approach. On the other hand, it is employing a distribution of the visual information across different neuron populations that code different features. This provides both a combinatorial representation of the input in terms of fewer processing units, and faster processing times than that provided by a sequential approaches. Feedback and lateral connections, as well as learning, might also be playing essential roles in these processes.

1.3 The binding problem

Assuming the brain processes information in a distributed manner, the problem of how to link features that have been processed by different areas arises. Distributed processing in the brain is a well accepted idea. From the most theoretical point of view, a parallel distribution of the different features a stimulus is composed of avoids the combinatorial explosion implied by having a *grandmother* cell for each different

feature combination. But it also involves the problem of how the brain knows which features, among all that are being simultaneously processed, must converge into single perceptions.

Solutions to the binding problem have been proposed from many perspectives. There are attention based approaches [101] that propose an intimate dependency between attentional mechanisms and binding; synchronization based approaches [43] that search for a solution in the precise spiking times of neurons coding each feature; and even approaches that rely on the capacity of the brain to encode information in a hierarchical way without leading to a combinatorial explosion [104]. It may also be that the brain does not use a single mechanism, but in fact combines many of them to achieve a solution to the binding problem.

The approach developed in this thesis follows the temporal correlation hypothesis [83, 43], which assumes that all the neurons representing the different features of an object are correlated in time with a millisecond precision. This hypothesis will be one of the main assumptions along this thesis, and for this reason it will be discussed in detail in chapter 2.

1.4 Entropy, information, optimal representations and factorial codes

Even if we could come to know the precise answers to the first two questions raised at the beginning, we would still have to address many important issues concerning the last one, that is, the development of optimal internal representations. The points discussed in the previous sections dealt mainly with how the brain processes information. There is still an even more important question to address: *Why?* Why do neurons respond to the kind of stimuli they do? Or, what are the basic principles that determine the brain function?

As a general rule, information theory has been used as an attempt to understand the kind of processing neurons are performing. Maximization of the mutual information between the output and the input has been usually proposed as one of the

objectives neurons are pursuing. However it must not be the only one, as a simple copy of the input maximizes mutual information, but it does not contribute much to knowledge. In the context of unsupervised learning, many attempts have been done to create artificial systems that develop optimal internal representations based on redundancy minimization criteria [5], independent component analysis [8], or the use of sparse and overcomplete representations [96]. Some of these approaches have led to first principles that are able to explain, for example, the receptive field properties of neurons in V1 from the statistics of natural images [95]. All these issues will be discussed in more detail in chapter 5.

1.5 Objectives of this thesis

This thesis is concerned with some aspects of information processing in neural systems related to previous points. The different problems will be focused from a computational modeling point of view. This approach consists of developing models of neurons and neural networks that provide a good description of real neural systems, so that they can be used to extract valid conclusions about the properties and functions of the systems they describe. The specific objectives of this thesis involve addressing the following three issues:

1. *Are there neural architectures that favor the brain function as we know it?*
2. *Is it useful to exploit oscillations and neural synchronization for practical purposes?*
3. *Which is the kind of coding the brain is performing?*

The work will be developed according to the following points.

I. Study of neural network architectures that optimize the network response in terms of oscillatory activity and fast response

This study is motivated by the following facts:

- Both activity oscillations and fast responses are observed in most neural systems.
- Other model studies tend to pay more attention to the neuron and synaptic dynamics than to the network architecture. Typically only regular (ordered) or random (totally disordered) architectures are considered.
- Recent work has shown that many real situations involving graphs can not be well described by neither a regular nor a random graph. A new kind of graph topologies, called *small-worlds*, seem to be more suitable to describe many real phenomena [128, 129], and I believe it could be the case for neural networks.

The study is developed according to the following stages:

- Study of the neural network response properties in terms of the network topology for model neurons with class 1 excitability.
- Study of the neural network response properties in terms of the network topology for model neurons with class 2 excitability.
- Comparison of the results obtained for each class of excitability.

The study has led to the following new results:

- Regarding class 1 excitability:
  - Ordered networks provide activity oscillations (synchronized activity) but the response time is quite low.
  - Random networks provide a fast response but they are not able to produce activity oscillations.
  - Small-world networks provide both fast response and activity oscillations.
- Regarding class 2 excitability:
  - Response time is generally low, except for random network architectures.
  - There is a high degree of synchronization regardless of the topology.
  - Spiking frequency of neurons strongly depends on the network topology.

II. Study of neural activity oscillations and spike synchronization, and applications to binding, binocular rivalry and image segmentation

This study is motivated by the following facts:

- Oscillations of neural activity have been observed in many neural systems.
- There is experimental evidence consistent with the idea that spike synchronization with millisecond precision could be used by the brain to associate the activity of neurons responding to different features of a single object [25, 41, 42].
- There is experimental evidence of a direct role played by activity oscillations in information processing in the insects olfactory system [70, 81, 82].
- Biological systems perform much better than artificial ones when dealing with real problems such as vision. Biologically inspired approaches could lead to improvements in some real applications.

The study is developed according to the following stages:

- Construction of a simplified model of the visual system with the following characteristics:
  - Different features are processed by different channels.
  - The main processing units are populations of neurons described by firing rate models.
  - Binding of different features is signaled by the simultaneous activation of the populations responding to each of them.
- Extension of the previous model to a model based on spiking neurons, so that:
  - It can account for the experimental measures of correlations between neurons in the visual cortex.
  - It is more consistent with the fast processing performed by the brain.

- Extension of the firing rate model to account for experimental results on binocular rivalry.

- Development of a segmentation mechanism based on synchronization in a network of integrate and fire neurons, and application to binary image segmentation.

The study has led to the following new results:

- A probabilistic model of spiking neurons that reproduces experimental results related to binding in the visual cortex. The simulations suggest that spike correlations can be due just to excitatory connections, and that the decorrelations may be due to the intrinsically noisy nature of the spike generation processes.

- A model of binocular rivalry based on competition between neuron pools with firing rate adaptation. Firing rate adaptation provides the alternation of winners, and the resulting phase durations coincide with experimental findings.

- A neural network of pulse-coupled oscillators that achieves segmentation of binary images using just local excitatory connections together with global inhibition. The use of pulse-coupled oscillators provides faster convergence and more robustness than other approaches based on continuously coupled oscillators.

III. Study of algorithms that lead to cause extraction and optimal internal representations of the input space

This study is motivated by the following facts:

- The brain uses internal representations that respond to the statistical structure of the input space [32].

- An input space is usually best described in terms of a set of generators, or hidden causes.

The study is developed according to the following stages:

- Analysis of the properties a good coding scheme should satisfy, namely discriminability and factoriality.
- Development of a measure for the code quality that combines these two requirements.
- Application of the measure to an example problem.

The study has led to the following new results:

- A new measure that takes into account the discriminability and the factoriality of a code has been introduced. For factorial and discrete input spaces, maximization of this measure leads to optimal codes in the absence of noise.

Chapter 2

Temporal coding and binding
A biological perspective

There is considerable evidence from neuroanatomy and neurophysiology that the brain uses different processing streams to process different aspects of visual information. It is quite well known that different features such as color, motion, object identity or position are separately processed by different cortical areas. From a theoretical point of view, this kind of processing has two main advantages:

1. Parallel processing is considerably faster than sequential processing.
2. A distributed representation of the information saves resources: expressing a stimulus as a combination of features coded by many neurons requires less coding units than having one neuron for each possible feature combination.

The second point has a side effect that leads to controversy: how does the brain manage to associate, or bind, the different features of a single stimulus that are spread across different cortical areas. This is know as the *binding problem*, and it becomes specially important when more than one object is present in the visual image. In this case, a wrong binding could lead to incorrect associations of features belonging to different objects, which is known as an *illusory conjunction*.

One possible hint on how the brain deals with the binding problem could reside on the large amount of lateral connections between different brain regions. These

connections may provide a cross-talk between areas that could serve to organize the response of all of them in some way that leaves no room for perceptual ambiguities.

The classical theory of binding assumed that information processed by specialized neurons responding to simple features converged onto neurons of gradually increasing specificity for certain classes of objects, which could even lead to the existence of *grandmother cells* that are selective to very precise combinations of features [4]. Although there are researchers that claim this kind of coding is possible [104, 40], it is generally believed that such a scheme would lead to a *combinatorial explosion* in the number of cells required for coding.

An alternative to this theory is the *temporal correlation hypothesis*. According to it, all the neurons involved in the coding of a single object could synchronize their spikes in order to signal their association [83]. Thus the different objects present in the visual field would be represented in the brain by synchronized neuron assemblies. The plausibility of this hypothesis from a biological perspective will be discussed in the next sections.

2.1 Oscillations in the brain: experimental evidence

At the end of the 80s, several experiments revealed the existence of coherent oscillations of the local field potential (LFP) in the cat visual cortex. These oscillations were assumed to be reflecting a synchronous pattern of activity of the neurons close to the recording electrode. Motivated by this findings, Eckhorn et al. [25] and Gray et al. [41] independently performed multielectrode recordings of both intracellular and extracellular potential in the cat primary visual cortex. They found that (i) the local field potential oscillated with a frequency of around $30-60Hz$ (*gamma oscillations*); (ii) the neurons' spiking activity was highly correlated with the LFP; and (iii) neurons inside an orientation column, as well as in different columns distant up to $7mm$ were able to synchronize their spike responses. This was the first evidence of synchronized spiking activity between neurons, and for many researchers it represented the proof

of the temporal correlation hypothesis. Later experiments have shown that spike synchronization may be driven by the stimulus [28, 62], can occur between different cortical areas [26], and even between the two brain hemispheres [27]. These and many other experiments during the last 15 years leave no doubt about the existence of spike synchronization, which is a reality for the visual cortex and for the nervous system in general [42, 123, 114]. However, whether or not this kind of correlated activity is being exploited by the brain to solve the binding problem remains controversial.

Recently, Gray [43] has reviewed the experimental evidences that support the temporal correlation hypothesis for binding. He remarks two main points in favor of it. Firstly, the abundance of experiments that have measured synchronous activity in the visual system leads to think that it must play a key role in the brain function. Secondly, in many experiments spike correlations are usually observed between neurons whose response properties share one or more of the Gestalt grouping features, such as proximity, similarity, or common motion [41, 28, 62, 74]. What this last observation implies is that neurons responding to features that the brain tends to associate seem to synchronize their spiking responses, and so it could be that this association is linked to the spike correlations. The experiments performed by Engel et al. [28] and Kreiter and Singer [62] are in favor of this view. They performed simultaneous intracellular recordings in pairs of orientation selective neurons of the visual cortex of the cat and the macaque monkey respectively; the neurons had overlapping receptive fields but different orientation preferences, and were stimulated with moving bars of different orientations. They reported that: (i) when the receptive field is stimulated with two bars of the preferred neurons' orientations, spike cross-correlograms between the neurons are flat, showing no correlations; and (ii) when only one bar, of an intermediate orientation between the two preferences, is presented, the neurons activation is lower, but the spiking times are correlated, which is shown by a high central peak in the cross-correlogram.

Of course there are also views that contradict the hypothesis of temporal coding for binding. Some studies reject the hypothesis based on the absence of gamma range oscillations resulting from experiments in the inferotemporal cortex of alert monkeys [119], and the striate cortex and the MT area in anesthetized monkeys

[133]. Other experiments in the cat visual cortex have shown no correlation between gamma oscillations and the stimulus [39], which suggests oscillations may be unrelated to binding. One of the most direct oppositions to the temporal correlation hypothesis is held by Shadlen [111, 112]. Taking into consideration anatomical constraints, he proposes that a code based on synchronization is biologically implausible because most of the input to a neuron comes in the form of synchronized spikes. So it is not imaginable how a neuron could differentiate which of its inputs are synchronized because of binding and which not. However he is not taking into consideration facts as inhibition or voltage-gated conductances, which may have profound effects on the excitability of cortical neurons [43].

In spite of all this controversy, I still believe there is enough experimental evidence not to reject the temporal correlation hypothesis, and even to think that oscillations and temporal correlation in the brain are not a casual phenomenon, but are indeed produced to achieve specific goals. One of the most direct evidence of the important role oscillations are playing in the nervous system comes from the results of studies performed by G. Laurent and coworkers in the olfactory system of the locust [70, 81, 82]. They have found that:

1. In response to odors, neurons in the locust olfactory system engage in synchronous coherent oscillations with a frequency of around $20Hz$.

2. Information about odors is encoded both by spatial and temporal patterns of spiking activity.

3. The ability of the locust to discriminate odors is deteriorated if synchronization is altered by external factors.

These observations seem to point to the fact that oscillations of neural activity play an essential role in the brain operation and are fundamental for correct information processing in neural systems.

2.2 Spikes vs rates. Processing speed

One of the hottest discussions in neuroscience is concerned with the kind of code neurons are using. There are two main perspectives. On the one hand, firing rate approaches, that defend that most of the information transmitted by a neuron is contained in its average firing activity. According to this view, a simple counting of the number of spikes that occur in a given time window is enough to encode the information the neuron is receiving. On the other hand, there are approaches in favor of a spike based coding. The main issue concerning spike coding is that the precise spiking times of a neuron could convey information, and it would be lost when considering just averages.

Firing rate coding schemes are motivated by the classical experiments of Adrian [3] in the muscle stretch receptors. He observed that the firing rate of the receptors increased with the forced applied to the muscle. Due to the relative ease of measuring firing rates, this kind of approach became a standard tool that is still in use. A firing rate code may be appropriate for almost stationary situations in which the input does not present strong variations with time. In such cases, firing rate measurements appear to be stimulus dependent and reproducible in different experiment repetitions. However some inconsistencies appear when one has to deal with fast varying inputs. In these cases, the time windows in which the input presents variations are not enough to compute firing rates, and a coding based on spikes seems more plausible.

A strong argument in opposition to firing rate coding comes from experimental measures of reaction time upon stimulation. Measured reaction times are often too short to permit the computation of averages over long time windows. Taking this to the limit, some researchers claim that the measured response times in humans under recognition task experiments not only contradict a firing rate coding, but also leave just time enough to process the first spike [116, 117]. Also in favor of a spike coding, the work of Bialek and coworkers [9, 103] shows that it is possible to reconstruct a time dependent stimulus from the precise spiking times of the H1 neuron of the fly. A coding scheme based on single spikes would be also compatible with the temporal correlation hypothesis and the experimental results of the group of Singer with cortical

neurons [41, 62].

Different coding schemes are possible in the framework of spike coding. A common approach is time to first spike. S. Thorpe [117] proposes that most of the information contained in a spike train is conveyed by the first spike, and that the relative order in which different neurons fire provides the substrate for different combinations that can code the stimuli. In this context, he has applied a method based on the firing order to codify and recover real images [124]. A deficiency that is present in this approach is how to determine which is the first spike when neurons are firing continuously. A simple solution could reside on the activity oscillations, which could be thought of as a mechanism that periodically resets the network. The coding could be then performed based on the precise spiking times of neurons relative to the average activity oscillations (phase coding, [80]). This assumption would be another point in favor of the importance of oscillations in the nervous system.

In spite of all these considerations, there is still some room for a firing rate based coding. Time averages are not biologically plausible because too large time windows are required to compute them. But it still could be possible to compute averages over populations of neurons with common dynamical and response properties. This kind of population rate could be computed in very short time windows and could respond to fast variations in the input. It will also provide the robustness derived from considering whole populations instead of single neurons.

This last approach could be seen as a convergence between spike based and rate based codings. On the one hand spiking times are important for sufficiently small time windows. On the other hand a population average provides the robustness that was absent in spike based codes. If the precise spiking time is in fact so important, it is not imaginable that the brain relies on the noisy processes that involve the spike generation in one single neuron. By averaging over a big population of similar neurons, however, this problem could be overcome.

2.3 Concluding remarks

Two main conclusions may be extracted from the considerations of this chapter that directly concern this thesis:

- The brain displays activity oscillations that seem to be essential for information processing. These oscillations could provide a framework for:
  - A temporal based solution to the binding problem.
  - A spike based coding in which information is contained in the precise spiking times of neurons relative to the average oscillation.
- Response to external stimulation is very fast, which indicates that the neural signal quickly propagates through the nervous system.

Chapter 3

Optimal network topologies for information processing

3.1 Introduction

In the previous chapters I have discussed two important elements for information processing in the biological brains. On the one hand, coherent oscillations of the local field potential and correlated spiking activity have been observed in a variety of studies [25, 41], and are believed to be essential for the correct processing of sensory information by biological systems [42, 82]. They are a key element when dealing with temporal coding and binding. On the other hand, a fast propagation of the neural activity is necessary to account for the fast response times measured in experiments [116, 117]. From a more Darwinian point of view, a fast reaction upon external stimuli implies higher survival chances.

In this chapter I will analyze neural networks with different topologies, searching for an optimal response in terms of these two facts. Artificial approaches to neural networks are usually characterized by an activation function, a synaptic dynamics, and a network architecture. Here I will study the effect of changing the architecture in networks with fixed activation function and synaptic dynamics, just constrained to provide a sufficiently realistic description of the biological processes involved in the action potential generation and the neural transmission. I will consider two different

neuron models that describe the two main types of neural excitability, the classes 1 and 2 proposed by Hodgkin [49]. Surprisingly, in most of the literature the network architecture is the "fixed" parameter. Usually only regular or random topologies are considered, and researchers tend to pay more attention to the dynamics in the network nodes than to the network structure itself. Here I want to state the importance of the topology, trying to find an answer to the following question:

Is there an optimal network topology that meets the two previous considerations?

And, if so:

How can it be characterized?

I will try to find an answer to these questions, but let us first take a glance into the brain, and how it is organized, to search for some inspiration. The structure of biological neural networks seems to have very specific patterns of connectivity. The human visual cortex, for example, presents a columnar organization of connections, with inter-columnar links and projections from and to very specific sites [21]. This structural organization is common to all brains and is far from being random. However we can not say it is regular. Everywhere in the brain we observe connections coming from and going to other brain areas, and connections which deviate from the general regularity. The brain connection scheme most often seems to be responding to an overall regular pattern with some additional connections that escape from the general rule. These extra connections break the regularity, but not completely. It appears that the topology nature has chosen for biological neural networks lays somewhere between randomness and regularity.

The need to characterize and formalize these ideas about the topological structure of natural neural networks leads the search toward graph theory and some recent research on the structure of complex networks. In this context a new kind of graph topologies, that are regular on average but present some special connections that escape from regularity, have been recently introduced [128]. They have been called *small-world* networks, and a lot of research have been carried out on them in the last few years.

These small-world topologies open new possibilities in the field of neural networks. One can characterize the network architecture in terms of its degree of randomness

or regularity, and study the network response properties for a variety of different topologies. Some of them, not necessarily regular or random, may appear to be interesting for particular problems. My motivation here is to elucidate which kind of networks are able to produce a biologically more plausible response. Using networks with spiking neurons and a good description of the action potential generation in terms of differential equations, I will search for the topologies that provide the network with the ability to quickly produce oscillations after being stimulated. I will show that, in many cases, networks with a small-world topology are the best choice.

The chapter is organized as follows. First, in section 3.2, I introduce the dynamical neuron and synaptic models that are used along the chapter. In section 3.3 I give an overview of the fundamental concepts of graph theory I will be using; I introduce the definitions of random graphs, lattices and small-world graphs, and their characterization in terms of the characteristic path length and the clustering coefficient. The section finishes with some examples of real small-worlds. Section 3.4 deals with the effects of the topology on the response of a neural network of Hodgkin-Huxley neurons; I study networks with different topologies and conclude that the small-world is the only one able to produce oscillations quickly after the stimulus is presented. In section 3.5 I extend the study to a new neuron model, the FitzHugh-Nagumo model, that presents different dynamical properties. An extensive comparison between the two models, each characteristic of a different kind of neural excitability, is performed. Finally, in section 3.6 I present the conclusions of the chapter and discuss some issues concerning the results.

3.2 Neuron models and synaptic dynamics

The basic information processing unit in the brain is the neuron. It is able to read information in the form of different synaptic currents, and produce a nonlinear response in the form of an action potential. There are many types of neurons, each adapted to particular functions in the brain. However what is common to all of them is their ability to respond to external currents by depolarizing their membrane, which

may eventually end up in the production of an action potential. Here I am not interested in the specific details of the neuron model, as far as it keeps the essentials of the generation of action potentials. I will consider two different models, for they reproduce the properties of the two main known types of neurons in terms of excitability, namely class 1 and class 2 neural excitability [49]. These models are the Hodgkin-Huxley model [50] and the FitzHugh-Nagumo model [33, 90]. I have chosen them because they are continuous (in contrast for example to integrate and fire models), biologically plausible, and well accepted in the neuro-scientific community. The synaptic transmission has been described with differential equations that model the fraction of open channels in the postsynaptic neuron in terms of the neurotransmitter concentration released after the presynaptic action potential [22].

3.2.1 Hodgkin-Huxley model, class 1 excitability

The first successful attempt to model the behavior of the membrane potential in real neurons was the Hodgkin and Huxley (HH) model for the generation of action potentials in the squid giant axon [50]. In 1952 A. L. Hodgkin and A. F. Huxley combined voltage clamp techniques with the usage of pharmacological agents which allowed to block different ionic currents, and were able to divide the membrane current into its main constitutive components. They proposed a detailed model of four coupled differential equations that describe the dynamics of the generation of action potentials, taking into account the two main ions that traverse the cell membrane, Na^+ and K^+:

$$C_m \frac{dV}{dt} = -g_l(V - V_l) - g_{Na} m^3 h (V - V_{Na}) - g_K n^4 (V - V_K) + I_{ext} \tag{3.1}$$

$$\frac{dm}{dt} = \alpha_m(V)(1 - m) - \beta_m(V)m \tag{3.2}$$

$$\frac{dh}{dt} = \alpha_h(V)(1 - h) - \beta_h(V)h \tag{3.3}$$

$$\frac{dn}{dt} = \alpha_n(V)(1-n) - \beta_n(V)n \tag{3.4}$$

In these equations, V represents the membrane potential; C_m is the membrane capacity per unit area; g_l, g_{Na}, g_K are the conductances for the leaky, sodium and potassium channels; and V_l, V_{Na}, V_K are the corresponding reversal potentials. The term I_{ext} involves all the external currents injected to the neuron, including synaptic currents. Finally, the variables m, h and n regulate the opening, closing and inactivation of sodium and potassium channels, and α and β are functions of V adjusted to physiological data by voltage clamp techniques. The parameters we use here are based on a model of Traub [120] for CA3 hippocampal neurons. The voltage dependent channel variables (α and β) are as follows, and the parameters are shown in table 3.1.

$$\alpha_m = \frac{-0.32(42+V)}{\exp(-(42+V)/4)-1}, \quad \beta_m = \frac{0.28(15+V)}{\exp((15+V)/5)-1} \tag{3.5}$$

$$\alpha_h = 0.128\exp(-(38+V)/18), \quad \beta_h = \frac{4}{\exp(-(15+V)/5)+1} \tag{3.6}$$

$$\alpha_n = \frac{-0.03(30+V)}{\exp(-(30+V)/5)-1}, \quad \beta_n = 0.5\exp(-(35+V)/40) \tag{3.7}$$

g_{Na}	$50.0mS/cm^2$
g_K	$10.0mS/cm^2$
g_l	$0.15mS/cm^2$
V_{Na}	$50.0mV$
V_K	$-95.0mV$
V_l	$-55.0mV$
C_m	$1.0\mu F/cm^2$

Table 3.1: Parameters for the HH model.

This model is an example of class 1 neural excitability. According to the classification of Hodgkin [49], neurons present two classes of excitability. Class 1 excitable

neurons are those that can present a spiking phase at arbitrarily low frequencies. In terms of dynamical systems, this kind of neurons are described by models which present a saddle-node bifurcation to the limit cycle [53, 105], such as the HH model[1]. As a proof of concept, I have numerically computed the solution of the HH equations (3.1-3.4) for different values of the external current, I_{ext}. Results are shown in figure 3.1A. Observe that the model presents a spiking phase for currents over a bifurcation value between 0.4 and $0.5\mu A/cm^2$; and that the frequency of the spikes can be arbitrarily low.

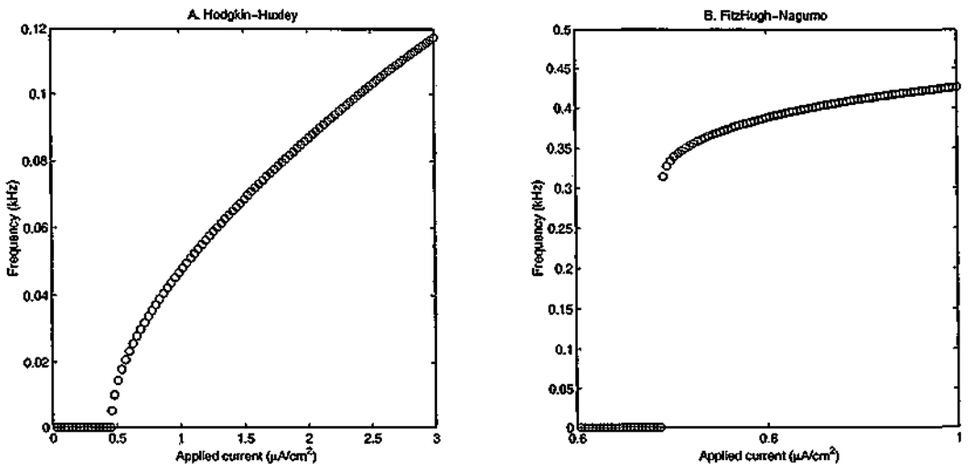

Figure 3.1: A. Frequency of oscillation versus external current for the Hodgkin-Huxley model. The presence of an oscillatory phase at arbitrarily low frequencies is a characteristic of class 1 excitability. B. Frequency of oscillation versus external current for the FitzHugh-Nagumo model. Class 2 excitable neurons present oscillations only in a limited frequency band.

3.2.2 FitzHugh-Nagumo model, class 2 excitability

The HH model provides a detailed description of the generation of action potentials in terms of the ionic currents that traverse the cell membrane. It reproduces with a high fidelity the physiological data; however, it is a quite complex four dimensional model

[1]This is true for the parameters I am considering. However the HH model exhibits class 2 excitability for the original parameters.

that requires a detailed knowledge of the kinetics of ionic channels. It is sometimes more interesting to develop simplified models that capture the essence of neuronal dynamics at a much reduced complexity. The FitzHugh-Nagumo model [33, 90] is a simplification of the HH equations, that comes out from the observation that in the HH model V and m evolve on similar, fast, time scales during the occurrence of an action potential; while h and n do on a much slower time scale. It was developed independently by R. FitzHugh [33] in 1961, and J. S. Nagumo, S. Arimoto and S. Yoshizawa [90] in 1962. They proposed a model of two variables, described by the following equations:

$$\frac{dV}{dt} = \alpha(V - \frac{V^3}{3} - W + I_{ext}) \tag{3.8}$$

$$\frac{dW}{dt} = \phi(V + a - bW) \tag{3.9}$$

The variable V represents the membrane potential, the fast variable; and W is a slow variable without a clear biological interpretation. The parameters a, b, α and ϕ are dimensionless and positive. Here I have used the following values: $a = 1.0$, $b = 0.8$, $\alpha = 20.0$ and $\phi = 1.2$. With such a selection, the model presents a subcritical Hopf bifurcation at a current $I_{ext} = 0.692\mu A/cm^2$ [53, 105]. Due to the lack of a clear biophysical interpretation of the model parameters, I have preferred to drop off the units and reinterpret V as a variable that measures the neuron state. However when applying a common synaptic dynamics to both the HH and the FN equations, I must rescale the variable V according to:

$$V' = \delta V + \kappa \tag{3.10}$$

with $\delta = 34mV$ and $\kappa = -10mV$. This new variable V' will be used as the presynaptic potential in the equations describing synaptic transmission.

The FN model is an example of class 2 excitability. Class 2 excitable neurons present oscillations only in a limited frequency band. They are well described by dynamical systems that lose their stability by means of a Hopf bifurcation [53, 105]. In figure 3.1B I show the frequency of oscillation versus the input current for the FN

model described by equations (3.8) and (3.9). Observe that the oscillations occur only within a frequency band, as characteristic of class 2 excitability.

3.2.3 Synaptic transmission

Synapses make possible the communication between neurons through chemical or electrical processes that initiate with the arrival of an action potential to the presynaptic site. Here I will consider only chemical synapses, which involve the liberation of neurotransmitter substances that are able to modify postsynaptic conductances and so generate ionic currents that affect the postsynaptic potential. In mathematical models, the postsynaptic current is generally expressed as:

$$I_{syn} = g_{syn}(V - V_{syn}) \tag{3.11}$$

where g_{syn} is the synaptic conductance, V is the postsynaptic potential, and V_{syn} is the synaptic reversal potential. The synaptic conductance increases after the occurrence of a presynaptic action potential as a consequence of the opening of ionic channels that are sensitive to neurotransmitter. It is generally modeled as an α-function [100, 58]:

$$g_{syn}(t) = Cte^{-t/\tau} \tag{3.12}$$

With the appropriate selection of the parameters C and τ, this kind of function reproduces well the time course of synaptic conductances measured in real neurons. However I will follow here the approach in [22], who model the fraction of open channels in the postsynaptic neuron, r, in terms of the following differential equation:

$$\frac{dr}{dt} = \alpha_{syn}x(1 - r) - \beta_{syn}r \tag{3.13}$$

where x is the neurotransmitter concentration in the synaptic cleft, and α_{syn} and β_{syn} are time-independent rise and decay constants. In terms of r, the expression for the synaptic conductance is simply:

$$g_{syn} = rg_{max} \tag{3.14}$$

where g_{max} is the maximum conductance per unit area. The parameter values used in the simulations are shown in table 3.2. The maximum synaptic conductance g_{max} is varied for different simulations in section 3.5.

Typically the transmitter concentration, x, is assumed to be a squared pulse that initiates with some delay after the presynaptic spike (as in [22]). This is the case for section 3.4, where we consider a square pulse of amplitude $A = 1mM$ and no delay, with a duration $\tau = 1.5ms$. However, in order to make an explicit dependence of x on the presynaptic potential V_{pre}, in section 3.5 I use the following equation:

$$\frac{dx}{dt} = \alpha(f(V_{pre}) - x) \tag{3.15}$$

where α is a constant and the function f is given by:

$$f(V_{pre}) = \frac{\sigma}{1 + \exp(-(V_{pre} - \theta)/T)} \tag{3.16}$$

This function represents the limit in transmitter concentration at a constant presynaptic potential V_{pre}, and has been fitted to reproduce experimental findings. In the present work I will consider only excitatory connections. The parameter values used in the simulations of sections 3.4 and 3.5 are shown in table 3.2.

3.2.4 Numerical integration

The differential equations describing the neuron and synaptic dynamics have been numerically solved using a Runge-Kutta 6(5) scheme with variable time step [52]. The absolute error was 10^{-15} and the relative error was 10^{-7} in all the calculations.

3.3 Network topologies and graphs

A neural network, either biological or artificial, can be described as a set of processing units, or neurons, and a set of directed connections between pairs of units. So, ignoring the dynamical behavior of neurons and synapses, the architecture of a neural network can be represented as a directed graph. The structure of this graph will influence the

section 3.4	V_{syn}	$0mV$
	α_{syn}	$0.94ms^{-1}mM^{-1}$
	β_{syn}	$0.18ms^{-1}$
	g_{max}	$0.015mScm^{-2}$
	A	$1.0mM$
	τ	$1.5mS$
section 3.5	V_{syn}	$0mV$
	α_{syn}	$2.0ms^{-1}mM^{-1}$
	β_{syn}	$1.0ms^{-1}$
	g_{max}	variable
	α	$5.0ms^{-1}$
	σ	$2.84mM$
	θ	$2.0mV$
	T	$5.0mV$

Table 3.2: Synaptic parameters.

dynamical properties of the network and the network response to external stimuli. In this section, I introduce some notions on basic graph theory that will be used along the rest of the chapter. For a complete review on graph theory see for example [44].

A *graph* is a set of elements, V, called *vertices* together with a set of *edges*, E, connecting pairs of vertices. I will denote the graph as $G(V, E)$, and use n for the number of vertices, or *order* of the graph, and M for the total number of edges, or *size* of the graph. Two vertices are said to be *adjacent* or *neighboring* vertices if there exists an edge joining them.

Let us define the *degree* of a vertex, k_i, as the number of edges converging on it. The average of k_i over all vertices is called the *connectivity* of the graph, and will be denoted by k. The following identities hold:

$$\sum_{i=1}^{n} k_i = 2M \tag{3.17}$$

$$\sum_{i=1}^{n} k_i = nk \tag{3.18}$$

And so,

$$nk = 2M \tag{3.19}$$

If $G(V, E)$ is a graph, we will define a *subgraph* $G'(V', E')$ of G as a subset V' of V with all the edges E' connecting the vertices of V' in G.

A *walk* between two vertices v_0 and v_l is a succession of vertices $v_0, v_1, ..., v_l$ such that the edge $e_{i,i+1}$ exists for all $i = 0, 1, ..., l-1$. The number of edges in the walk is called the *length* of the walk. A walk is called a *path* if all the vertices are distinct.

The *distance* l_{ij} between vertices v_i and v_j is defined as the minimum length of a path connecting them. With the concept of distance, we can extend the definition of *neighboring* vertices as follows: two vertices v_i and v_j are *r-neighbors* if $l_{ij} = r$; two vertices are *neighbors* if they are 1-neighbors. The *neighborhood of degree r* (or *r-neighborhood*) of a vertex v_i, $\Gamma^r(v_i)$, is defined as the subset of vertices v_j that are r-neighbors of v_i:

$$\Gamma^r(v_i) = \{v_j \in V : l_{ij} = r\} \tag{3.20}$$

Given a vertex v_i, we will define the *r-subgraph* associated to v_i as $G'(\Gamma^r(v_i), \mathcal{E})$, where $\Gamma^r(v_i)$ is the r-neighborhood of v_i and $\mathcal{E}$ is the subset of edges in the original graph that connect vertices in $\Gamma^r(v_i)$.

A graph is said to be *directed* if the edges have a preferred direction, i. e., the edge e_{ij} begins at vertex v_i and ends at vertex v_j. Otherwise it is *undirected*; in this case we have $e_{ij} = e_{ji}$.

A graph is *simple* if there are no multiple edges between any given pair of vertices and no edges connecting a vertex to itself.

A graph is *sparse* if, being simple, the number of edges is a small fraction of the maximum allowed one. That is:

$$M << \frac{n(n-1)}{2} \tag{3.21}$$

In the limit $n >> 1$, we can use equation (3.19) to express the sparseness condition as:

$$k << n \tag{3.22}$$

Finally, a graph is *connected* if there exists a path joining any pair of vertices.

For the present analysis, I will only consider graphs that are undirected, connected, simple and sparse; and I will always work in the limit of large order, $n >> 1$. Of course the graph describing the architecture of a neural network should be a directed one; I will take this fact into account later on in this chapter. Now let us introduce a couple of definitions that will be useful to characterize the structure of a particular graph [128, 129].

Characteristic path length:

The *characteristic path length* (L) of a graph is the average distance between all pairs of vertices:

$$L = \frac{2}{n(n-1)} \sum_{i \neq j}^{n} l_{ij} \tag{3.23}$$

Clustering coefficient:

The *clustering coefficient*, C_i, of a vertex v_i in a graph is the quotient between the size M_i of the 1-subgraph associated to v_i, $G'(\Gamma^1(v_i), \mathcal{E})$, and the maximum allowable size of $G'(\Gamma^1(v_i), \mathcal{E})$. That is:

$$C_i = \frac{2M_i}{k_i(k_i-1)} \tag{3.24}$$

It measures, somehow, the fraction of neighbors of the vertex that are also neighbors among themselves. The *clustering coefficient* of graph, C, is simply the average of C_i over all the vertices:

$$C = \frac{1}{n} \sum_{i=1}^{n} C_i \tag{3.25}$$

In what follows I will use these two structural properties to characterize graphs with constant order, n, and connectivity, k, but different topologies. In particular we will evaluate L and C for two special kinds of graphs, random graphs and lattices, which have been typically the most studied graph topologies applied to neural networks.

3.3.1 Random graphs

A *random graph* consists of a set of n vertices and a set of M randomly chosen edges connecting them. An example of a random graph is shown in figure 3.2. Special care about connectedness should be taken when dealing with sparse random graphs: when the degree of sparseness is very high, the probability of the random graph to be disconnected can be very high as well. To ensure connectedness we can use the result of a theorem stated by Erdös and Rényi [29]. We can guarantee that the probability of a random graph to be connected is very high as far as the condition $k > ln(n)$ is satisfied. For details on this result see also [12]. With this result in mind, we can guarantee the requirements of sparseness and connectedness as long as the following condition is verified:

$$n >> k >> 1 \tag{3.26}$$

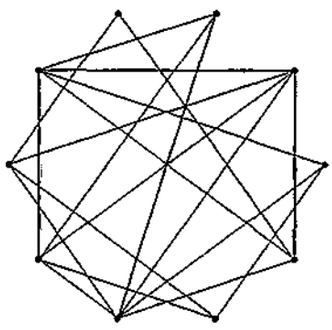

Figure 3.2: A random graph with $n = 10$ and $k = 4$.

Let us now study L and C for a random graph. I will first evaluate the probability

of an edge between a given pair of vertices to exist. It can be expressed as the quotient between the number of edges M and the number of pairs:

$$p = \frac{2M}{n(n-1)} \tag{3.27}$$

Using equation 3.19 and the assumption 3.26 we can write:

$$p \approx \frac{k}{n} \tag{3.28}$$

The clustering coefficient, as defined in equations 3.24 and 3.25, is an average over all graph vertices of the fraction of edges existing in the 1-subgraph associated to each vertex. In a random graph, the fraction of existing connections is the same for any subgraph, and equal to the connection probability p. So we obtain:

$$C \sim \frac{k}{n} \tag{3.29}$$

To calculate the characteristic path length, we must take into account that in a sparse random graph, if v_i is a vertex and $v_j \in \Gamma^1(v_i)$, then $\Gamma^1(v_i) \cap \Gamma^1(v_j) = \emptyset$ with a high probability. So the number of vertices in $\Gamma^2(v_i)$ approximates $k_i(k_i - 1)$, and in general the number of vertices in $\Gamma^r(v_i)$ is:

$$n(\Gamma^r(v_i)) \approx k_i(k_i - 1)^{r-1} \tag{3.30}$$

Based on this result and with a little algebra, we obtain that L grows with n as:

$$L \sim \frac{ln(n)}{ln(k)} \tag{3.31}$$

3.3.2 Regular graphs and lattices

A *regular graph* is a graph in which the degree of each vertex is a constant:

$$k_i = k,\ i = 1, ..., n \tag{3.32}$$

A particular case of a regular graph is a *lattice*, where the spatial structure resembles that of a periodic crystal. I will consider here just one-dimensional lattices and even vertex degree, $k = 2r$, for this simplifies the analysis. I will build the lattice by arranging the vertices in a ring and connecting each one to its k nearest neighbors, r on either side (see figure 3.3). That is, vertex v_i is connected to the vertices:

$$v_j : j = [(i - l) + n] \bmod n \tag{3.33}$$

and

$$v_k : k = (i + l) \bmod n \tag{3.34}$$

where

$$1 \leq l \leq r \tag{3.35}$$

I will only consider regular graphs that are lattices, so from now on I will use the terms regular graph and lattice indistinctly.

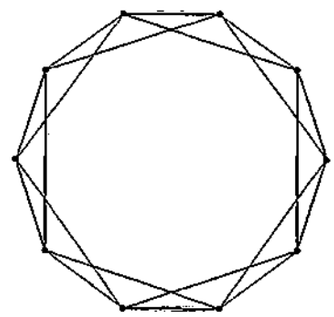

Figure 3.3: A regular lattice with $n = 10$ and $k = 4$.

As I did for the random graphs, I will give expressions for L and C for one-dimensional lattices. In this case it is possible to explicitly calculate L and C, but we are just interested in how they scale with n and k in the limit of condition 3.26. It is not difficult to show that the characteristic path length grows linearly with n:

$$L \sim \frac{n}{2k} \tag{3.36}$$

For the clustering coefficient we get:

$$C \sim \frac{3}{4} \tag{3.37}$$

3.3.3 Small-world graphs

So far we have seen that the characteristic path length and the clustering coefficient have quite different scaling properties for random and regular graphs. For given n and k, the regular graph is highly clustered and presents a very high characteristic path length, whereas the random graph presents both very small C and L.

The question that arises is whether there exists a kind of graphs that, while being highly clustered, present a characteristic path length similar to that of a random graph. Intuitively, we can try to do the following reasoning. Let us start with the regular graph of figure 3.3, and replace a few edges by random ones. We obtain a graph similar to that of figure 3.4, in which only two edges have changed. This new graph presents two characteristics:

- The clustering properties have hardly changed with respect to the regular graph. The overall structure of both graphs is mostly the same.
- The characteristic path length of the new graph has greatly decreased, because the new edges act as *short paths*.

This graph is placed somewhere between regularity and randomness, and it will be called a *small-world*[2] graph [128, 129]. Before we give a definition for small-world graphs, we will introduce a procedure to generate graphs of increasing randomness, and we will study the structural properties of these resulting graphs.

[2]The name small-world comes from the study of social networks, where it has been shown that two randomly chosen human beings can be connected by a very short chain of intermediate acquaintances, the so-called small-world effect [86].

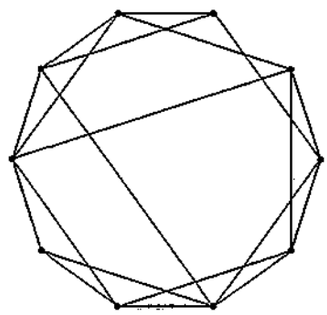

Figure 3.4: A small-world graph with $n = 10$ and $k = 4$.

Let us start with a regular graph G, and introduce a new parameter, p, with $0 \leq p \leq 1$, which represents the probability of replacing an edge in G by a new, randomly selected[3], one. After rewiring each of the edges with probability p, we have a new graph G'. Obviously, for $p = 0$, we have $G' = G$, so regular graphs are characterized by $p = 0$. On the other hand, for $p = 1$ every edge has been rewired and we have a random graph. By smoothly varying p between 0 and 1, we can interpolate between regularity and randomness.

If we study the behavior of L and C as functions of the rewiring probability, p, we observe that there is an interval in which high C coexists with low L. There is a range of probabilities (with $p \to 0$ as $n \to \infty$) that, while not altering the clustering structure of the graph, greatly reduce its characteristic path length. A graph lying on this interval is called a *small-world* graph. As an example, we have performed numerical calculations of L and C in graphs with $n = 797$ and $k = 30$, for different values of the rewiring probability. The results are shown in figure 3.5. In the figure, $L(p)$ and $C(p)$ have been normalized by the values $L(0)$ and $C(0)$ respectively, for a clearer comparison. There is an interval for p where L has decreased to almost the minimum value while C has not changed. Probabilities within this interval determine small world graphs.

The mechanism that allows for the appearance of such a small-world has been

[3]We take care of not creating multiple or recurrent connections with this procedure, as the graph must remain simple.

discussed before. For very small probabilities only a few edges change. Changing one edge in the regular graph by a randomly selected one represents the substitution of a *short-range* connection by a *long-range* one, which can act as a short path, reducing the average length between graph vertices. So the appearance of just a few long-range edges is able to highly reduce the characteristic path length. However, such a few number of rewired edges is not enough to alter the clustering structure of the regular graph.

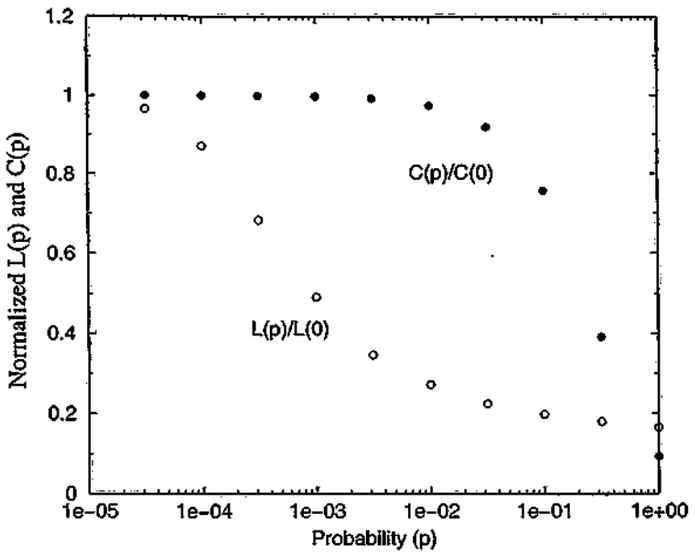

Figure 3.5: Characteristic path length L and clustering coefficient for different values of the probability p in a graph of $N = 797$ vertices and a mean connectivity $k = 30$. The results are normalized by the values of the regular graph $L(0)$ and $C(0)$, and are averages over 10 different simulations.

3.3.4 Some real life examples

The small-world is not just a theoretical speculation, and in this section I show some examples of real networks that present small-world properties. The first evidence for the existence of graphs with small-world structure comes from the study of social

networks, which can not be considered either regular or random. This in fact motivates the name *small world*. It is estimated that two randomly selected human beings can be connected, on average, by a short chain of intermediate acquaintances [86]. This is the so-called "six degrees of separation" [45]. Despite the big size of social networks, the average distance between vertices is very small. However they can not be well described by random graphs, because people's circles of acquaintances tend to overlap. In a social network, if A and B are *friends* of C, the probability that A and B are also friends is higher than in a random graph of the same characteristics. Social networks are an example of highly clustered graphs with small characteristic path length, which is precisely the definition of a small-world.

Although this result is quite intuitive, a complete analysis would imply the calculation of L and C, and results impossible for almost any social network, due to its enormous size. However, some calculations have been performed for a few special cases, such as the network of collaborations between movie actors [129]. The study revealed a clustering level close to a regular network, and a characteristic path length close to a random one (table 3.3).

Beyond social networks, other real graphs have been studied in terms of L and C. Analyses of the neural network of the worm *C. Elegans* and the electrical network of the western United States were also performed by [129]. His results are summarized in table 3.3. Other empirical examples of small-world connectivity have been reported in metabolic networks [54], scientific collaboration networks [93], or communication networks [2]. All these examples present clustering coefficients close to that of a regular graph of the same n and k, and characteristic path lengths that resemble those of a random graph.

Since the introduction of the small-world graphs by Watts and Strogatz [128], many authors have applied this new kind of graph topologies to a variety of problems: cellular automata, simple games and networks of coupled oscillators [129]; the Ising model [7]; the problem of disease spread [91]; or the eigenspectrum of the Laplacian operator [89]; among others. For a review see [92].

I have applied small-world topologies to neural networks of dynamically coupled Hodgkin-Huxley and FitzHugh-Nagumo neurons [63, 65]. In the next sections I will

Network	Actors	Electrical Network	C. Elegans
n	225226	4941	282
k	61	2.67	14
L	3.65	18.7	2.65
C	0.79	0.08	0.28
L_{rand}	2.99	12.4	2.25
C_{rand}	0.00027	0.0005	0.050
L_{reg}	1846.6	926	10.5
C_{reg}	0.74	0.3	0.69

Table 3.3: Statistics of three real graphs (network of collaborations between movie actors; electrical network of the western United States; and neural network of the worm *C. Elegans*) and comparison with the statistics of random and regular graphs of the same n and k. Results taken from [129].

show that small-world topologies provide the network with special properties that make them interesting from the point of view of information processing in biological systems.

3.4 Effects of the topology on the network response

Now that I have introduced the models for neuron dynamics and synaptic interaction, and quantified the network topology in terms of the characteristic path length and the clustering coefficient, let us turn to the study of how the topological structure influences the response of a biologically plausible neural network. I will start by considering the Hodgkin-Huxley model, characteristic of class 1 excitability, and then I will turn to the comparative study of classes 1 and 2 in section 3.5. I will use neural networks with constant structure parameters n and k. The network topology is characterized by the rewiring probability, p, which measures the degree of randomness in the graph. For $p = 0$ a regular network is obtained, whereas for $p = 1$ a random one results. By varying the value of p between 0 and 1 we can interpolate between the two limiting cases, passing through the small-world region.

Before going on, I will consider some points that I postponed, concerning the

directness of the graph associated to the neural network. The flow of information in a synapse has a specific direction, from the presynaptic neuron to the postsynaptic one. So the graph describing a neural network architecture should be a directed graph. Some of the concepts introduced in section 3.3 must be revisited when dealing with neural networks. For each vertex in the graph, we can define two different degrees, one for the incoming edges, k_i^I, and another one for the outgoing edges, k_i^O. Their corresponding averages will be denoted without the subscript, k^I and k^O. Obviously the total number of incoming connections equals the total number of outgoing ones:

$$k^I = k^O = k \tag{3.38}$$

The generation of the different network topologies is performed as follows:

1. We start from a regular graph as defined in section 3.3.2, and for each edge we consider two different connections, one in each direction. We obtain a regular neural network with $k_i^I = k_i^O = k$ for all neurons i.

2. With a probability p, we change each connection in the following way. We maintain the presynaptic neuron and randomly select a postsynaptic one. We avoid choosing the same presynaptic neuron and generating multiple connections. This procedure produces no change in the outgoing degree of network vertices, $k_i^O = k$, but modifies the incoming degree k_i^I. In the limit of $p = 1$ we approach a quasi-random[4] network structure.

The definitions of characteristic path length and clustering coefficient must be refined:

For the characteristic path length, L, we need to measure the minimum distance between all network pairs, but always following the direction of edges. The distance between vertices i and j may be different from the distance between vertices j and i, so we can redefine L as:

[4]Strictly speaking this is not a random graph, as the number of outgoing connections is constant for all vertices.

$$L = \frac{1}{n(n-1)} \sum_{i=1}^{n} \sum_{j \neq i}^{n} l_{ij} \tag{3.39}$$

For the clustering coefficient, C, we can define two different quantities, one for incoming and another for outgoing connections. This is because two neurons i and j can be neighbors in two different ways: because there exists a connection from i to j or because there exists a connection from j to i. Using the first kind of neighborhood, we define the outgoing clustering coefficient, C_i^O, and using the second one we define the incoming clustering coefficient, C_i^I. Averages over all network neurons are denoted without the subscript, C^O and C^I. Along this work we will consider always the incoming clustering coefficient, C^I.

With these explanations in mind, we can continue the study. I will investigate the response properties of a neural network in terms of its topology. In particular I am interested in response time and the ability to generate correlated activity, as they both are interesting properties from a biological point of view. The results from section 3.3 lead us to make some predictions. We should expect the following results:

- *Correlated network activity and very long response time for regular networks.* In highly clustered networks, two neighbor neurons receive afferent connections from almost the same subset of neurons; so we expect them to fire with a high synchrony. On the other hand, the characteristic path length is too large, so we expect long response times.

- *Uncorrelated network activity and short response time for random networks.* In networks with very small characteristic path length, neural activity can rapidly propagate through the whole network, and so we expect short response times for random networks. However, the absence of clustering lead us to believe that network activity will show no correlations.

The case of small-world networks is a special one. In a small-world graph some properties of random and regular graphs coexist. Simultaneously having high C and low L may allow a fast network response and the presence of correlated activity. As pointed out before these properties are both desirable in any biological system.

In order to test these hypothesis, I have simulated a variety of neural networks with different topologies. I used the HH model of section 3.2.1 for the network vertices, with synaptic interactions as described in section 3.2.3. The results of all the simulations are shown in the following sections.

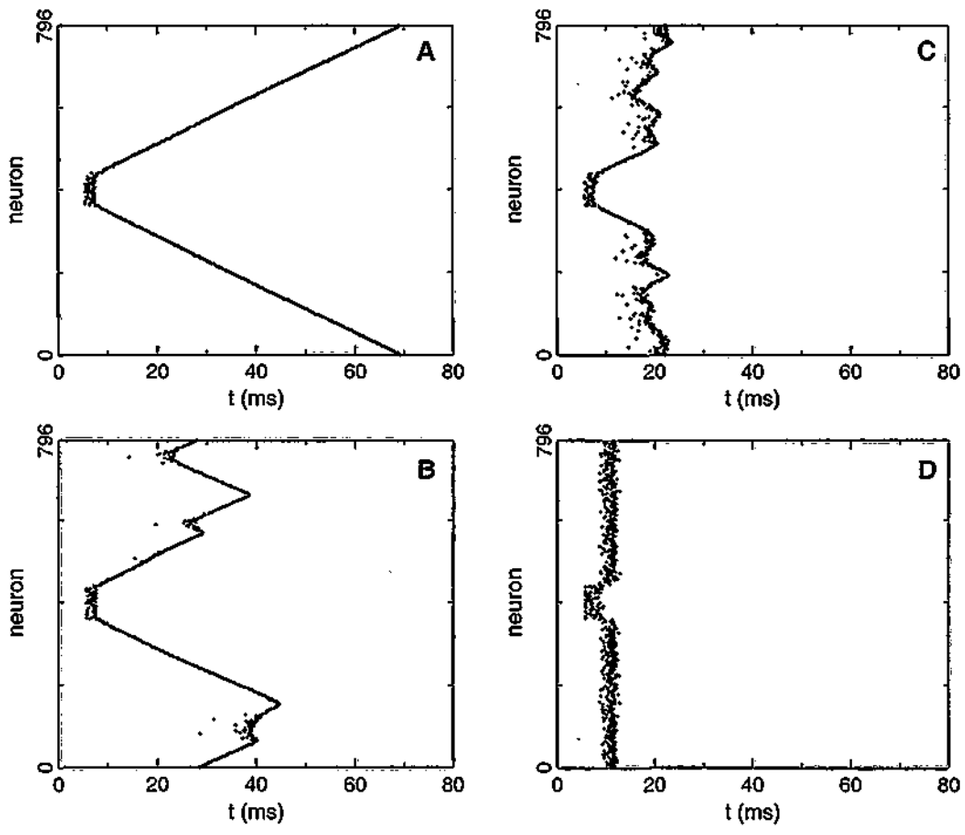

Figure 3.6: First spike of every neuron in a network of HH units with parameters $n = 797$ and $k = 30$, for different rewiring probabilities. A. $p = 0.000$, $L = 12.36$. B. $p = 0.001$, $L = 6.78$. C. $p = 0.032$, $L = 3.10$. D. $p = 1.000$, $L = 2.26$. The input stimulus consisted of a current pulse of amplitude $I_{ext} = 1.5\mu A/cm^2$, injected at $t = 0ms$ to a subset of 80 contiguous neurons.

3.4.1 Low characteristic path length produces a fast response

Here I will study the relation between the characteristic path length, L, of a neural network and its response time, T_r, upon presentation of a stimulus, which I define as the time the stimulus signal needs to reach the whole network. To be more precise, I will define T_r as the time interval between the stimulus onset and the instant when all the neurons have fired at least once. Assuming that the synaptic transmission between two neighbor neurons takes a constant finite time, then the expected relation between T_r and L is linear:

$$T_r = \alpha L \tag{3.40}$$

In order to test this relation I performed a series of simulations using the HH model in networks with $n = 797$, $k = 30$ and different topologies ranging between regularity and randomness. The initial state for the network neurons is selected at random in the vicinity of the equilibrium point. The input stimulus consisted of a current pulse of amplitude $I_{ext} = 1.5\mu A/cm^2$, injected at $t = 0ms$ to a subset of 80 contiguous[5] neurons. In figure 3.6 I have plotted the first spike of all the neurons in the network for different values of the rewiring probability p. In the regular network (A, $p = 0.000$) the signal takes a long time to reach the whole network because it has to travel along regular connections. As soon as p increases (B, $p = 0.001$ and C, $p = 0.032$), short paths appear, which allow a faster propagation of the signal. Finally, for the random network case (D, $p = 1.000$), the signal rapidly reaches the whole network.

If we plot the network response time, T_r, versus the rewiring probability, p, we get the results of figure 3.7A. For clarity of comparison with the normalized characteristic path length, $L(p)/L(0)$, also plotted in the figure, the values of $T_r(p)$ have been normalized by $T_r(0)$. Both measures show the same behavior with p, which indicates the expected linear relation between T_r and L. This is better observed in figure 3.7B, where I have represented T_r versus L. The points are well fitted by a straight line

[5]Contiguous in a physical sense, not a topological one. This means that two neurons are contiguous if they are located one next to the other in the ring; however they may not be neighbors in the sense of section 3.3.

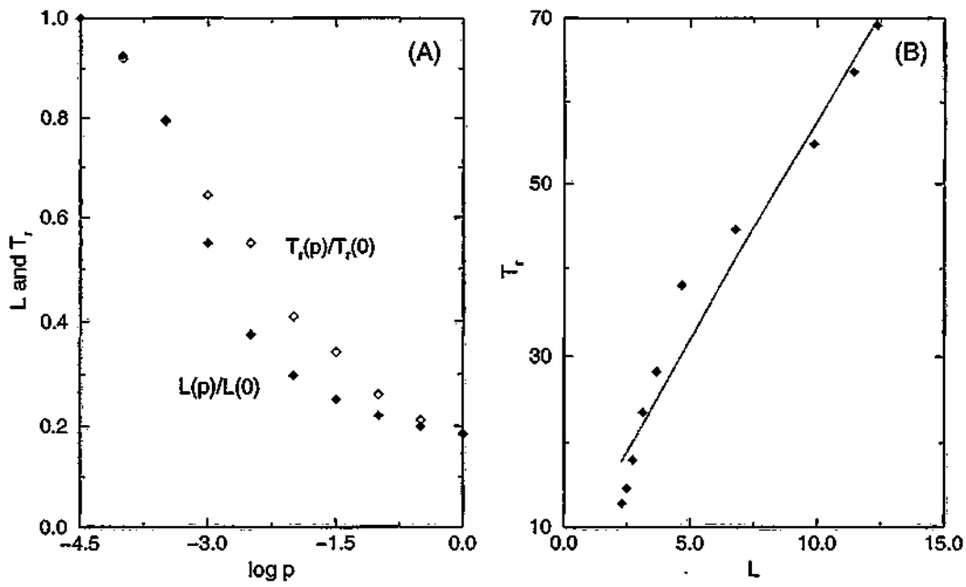

Figure 3.7: A. Normalized characteristic path length, L, and response time, T_r, versus rewiring probability, p, for a network of 797 HH neurons and $k = 30$. The normalization values are those for the regular network ($p = 0$): $L(0) = 12.36$ and $T_r(0) = 119.13ms$. B. T_r versus L for the same network showing the expected linear relation. The points have been fitted using linear regression, giving a slope $\alpha = 5.16$.

with slope $\alpha = 5.16$ (with a correlation coefficient $\rho = 0.97$).

Finally, if we study the behavior of T_r with L for regular networks of increasing size we obtain similar results. We have performed simulations in networks of HH neurons with $k = 30$ and n ranging between 600 and 1500. The results are shown in figure 3.8. Part A shows the dependence of L and T_r with n, which is linear in accordance to equations 3.36 and 3.40. In part B we plot T_r versus L and the linear regression fitting to the points, which gives a slope $\alpha = 5.01$, in clear accordance with the previous results. The correlation coefficient is $\rho = 0.99$.

3.4.2 High clustering produces coherent activity

Let us turn now to the study of the clustering coefficient C and its effect on the correlations in the network activity. Intuitively we expect a higher correlation between two

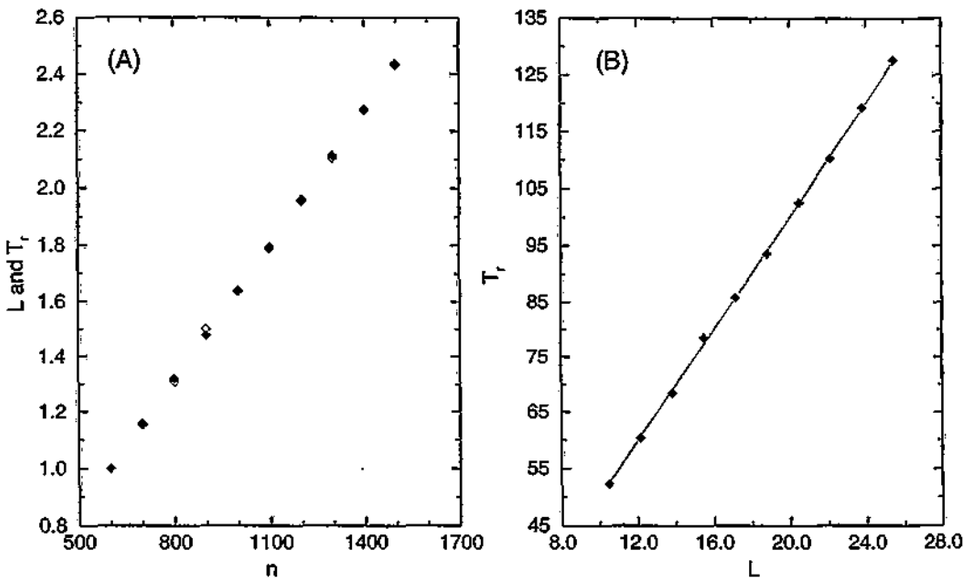

Figure 3.8: A. Normalized characteristic path length ($L(n)/L(600)$, filled diamonds) and response time ($T_r(n)/T_r(600)$, open diamonds) versus network size for regular networks with $k = 30$. The normalization values are those for $n = 600$: $L(600) = 10.47$ and $T_r(600) = 52.33ms$. B. T_r versus L. The points have been fitted using linear regression, giving a slope $m = 5.01$.

neighbor neurons for highly clustered networks, because they have a higher number of common afferents. In other words, a high clustering implies a high overlapping between the receptive fields of neighbor neurons. So neighbors are receiving a very similar input and its activity should reflect this fact showing a high correlation.

To see how different topologies influence the level of correlation in the network response, I show in figure 3.9 the spike diagrams for four networks of HH neurons with $n = 797$ and $k = 30$, but different rewiring probabilities. In all cases the network was stimulated with a constant current pulse that was injected to a subset of 80 contiguous neurons, as in section 3.4.1. I waited until the network response was stable and then took the time windows that are shown in the figure. Although a detailed analysis of the correlations is left for next section, we can observe that in high clustering cases (A, B and C) the network shows highly correlated activity; all the neurons tend to fire at almost the same time. However in the random network case (D), with very

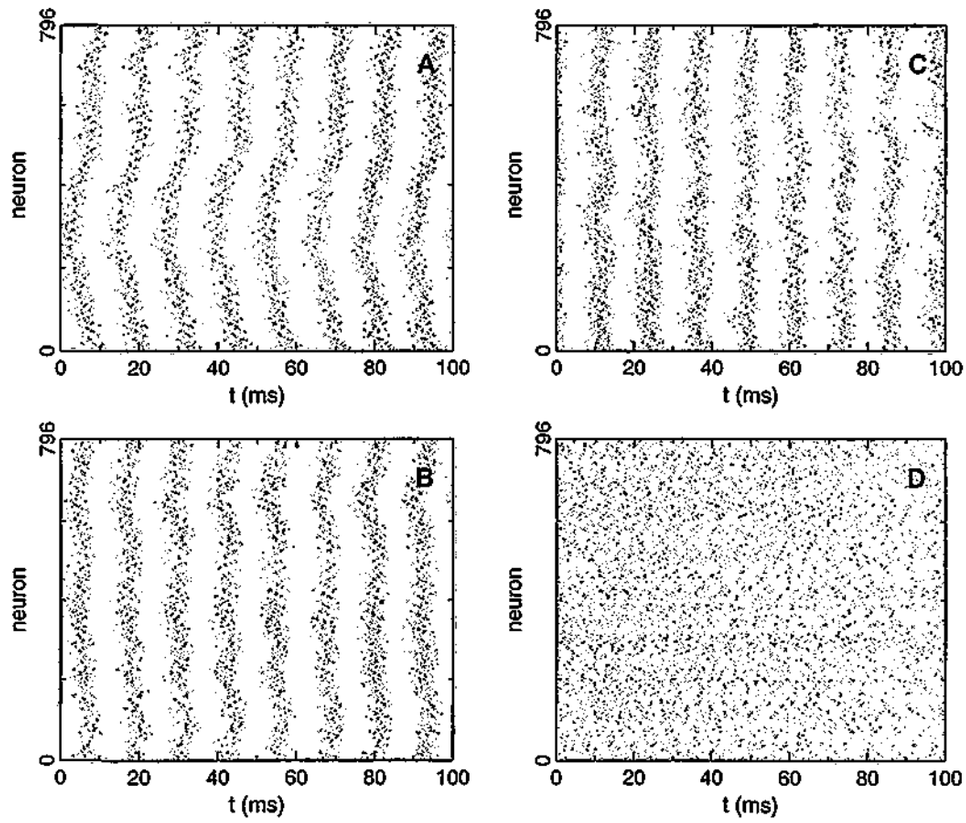

Figure 3.9: Spike rasters for different values of the rewiring probability p in a network of HH neurons with $n = 797$ and $k = 30$. A. $p = 0.000$, $C = 0.74$. B. $p = 0.001$, $C = 0.74$. C. $p = 0.032$, $C = 0.68$. D. $p = 1.000$, $C = 0.07$. A clear dependence of the correlation properties of the network activity on the clustering level is observed. We have coherent activity for highly clustered networks (A, B, C), and incoherent activity for low clustering (D).

small clustering, the spikes are very uncorrelated and the number of spikes is almost constant for all times. To make the results clearer, we show in figure 3.10 the total number of spikes versus the simulation time for the same four cases.

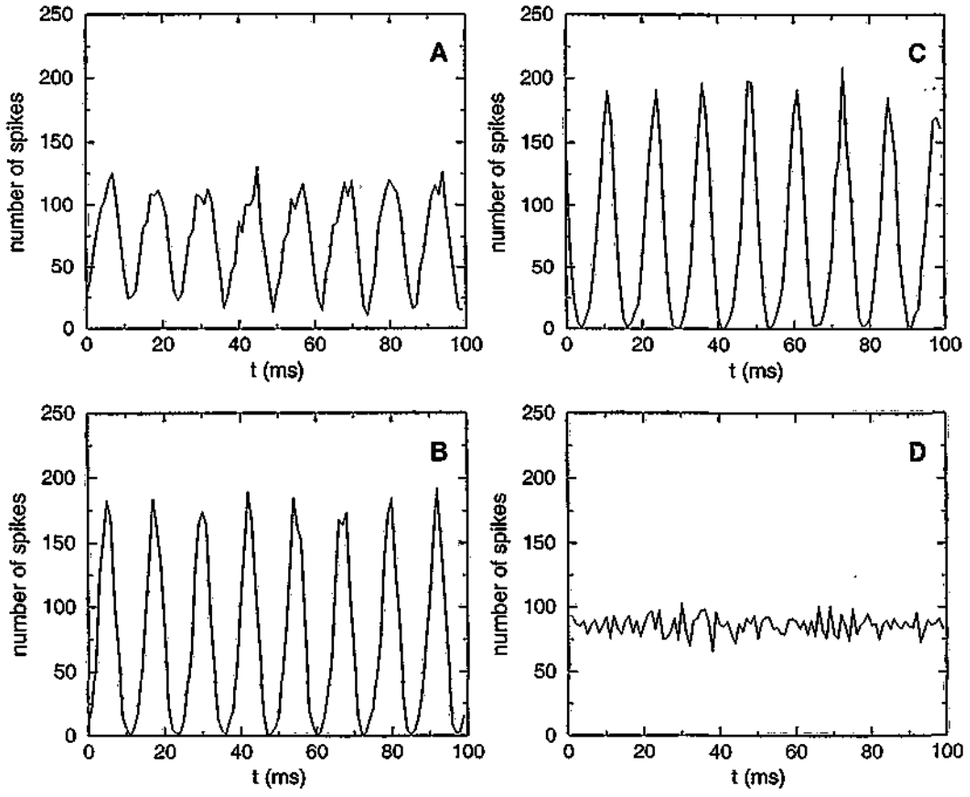

Figure 3.10: Number of spikes versus simulation time for networks of HH neurons with $n = 797$ and $k = 30$. A. $p = 0.000$, $C = 0.74$. B. $p = 0.001$, $C = 0.74$. C. $p = 0.032$, $C = 0.68$. D. $p = 1.000$, $C = 0.07$. A clear dependence of the correlation properties of the network activity on the clustering level is observed. We have coherent activity for highly clustered networks (A, B, C), and incoherent activity for low clustering (D).

3.4.3 Optimal topologies

Up to this point I have investigated the behavior of the neural network response time and its ability to show correlated activity in terms of the characteristic path length and the clustering coefficient of the graph that describes the network. The results that I have obtained can be summarized as follows:

- The behavior of T_r with p closely resembles that of L. Even for very small

rewiring probabilities, the presence of a few short paths allows a very fast propagation of the input signal to the whole network. Only regular topologies ($p \approx 0$) present high response times.

- The correlations in the network activity depend on the clustering coefficient. I have shown that in highly clustered networks all the neurons tend to synchronize their spikes, while when the clustering is low (almost random topologies) no correlations are observed.

Now I want to extend these results, first by introducing some measure of the correlation degree, then by establishing the range of optimal topologies that allow the rapid onset of synchronous network activity after the presentation of a stimulus. As a source of inspiration, let us put the study in a biological context by comparing the neural network with the antennal lobe of insects. The antennal lobe is a group of around 800 neurons in the insect olfactory system, whose functional role is to relay information from the olfactory receptors to higher areas of the brain for further processing. The experiments, carried on mainly with locusts [70, 82, 81], reveal two main features in the antennal lobe dynamics after an odor is presented to the insect:

- First, the response of the antennal lobe is very fast; neurons become active within a few milliseconds after the stimulus presentation.

- Second, coherent oscillations of around $20Hz$ in the local field potential are measured. Without these coherent oscillations the insect seems to lose its ability to process the information incoming from the sensors.

Summarizing, there is a very fast onset of coherent oscillations in the antennal lobe after the presentation of a stimulus to the olfactory receptors. The question that arises is whether it is possible in our neural network model to have this kind of response. In other words, is there any network topology that allows a fast response together with coherent oscillations in the network activity? To answer to this question we must unavoidably look at the small-world topologies introduced in section 3.3.3. Recalling the properties of small-world graphs (high clustering coefficient and low characteristic

path length), we expect that neural networks with a small-world topology present the desired kind of response.

To study the global dynamical properties of the network I will compute its average activity $V(t)$, which is the average of the membrane potential over all the network neurons:

$$V(t) = \frac{1}{n}\sum_{i=1}^{n} V_i(t) \tag{3.41}$$

This quantity is usually related to the local field potential measured in experiments. In figure 3.11 I have plotted the average activity for three typical cases, a regular network (A, $p = 0.000$), a network in the small-world range (B, $p = 0.032$), and a random network (C, $p = 1.000$). There are two remarkable facts to be extracted from the figure. First, the long response time in case A in comparison with the other cases (note that the stimulus onset is at $t = 50ms$). Second, the presence of coherent oscillations in cases A and B. These two facts lead us to reinforce our previous conclusions on the influence of L and C on T_r and the correlation degree respectively.

The network in the small-world regime (figure 3.11B) seems to be the only one that combines a fast response with the presence of coherent oscillations. Even more, comparing cases A and B, we observe that the small-world network not only presents a much faster onset of the oscillations, but also more coherence. It seems that the fast signal propagation of the small-world cases not only produces a faster network response, but also favors a faster organization of the network activity in the form of coherent oscillations. In random networks, in spite of the low L, we observe no coherent oscillations due to the small clustering.

We need to quantify the quality of the oscillations in order to be able to compare the different topology regimes. To do so I will introduce two different measures, the *average activity oscillation amplitude* and the *degree of coherence.*

Average activity oscillation amplitude:

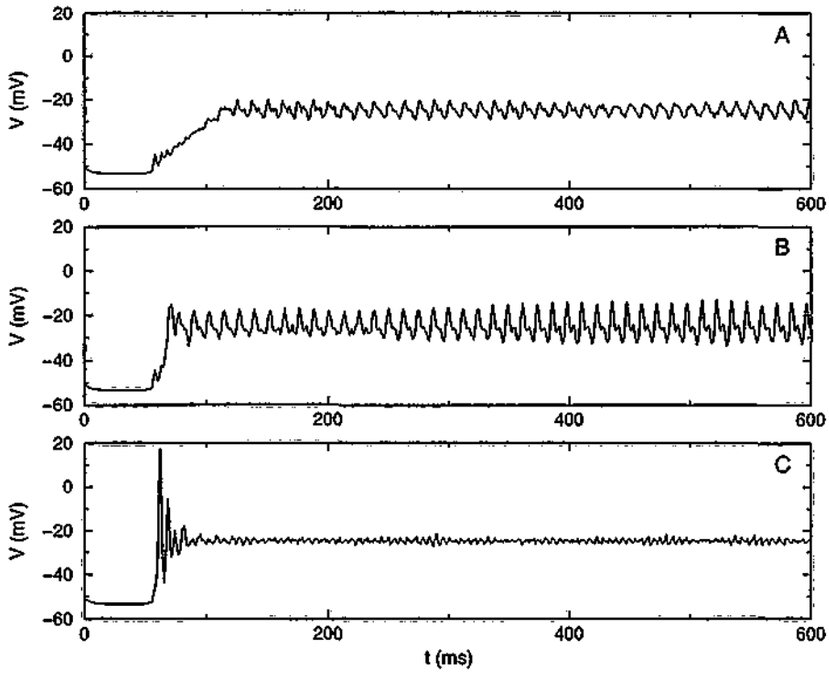

Figure 3.11: Average activity, $V(t)$, in networks of HH neurons with $n = 797$, $k = 30$ and different rewiring probabilities. A. $p = 0.000$, $L = 13.57$, $C = 0.47$, regular network. B. $p = 0.032$, $L = 3.09$, $C = 0.68$, this network falls into the small-world range. C. $p = 1.000$, $L = 2.26$, $C = 0.07$, random network. Stimulus onset at $t = 50ms$.

If we assume oscillatory behavior for the average activity, $V(t)$, we can use the deviation of $V(t)$ with respect to its temporal average as a measure of the oscillations amplitude. For each of the network topologies characterized by a rewiring probability p, I will evaluate the quantity [51]:

$$\sigma^2(p) = \frac{1}{T_2 - T_1} \int_{T_1}^{T_2} [\langle V_p(t) \rangle - V_p(t)]^2 dt \tag{3.42}$$

where the subindex p refers to the rewiring probability and the angle brackets denote temporal average over the integration interval, that is:

$$\langle V_p(t) \rangle = \frac{1}{T_2 - T_1} \int_{T_1}^{T_2} V_p(t) dt \tag{3.43}$$

The integration interval is taken once the oscillations have been established; for the present calculations we have used $T_1 = 500ms$ and $T_2 = 600ms$. In figure 3.12 I show the results. Observe that the highest values of $\sigma(p)$ are for probabilities lying in the small-world range.

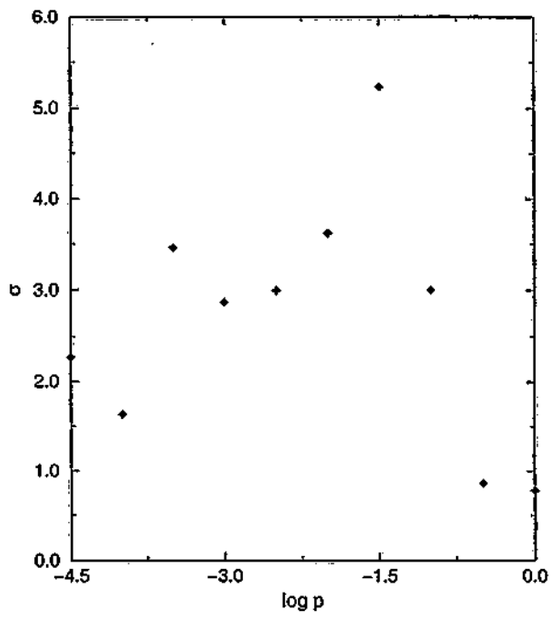

Figure 3.12: Average activity oscillation amplitude, $\sigma(p)$, versus the rewiring probability in a network of $n = 797$ HH neurons with connectivity $k = 30$.

Degree of coherence:

A more robust measure for the oscillations quality is the degree of coherence. It is related to the Fourier transform of the average activity, which gives us its frequency decomposition. I have evaluated the Fourier transforms of each of the time series in figure 3.11, obtaining the results of figure 3.13. Now the quality of the oscillations results more evident in the regular and small-world cases (A and B). They both present a dominant frequency of around $80Hz$. In the random case (C), however, we can not deduce any oscillatory behavior from the observation of the power spectrum.

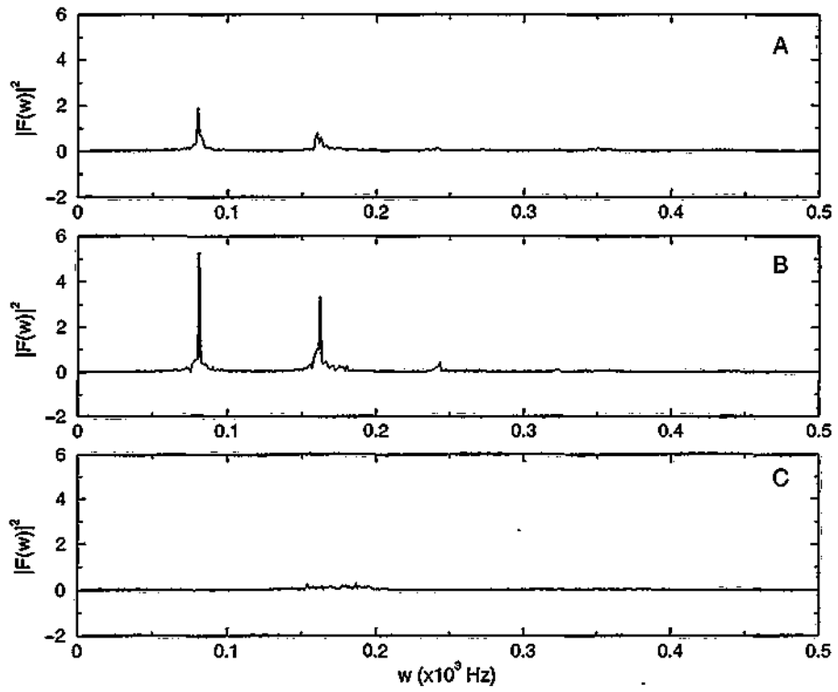

Figure 3.13: Power spectra for the time series of figure 3.11. A. $p = 0.000$, $L = 13.57$, $C = 0.47$. B. $p = 0.032$, $L = 3.09$, $C = 0.68$. C. $p = 1.000$, $L = 2.26$, $C = 0.07$.

I have used the first peak in the power spectra of the average activity to compute the degree of coherence [36], $\beta(p)$, which is defined as follows:

$$\beta = H\frac{\omega}{\Delta\omega} \tag{3.44}$$

where H is the height of the peak, ω is the frequency at which it appears and $\Delta\omega$ is its width at half maximum height. The degree of coherence is a good measure of oscillatory behavior, and I will use it to characterize the network response as a function of p. As done for $\sigma(p)$, I have computed the value of β for different values of p, obtaining the results of figure 3.14. These results are in accordance with previous ones for $\sigma(p)$, and show that the oscillation coherence increases in the small-world region. As pointed out before, the reason for this fact is not only the high clustering, that is present in the regular networks as well, but also the small characteristic path

length, which permits a rapid organization of the network response.

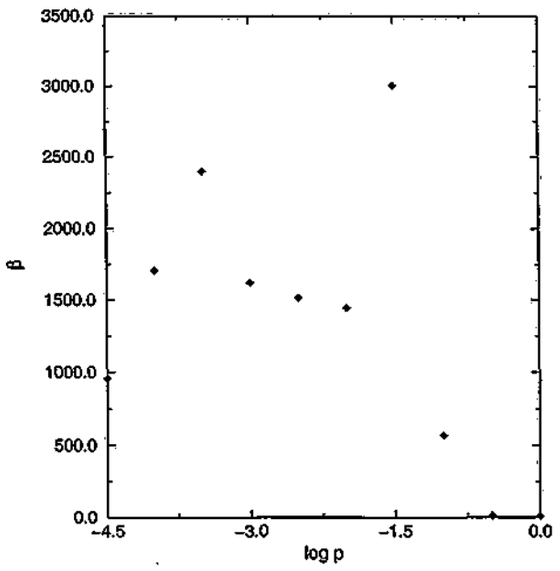

Figure 3.14: Degree of coherence, β, versus rewiring probability, p, for networks of HH neurons with parameters $n = 797$ and $k = 30$.

3.4.4 Partial conclusions

In the simulations performed in the previous section, we observed the following behaviors:

- Only highly clustered networks are able to generate a synchronized response to input stimuli. These are the regular and small-world networks ($p \leq 0.032$).
- It takes much longer time to synchronize in regular networks than in small-world networks. In the former case the localized input needs to propagate through regular connections, yet the small-world topology overcomes this problem thanks to the existence of a few long range connections.
- In the random case, the low clustering implies an absence of coherent oscillations because the input to any neuron comes from all over the network and is highly

uncorrelated. The response time is small due to the low characteristic path length.

To have a fast network response we need low L, which is impossible in a regular network. To have coherent oscillations we need high C, and this is impossible in a random network with small connectivity. This is what makes the small-world interesting, as the only topology that allows a fast network activation in the form of coherent oscillations (Figure 3.15 summarizes the results).

I will finish this section with a more extensive study in which I vary both the connectivity, k, and the rewiring probability, p, in order to establish the limits for the appearance of coherent oscillations. The study shows that previous results can be generalized within a certain range of parameters. I computed the average activity oscillation amplitude, σ for a total of 180 points in the (k, p) plane. An interpolation of these results is plotted in figure 3.16, where the clear zones indicate high values of σ. We can conclude from this figure that fast coherent oscillations appear only in the region of intermediate probabilities, the small-world, for different values of k. The a priori limits on k are based on the fact that for k lower than ~ 10 and the actual parameters of the simulations, the activation of the network is very weak; on the other hand for k higher than ~ 35 some neurons become saturated.

In conclusion, regular networks produce coherent oscillations and long response times; whereas random networks give rise to fast response but without coherent oscillations. We have observed that SW networks show both coherent oscillations, necessary for temporal coding, and fast reaction times. The dynamical system introduced in the vertices of the network is the Hodgkin-Huxley model that presents a saddle-node bifurcation to the limit cycle (class 1 excitability). Another research direction could analyze a different dynamical system, with a different bifurcation, such as the Hopf, in the network vertices. It remains to be seen if these results can be extrapolated to other dynamical systems with different bifurcations, and it will be explored in the next section.

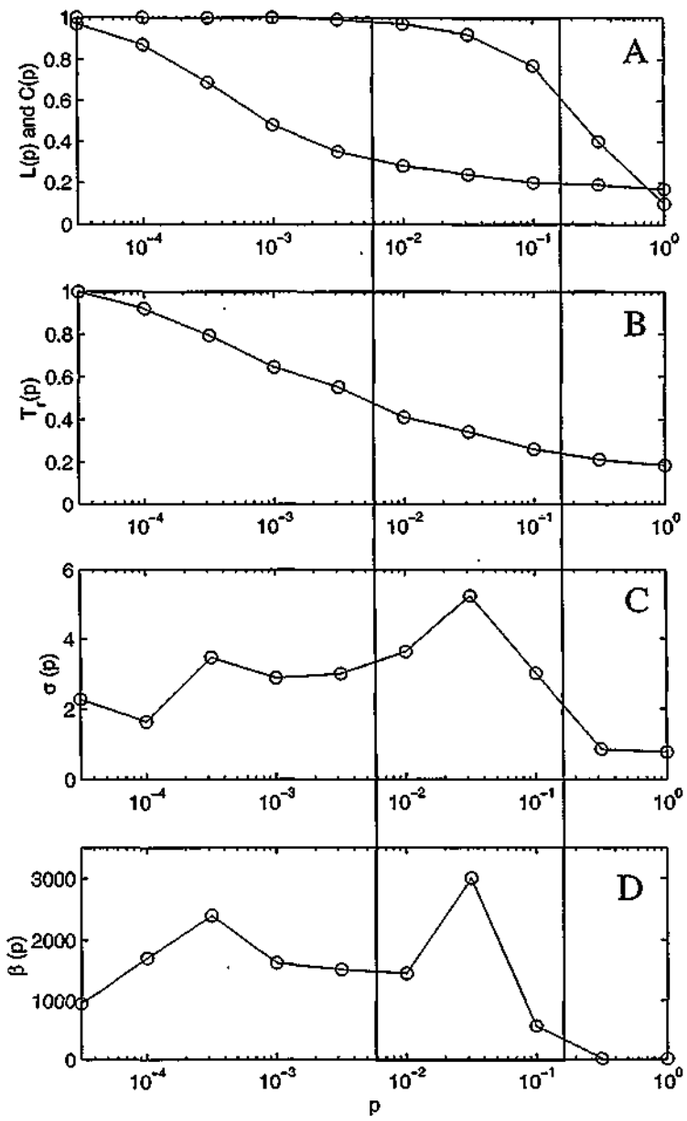

Figure 3.15: Different properties of the network versus rewiring probability. A. Characteristic path length and clustering coefficient. B. Response time. C. Average activity oscillation amplitude. D. Degree of coherence. The small-world (high C and low L) has been marked, and shows a coexistence of low response times with oscillatory activity.

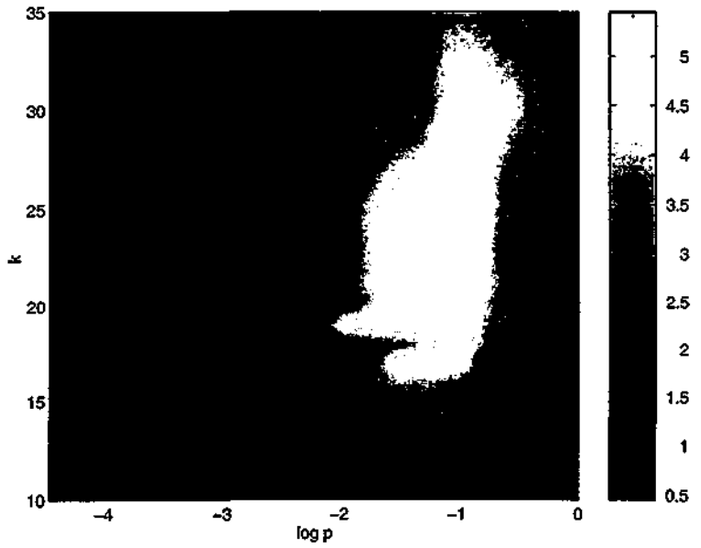

Figure 3.16: Average activity oscillation amplitude, σ, versus connectivity, k, and rewiring probability, p, in networks of HH neurons. Network size is $n = 797$.

3.5 Dependence on the neuron model and coupling strength

The results of previous section could be highly dependent on the specific neuron model we used, the Hodgkin-Huxley model, which presents a saddle-node bifurcation to the limit cycle. If we used a different dynamical system in the network vertices, the network behavior could qualitatively change. We also expect the results to be dependent on synaptic parameters, such as the coupling strength. In this section I extend the previous work and analyze the behavior of the two main classes of excitable neurons, the Hodgkin classes 1 and 2 [49], in terms of the connection topology and the coupling strength. We have seen that class 1 excitability shows a strong dependence of the signal propagation speed and the synchronization properties on the connection topology. In addition no spiking frequency dependence on the network topology is observed. Now we will see that class 2 excitability presents a fast wave-like propagation of the activity, a strong frequency dependence on the connection topology and a good level of synchronization regardless of the topology. In this comparative study I

consider the HH and FN models previously described, as representative of class 1 and 2 excitability respectively. I intend to determine the differences in synchronization and response speed for both models and different network topologies.

The general structure of the networks and the mechanism for changing topologies are essentially the same as in previous sections. For both neuron models, we will deal with networks with $n = 797$ neurons and connectivity $k = 30$, with different topologies which depend on a rewiring probability p. As before, we will quantify the structural properties of the graph describing the network architecture by using the characteristic path length, L, and the clustering coefficient, C. The details of the models and the numerical integration were fully described in section 3.2. However, in the current approach two main differences must be remarked with respect to section 3.4. Firstly, concerning synaptic transmission, the transmitter concentration has been explicitly modeled with equations (3.15) and (3.16). Secondly, the measure of synchronization is slightly different from those of section 3.4.3. Here, based on the fact that the LFP registered in extracellular recordings is a local measure of the network activity, I consider just local correlations between neighbor neurons. In the present analysis I have also included a study of the network responses for different connection strengths.

3.5.1 Class 1 excitability. Hodgkin-Huxley model

The HH model used in this section is described by equations (3.1-3.4), with the parameters given in section 3.2.1. As seen before, the model undergoes a saddle node bifurcation to a limit cycle, which means that it is possible to have oscillations at arbitrarily low frequencies (see figure 3.1). I have simulated neural networks of HH neurons with $n = 797$ and $k = 30$, with the synaptic dynamics described in section 3.2.3 and a maximum synaptic conductance (coupling strength) that varied between 0.01 and $0.10 mS/cm^2$. The network topology was determined by a rewiring probability p, which was varied logarithmically between 0 and 1.

In all the simulations performed, the neurons started in a random state very close to their equilibrium point, and a constant current pulse of amplitude $I = 0.7 \mu A/cm^2$ was injected to a subset of 30 contiguous *input neurons*.

In the following sections I will show the results of the simulations, which have been divided into three different ranges of synaptic conductance for clarity of analysis. I have observed that for *low* conductances (approx. $0.02mS/cm^2$) there is a poor activation of the network, and usually the activity is not able to reach all the neurons. For *medium* conductances (approx. $0.05mS/cm^2$) the input activity reaches all the neurons in the network, and we observe network properties, namely the response time and the local coupling, that resemble the behavior of $L(p)$ and $C(p)$ respectively. The network response time to the stimulus quickly decreases with increasing p, while the local coupling keeps almost constant at a high value through both the regular and small-world topology regimes, and it decays very sharply as soon as the rewiring probability reaches values near 1 (random topology). This particular result corroborates that of section 3.4. Finally, for higher conductances we observe saturation in the network, which is more explicit in the high clustering cases (regular and small-world).

Low conductance, $g \sim 0.02mS/cm^2$

When the synaptic conductance is of the order of $0.02mS/cm^2$, we observe that, in the regular and the small-world topologies, a propagating wave is initiated at the input neurons, and travels along the ring (figure 3.17, upper panels). However, in the random topology, only input neurons show spiking activity (figure 3.17, bottom panel), since at very low synaptic conductances single connections are not able to elicit a postsynaptic response. Due to the localized input, long range connections are not sufficient by themselves to activate post-synaptic neurons because of the low conductance, and so the effect of rewiring connections is somehow equivalent to reducing the number of synaptic inputs to single neurons.

There are not important differences between regular and small-world connection topologies, because network response mainly depends on the clustering properties, which are essentially the same for both regimes. However we observe a very abrupt change when the networks approach a random topology. In these cases the absence of clustering makes the signal transmission impossible, and so only the input neurons show spiking activity.

Summarizing, the results show that network response is completely determined

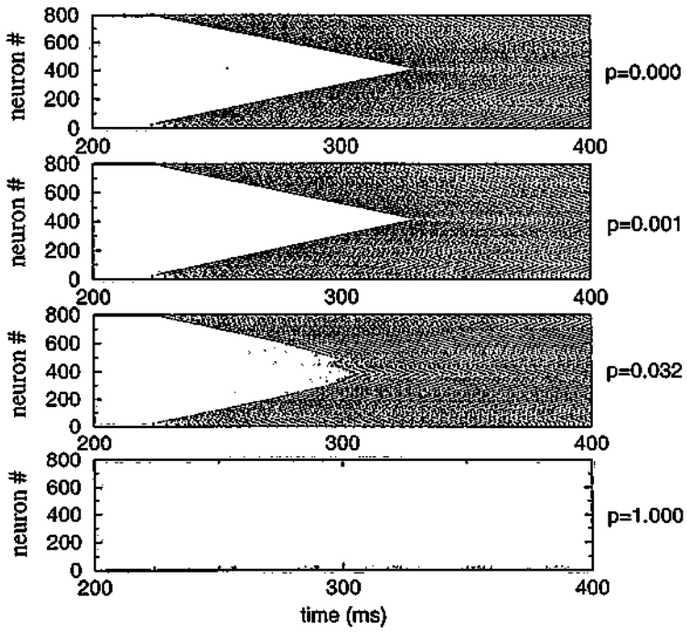

Figure 3.17: Spike rasters for the HH model and different network topologies ranging from regularity to randomness. Synaptic conductance $g = 0.02mS/cm^2$.

by the clustering coefficient, $C(p)$, and does not depend on the characteristic path length, $L(p)$. The activation of the network seems to occur only at high clustering levels; and the response time depends only slightly on L, as the network activity is mainly propagated through regular connections.

Medium conductance, $g \sim 0.05mS/cm^2$

For medium synaptic conductances, of the order of $0.05mS/cm^2$, the behavior qualitatively changes (see figure 3.18). Now long range connections acquire importance, as they are able to transmit the activity through short paths, giving rise to a decrease in the network response time. The input activity can reach the whole network regardless of the topology, and we observe that network response properties depend both on the characteristic path length and the clustering coefficient, which makes the small-world regime advantageous over the regular and random ones. Due to the

propagation of activity through long range connections, the network response time reflects the behavior of $L(p)$. On the other hand, local correlations highly depend on $C(p)$. This result confirms that from section 3.4.

In figure 3.18 I show the results of the simulations. Observe that, for regular topologies, the network response presents a very high correlation between neighbor neurons; however the response time is too long. For small-world topologies the local correlation is maintained, but the response time decreases as $L(p)$ does. Finally, for random topologies, we have a very fast response, but the local correlation is completely lost.

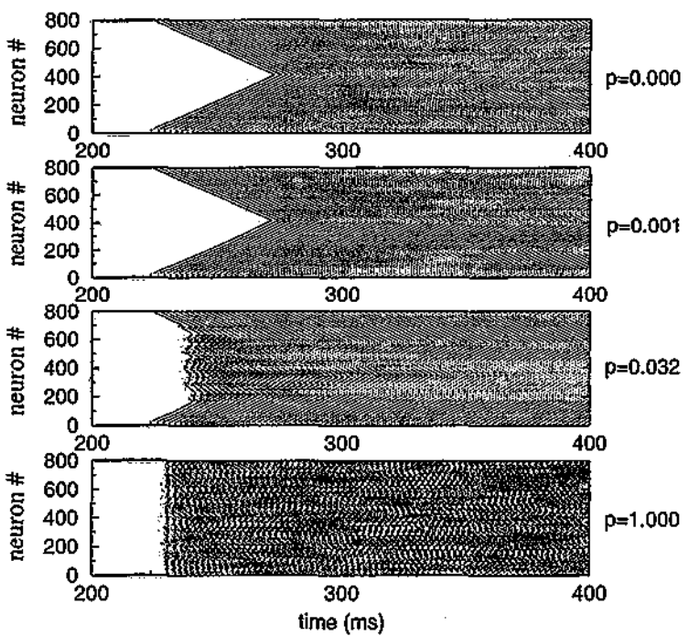

Figure 3.18: Spike rasters for the HH model and different network topologies ranging from regularity to randomness. Synaptic conductance $g = 0.05mS/cm^2$.

Fast response and synchronization are best achieved in a neural network with small-world topology, which makes the small-world the most likely choice to achieve both responsiveness and synchronizability using class 1 excitability.

For higher values of the synaptic conductance, from $0.06mS/cm^2$ on, I have observed that some neurons in the network are overexcited. This is the reason why I do not perform any analysis under the high conductance regime.

Response time and local correlation

To classify the topologies that are relevant for the present study, I use two different measures, the response time and the local correlation. The response time of the network, T_r, measures the time it needs to react upon the presentation of an external stimulus. It is defined in the same fashion as in section 3.4.1, as the time interval between the stimulus onset and the instant when all the neurons have fired at least once. This quantity decreases with the rewiring probability, p, as a result of the appearance of long range connections, that allow faster transmission of neural signals. In figure 3.19 I show (open circles) the evolution of T_r with p for the two considered conductances, $g = 0.02mS/cm^2$ and $g = 0.05mS/cm^2$. The values of T_r have been normalized for a more straightforward comparison with the local correlation.

To estimate the local correlation in the network I have calculated spike correlograms between pairs of neighbor neurons, and averaged over all neighbor pairs. The correlograms for $g = 0.05mS/cm^2$ and different values of p are shown in figure 3.20. We observe high local correlation along the regular and the small-world topologies, that disappears as we approach the random topologies. To obtain a quantity that measures the quality of the local correlation for each probability, I have fitted a Gaussian to the central peaks of the correlograms and evaluated the quantity[6] [36]:

$$b = H/\sigma \tag{3.45}$$

where H is the amplitude and σ the standard deviation of the fitted Gaussian. A normalization of $b(p)$ is also shown in figure 3.19 (filled circles), together with $T_r(p)$. We can observe that, regardless of the synaptic conductance, $b(p)$ is almost constant

[6]This is in fact the same measure as in equation (3.44). Here the standard deviation is not related to the average because all the correlograms are centered around 0.

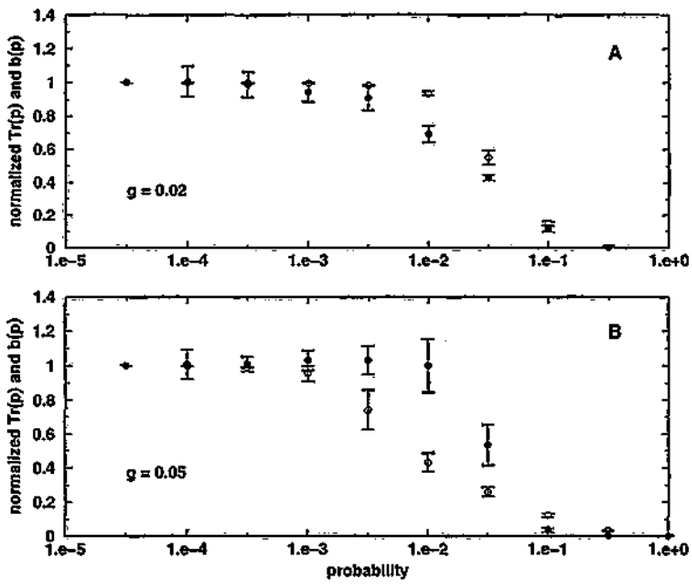

Figure 3.19: Response time $T_r(p)$ (open circles) and local correlation $b(p)$ (filled circles) as a function of the rewiring probability p for the Hodgkin-Huxley network and two different synaptic conductances: A. $g = 0.02mS/cm^2$, B. $g = 0.05mS/cm^2$. Note the absence of points for $p = 1$ in figure A; the lack of global activity in the random network does not allow to calculate the quantities $T_r(p)$ and $b(p)$.

for the regular and small-world topologies, and it decreases as we reach high probabilities. The response time, however, starts to decrease at lower probabilities when the synaptic conductance is higher, because the long range connections are more effective. This fact makes possible the appearance of a range of probabilities where the network response time decreases yet the local correlation does not vary, which makes the case very favorable for sensory systems where fast response and locally correlated neural activity are needed.

3.5.2 Class 2 excitability. FitzHugh-Nagumo model

In this section I use the FitzHugh-Nagumo model (equations (3.8-3.9)) with the parameters of section 3.2.2. With these parameters the model presents a subcritical Hopf bifurcation when the applied external current exceeds the value $I_{ext} = 0.692\mu A/cm^2$

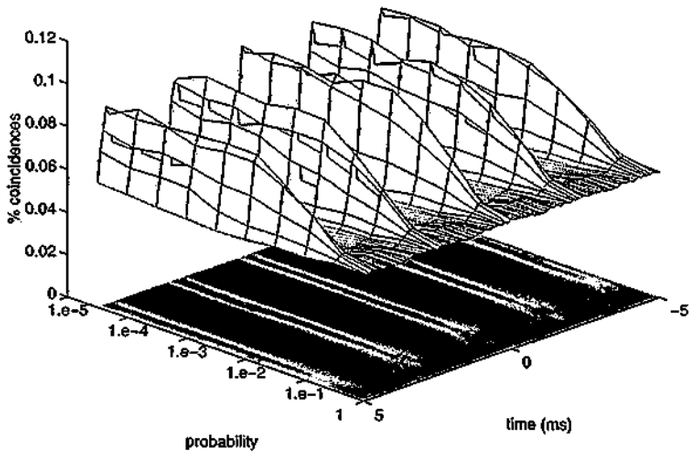

Figure 3.20: Spike cross-correlograms between neighbor neurons, averaged to all pairs of neighbor neurons. $g = 0.05mS/cm^2$.

(see figure 3.1). As I did for the HH model, I will study the behavior of networks of FN neurons for different values of the rewiring probability p. The network parameters are, as before, $n = 797$ and $k = 30$. I have studied different synaptic conductances, varying between 0.001 and $0.010mS/cm^2$. The rewiring procedure and the rest of the settings are as for the HH case (see previous section).

The results for the FN model are quite different from those for the HH model. One of the reasons is that the dynamics of the FN neuron model, with a Hopf bifurcation, make the membrane potential react very quickly to the stimulation by a current pulse. The integration time of a FN neuron is therefore very short, and as a consequence it only responds to highly correlated input for low synaptic conductances. I have also observed a very fast signal propagation to the whole network, with a propagation speed that shows small variation with p.

The dependence of the network response with respect to the synaptic conductance is very strong. So, following the analysis performed for the HH model, I divide the study into three different subsections: *low*, *medium* and *high* synaptic conductances.

Low conductance, $g \sim 0.003 mS/cm^2$

For very low synaptic conductances a neuron that does not receive external input can only be activated if it is simultaneously stimulated by many neurons. In the regular and small-world cases the clustering is very high, so when a group of neurons fire their activity can be propagated to the close neighbors. The activity initiates in the cluster of input neurons and propagates to the whole network like a wave. The long range connections in the small-world networks have very little effect, since one single synaptic contact is not able to activate the postsynaptic neuron.

We observe a quite different behavior in the random topology. Now there is no local clustering, and one neuron receives connections randomly from all over the network, with no correlation between its afferents. A neuron that does not belong to the input cluster will not receive enough connections from the input neurons to become activated, and so we observe that only the input neurons display spiking activity. These results are shown in figure 3.21.

One important aspect to note in the figure is the extremely low spiking frequency for high clustering values in comparison with the normal frequency of single isolated neurons. One would expect that the synaptic coupling gave rise to higher oscillation frequencies, but that seems not to be the case. The reason can be found in the mechanism underlying the Hopf bifurcation that characterizes the FN model. The addition of an external current to an input neuron gives rise to a limit cycle with an unstable focus in the middle. If we start with initial conditions very close to the fixed point, the neuron will be trapped around it for some time before it reaches the limit cycle. Now, if we couple the input neuron to a non-input one, the former will make the latter spike. I have observed that the synaptic effect of the non-input neuron on the input one is to push it toward the fixed point, where it gets trapped for some time before it can fire again. This is the reason why we observe lower frequencies than expected: the neurons that initiate the activity in the network get trapped for some time around their fixed point due to the synaptic excitation they receive from other neurons. During this time no activity is observed in the network.

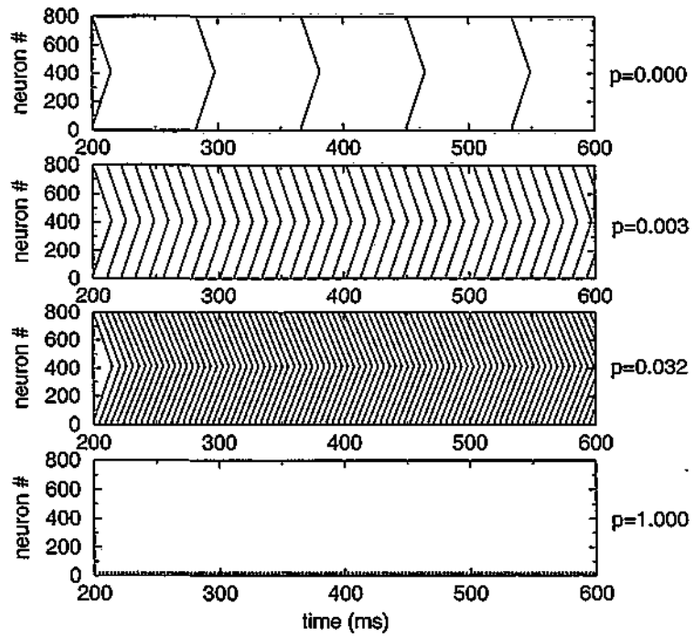

Figure 3.21: Spike rasters for the FN model and different network topologies ranging from regularity to randomness. Synaptic conductance $g = 0.003mS/cm^2$.

Medium conductance, $g \sim 0.006mS/cm^2$

In the case of conductances close to $0.006mS/cm^2$, a non-input neuron may become active by the simultaneous input received from a few neurons. This change in conductance has no effect on the behavior of the regular or small-world networks (see figure 3.22). Long range connections are ineffective unless there exist a few of them connecting a non-input neuron with the input cluster, and the probability for this to occur is very small.

In random topologies, however, the number of rewired connections is very high, and it is not so unlikely that some non-input neurons receive enough connections from the input cluster to become active. So, immediately after the first spikes of the input neurons occur, some non-input neurons also fire. The dynamics of the FN model makes the neurons respond very fast to a excitatory stimulation of their afferents, and when the second group of neurons fire the synaptic inputs from the input neurons

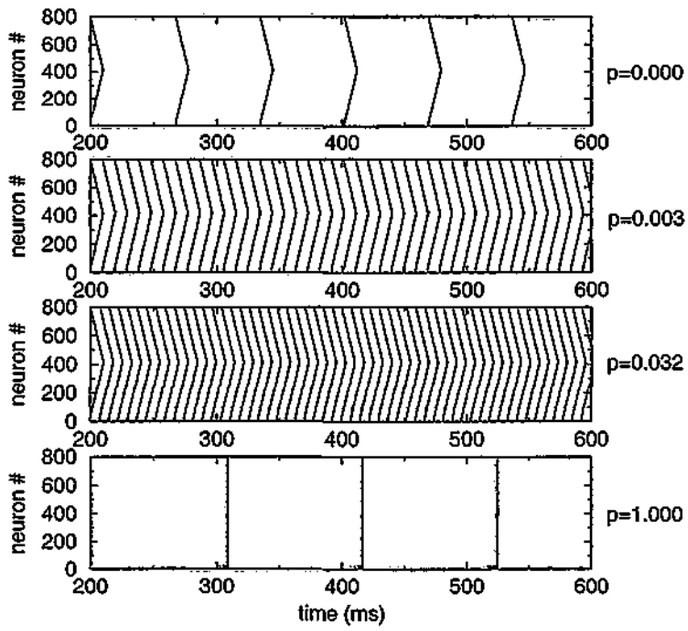

Figure 3.22: Spike rasters for the FN model and different network topologies ranging from regularity to randomness. Synaptic conductance $g = 0.006mS/cm^2$.

are still active. Thus the synaptic currents due to the active input neurons and those secondly activated neurons add up on other neurons that remained inactive. This generates a chain reaction which makes all the neurons fire in a very short time frame. The subsequent synaptic input to the input neurons gives rise to a period of inactivation since they get trapped around the fixed point, as explained before. We end up with a highly synchronized network response at a very low frequency.

High conductance, $g \sim 0.009mS/cm^2$

Finally let us consider the case of very high synaptic conductances. Now the input connection from just one neuron is able to produce a postsynaptic spike. In the regular and small-world cases we have a very high saturation that produces just one spike per neuron in the time window I considered (figure 3.23). The high correlations between the different afferents to a given neuron make it receive almost simultaneous input

from all of them, which together with the high value of the synaptic conductance produces a high inactivation time for the input neurons. This is the reason why we typically observe just the first spike of each neuron. We also observe that there is a decrease of the network response time as we approach the small-world region (see figure insets), due to the effect of long range connections, which are now fully effective.

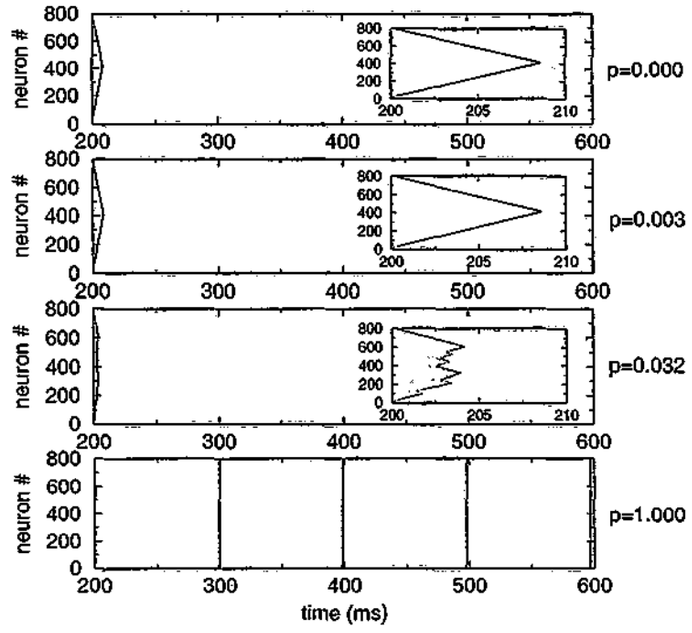

Figure 3.23: Spike rasters for the FN model and different network topologies ranging from regularity to randomness. Synaptic conductance $g = 0.009 mS/cm^2$.

In the random network the situation does not vary much from the previous one for medium conductances. Random connections produce an absence of correlations and the average input to a neuron is much lower than in the regular and small-world cases.

Response time and local correlation

In figure 3.24 I show the normalized response time, $T_r(p)$ (open circles), and the local correlation, $b(p)$ (filled circles), for the different connection topologies and synaptic

conductances. For small and medium conductances (A, B), we see that $T_r(p)$ keeps almost constant until we reach very high probabilities. The reason is, as previously indicated, that single long range connections are not able to transmit any signal. The neural activity propagates through regular connections and, therefore, the network response time is given by that corresponding to $p = 0$. We even observe a small increase in the network response time with p, which I associate to the negative effect of the rewiring process on the normal propagation of network activity. As we approach random topologies we observe infinite response times for the low conductance network (some neurons do not activate), and an abrupt decrease for the medium conductance network. In the last case long range connections have started to carry information.

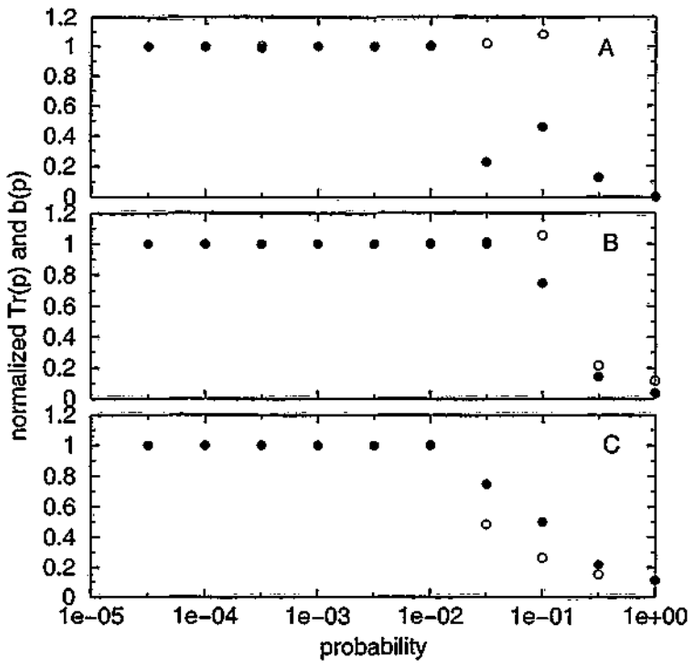

Figure 3.24: Response time $T_r(p)$ (open circles) and local correlation $b(p)$ (filled circles) as a function of the rewiring probability p for the FitzHugh-Nagumo network. A. $g = 0.003 mS/cm^2$, B. $g = 0.006 mS/cm^2$. C. $g = 0.009 mS/cm^2$. The absence of global activity in the network does not allow to calculate the response time $T_r(p)$ for the two highest probabilities in figure A.

The results for high synaptic conductance (C) are very similar to those for medium

one, but now the response time starts decreasing at lower probabilities. The higher value of g allows propagation through short paths for a smaller density of long range connections.

Let us now turn to the behavior of $b(p)$. In figure 3.24 we can observe that it does not vary significantly with the synaptic conductance. The network activity is locally highly correlated for high clustered topologies, and partially loses this correlation for random topologies, where the clustering also decreases. The behavior of $b(p)$ appears to closely resemble that of the clustering coefficient $C(p)$.

3.5.3 Partial conclusions

I have analyzed the dynamics of neural networks in terms of the topology and the class of excitability that underlies the network vertices. The results of the analyses can be summarized as follows. For the HH model we observe that:

- The signal propagation speed is strongly dependent on the connection topology.
- There is a weak frequency adaptation: spiking frequency is almost independent of the network topology.
- Synchronization is lost in random topologies.

On the other hand, the FN model shows:

- Weak dependence of the propagation speed on the connection topology.
- Strong spiking frequency dependence on the connection topology.
- High degree of synchronization regardless of the topology.

The main feature that we detect by using class 2 excitability is that there is a strong frequency regulation of the network response as a function of the topology. Moreover, the propagation time of the signal does not strongly depend on the topology. It, therefore, seems that those biological networks with a high variation in the frequency of the oscillations are good candidates for having a class 2 excitability in

their vertices. The mechanisms that regulate the frequency may be found in the inhibitory neurons, that could be able to reconfigure the network.

On the other hand, class 1 excitability does not have such a strong frequency dependence on the connection topology. However, the propagation speed is highly dependent on the topology. For random topologies, where high responsiveness is achieved, the network is not able to display any kind of synchronization. This is the reason why I believe that some sensory systems must be sitting near the small-world configuration, where the balance between responsiveness and synchronization is accomplished.

Finally, I would like to add that biological sensory systems present inhibitory neurons that could dynamically rearrange the connection topology of the network. They seem to play an important functional role in discriminating between similar messages, but are not necessary for gross recognition [70, 82, 81]. The dynamically changing connection topology due to the inhibitory neurons introduces a degree of complexity that is the goal of future work.

3.6 Discussion

The small-world is a concept that applies to networks or graphs whose topology is placed somewhere between order and randomness. A small world network can be imagined as an overall regular network, in which some long-range connections highly reduce the average distance between vertices. It keeps the clustering properties of the regular network, but the characteristic path length takes values close to those of a random graph. Small-worlds were introduced as an attempt to explain the structure of social networks, but they have shown to be applicable to many other systems.

When applied to neural networks, I have shown that small-world topologies can provide the network with properties given neither in regular nor in random networks. In networks with class 1 excitability in their vertices, they provide a fast response due to the small characteristic path length; and a high level of synchronization due to the high clustering coefficient. This is the kind of response desirable in any biological

or artificial system that has to deal with big amounts of information and rapidly respond to external stimuli. Regular and random networks are not able to produce this kind of response because they fail to produce fast response and coherent oscillations respectively.

On the other hand, in networks with class 2 excitability in their vertices, the main observed result is a strong frequency regulation as a function of the topology. The network response time and synchronization properties seem not to strongly depend on the topology. In biology, some systems with great variations in the oscillation frequency exist. They could be good candidates for containing neural networks with class 2 excitability. The topology varying mechanisms could be found in inhibitory neurons, that are able to cancel some vertices and edges, hence reconfiguring the graph.

Maybe the most interesting result of this chapter is the ability of the small-world network to provide coherent oscillations. The fast response was not so surprising, given the quite intuitive relation between the response time and the characteristic path length. So what makes the small-world topologies really attractive from the point of view of neurosciences, is their capacity, at least for some neuron models, of producing an oscillatory activity. So far I have been talking about the importance of coherent oscillations for information processing in biology. This assumption was one of the motivations of the study, and it can be justified both by experimental evidences [25, 41, 82] and theoretical analyses [83]. However I would like to show that, apart from pure experimental results and theoretical speculations about the brain, the concepts of correlated activity and temporal coding can be applied to a variety of problems, from binding to image segmentation. These issues are the aim of the next chapter.

Chapter 4

Neural synchronization and applications

4.1 Introduction

In previous chapters we have seen that the presence of coherent oscillations in the neural activity seems essential for the processing of sensory information by the brain. I presented the correlation hypothesis of von der Malsburg [83], which solves the binding problem in an elegant manner and avoiding the combinatorial explosion implied by the grand-mother cell hypothesis. Some experiments in the last decade seem to confirm this theory with the observation of temporal correlations, in the millisecond range, between neurons responding to a single stimulus even across different cortical areas [25, 41, 42]. In addition, some experiments performed in the olfactory system of insects show that these oscillations are not just a residual effect of neural activity, but are in fact essential for a good information processing [70, 82, 81].

The aim of this chapter is to discuss the kind of neural mechanisms that are able to generate synchronization among different groups of neurons in the brain, and to show some applications of these ideas to binding, image segmentation, and the study of psychophysical problems such as binocular rivalry and visual illusions.

In the analysis performed in chapter 3, the presence of oscillations in the neural network activity was taken as a basic requirement, and the study was centered

on the search of network topologies that provide this kind of response for a given neuron model. Based on the results of physiological experiments, I worked under the assumption that oscillatory neural activity provides a better substrate for coding and information processing. However, up to now, we have not seen any practical application where oscillations show advantageous over other approaches.

Here I want to show, with the aid of some specific examples, that oscillations, and in particular spike correlations, may be useful for some kind of applications. I will study three different problems. First, a typical example of binding in the visual system, which will be focused both from a firing rate based and from a spike based point of view. In particular, the solution in terms of spikes provides results that are quite coincident with experimental observations, under the assumptions that: (i) spike correlations are a direct consequence only of excitatory connections between neurons; and (ii) spike decorrelations are provided by the intrinsically noisy processes of spike generation. The firing rate model will later be applied to the study of a phenomenon that implies oscillations in a much longer time scale. Binocular rivalry and other perceptual illusions are characterized by an alternation of two competing perceptions in a time range of several seconds. This alternation can be explained assuming a competition between two neuron pools with firing rate adaptation. Finally, I will present a network of integrate and fire neurons that exploits synchronization to achieve segmentation of binary images. Groups of neurons responding to a connected component in the image reach a synchronized oscillatory state, while different neuron groups tend to oscillate with a constant phase difference. The use of pulse coupling provides more robustness and less sensitivity to parameters than in other similar models based on continuous coupling.

The neuron models used along this chapter are quite different from those of chapter 3. There I was motivated by biological aspects, and here I am constrained by more computational and practical terms. I will use models that simplify the neuron's behavior, following two different approaches. On the one hand I will consider firing rate models that describe the mean activity of a population of similar neurons that present common dynamical properties. On the other hand I will consider spiking models that simplify the neuron's dynamics to a simple integrator which fires when it

reaches a threshold, or even more to a Poisson process with a time varying probability. These assumptions lose biological detail but keep the image of a neuron as a processing unit that is able to generate a spiking response under external stimulation. The simpler dynamics also provide faster simulations and results that are easier to analyze and interpret.

The chapter is organized as follows. In section 4.2 I overview the neural mechanisms that produce oscillations in the brain, as well as the different artificial approaches that have been made to explain this phenomenon with artificial neural networks. In section 4.3 I show an example of application of synchronization to binding in the visual system. Section 4.4 extends these results to explain the phenomenon of binocular rivalry. Section 4.5 presents a network of integrate and fire oscillators used for binary image segmentation. And finally I discuss some conclusions in section 4.6.

4.2 How to achieve synchronization Neural mechanisms

Oscillations in the local field potential registered in extracellular recordings reflect a synchronous, repeating pattern of spiking activity of the neurons that are located close to the electrode. In fact, after the discovery of coherent oscillations in the cortical activity, different experiments proved the existence of spike correlations between different neurons. This kind of activity has been observed in localized areas in the cortex [25, 41], across different cortical areas [26], and even between the two brain hemispheres [27]. However the mechanisms that permit the appearance of such spike synchronization are not clear.

The original idea of von der Malsburg seems the most plausible one. Mutual synaptic excitation creates correlations in the brain. If one neuron makes some other fire, then the two will be correlated (disregarding a synaptic delay). Also temporal correlations between two neurons can be imposed by a common input even if there are no mutual connections between them. The discovery of lateral connections between columns of similar orientation preference supposed a point in favor of this view.

However, theoretical and simulation works have shown that synchronization is not easily achieved in networks of biological neurons with excitatory coupling. In consequence many different mechanisms that may lead to synchronization have been proposed. Lytton and Sejnowski [79] proposed that certain classes of inhibitory interneurons could play a functional role in the maintenance of cortical phase-locking. Bush and Douglas [14] proposed a model of bursting neocortical neurons in which synchronization is achieved by means of global inhibition. Hansel and Sompolinsky [46] studied networks of chaotic neurons with global coupling, and found that certain values of the coupling parameters provided global synchronization. König and Schillen [59, 110] used a network of neural oscillators synchronized by local connections that accounted for the experimental results with orientation selective neurons. More recently Bondarenko and Chay [13] have studied synchronization and desynchronization in neural networks with random coupling, and found that the type of activity displayed by the network is highly sensitive to the input, the connection strength and the neurons' degree of excitability. Even mechanisms based on depressing synapses have been proposed [35].

Common to almost all of the cited approaches is a high sensitivity to the parameters selection, and some of them also present deficiencies when dealing with noise. Despite the big effort realized, the answer to what kind of neural mechanisms are able to generate synchronization in the brain remains unclear. But maybe we are not setting the correct questions.

The study of synchronization in networks of coupled oscillators has been a matter of interest since much earlier than the introduction of the temporal correlation hypothesis or the first experimental evidences of correlated spiking activity in the brain. Synchronization in populations of mutually coupled oscillators takes place in several mathematical, chemical, or biological systems [132]. The mechanisms that provide synchronization in such assemblies of mutually coupled oscillators have been the matter of extensive study [132, 30, 61, 125]. In most of these approaches it is generally assumed that the coupling interactions are smooth, that is, the equations describing the oscillators' activity are continuously coupled in time. However neurons are not continuously coupled; synaptic coupling between neurons occurs only when

an action potential is produced. This kind of coupling is also characteristic of many other systems: fireflies that flash in unison, chirping crickets or heart pacemaker cells are some examples. Theoretical research has also been carried out on the synchronization of these kind of pulse-coupled oscillators [98, 88, 31, 18]. In all these studies, synchronization is understood as a global property of the system in which all the oscillators evolve in time with zero phase difference. All the oscillators are in the same state at the same time. I am afraid that theoretical approaches to synchronization in the brain have in many cases inherited this view, and try to view neural networks as pools of coupled oscillators, and the phenomenon of spike synchronization as a global network property. However, it should be remarked that (i) neurons are not perfect oscillators, for instance they do not have a constant spiking frequency; and (ii) when we talk about neural synchronization we are not talking about a global network property, but rather about pair-wise correlations between spiking times of neurons. Synchronization is a complex phenomenon in networks of coupled oscillators, but a simple mutual excitatory connection between two integrate and fire neurons can lead to correlated spiking activity, as originally hypothesized by von der Malsburg. So what maybe happens is that we are misunderstanding the concept of neural synchronization. Probably excitatory connections in networks of spiking neurons is all that is needed to produce the spike correlations that are observed in experimental work.

In conclusion, global synchronization in oscillator assemblies is a hard terrain to explore. Mechanisms are complex and solutions quite parameter dependent. But *"who says neurons are perfect oscillators"*, and *"who says neural networks have to reach global synchronization"*. Up to now only spike correlations have been observed, and these could be achieved by mutual excitatory connections. However oscillations and synchronization in networks of oscillators still provides interesting applications to many practical problems.

4.3 Binding of objects and positions in the visual system

As a first application of the ideas presented in the previous chapters, I want to show here that it is possible to exploit synchronization to link the different features of a single stimulus that are being processed in parallel by different brain areas. In particular I will focus on the visual system of mammalians and the two paths of visual information. It is well known that the mammalian brain processes spatial information and object properties by two differentiated neural streams [121, 85]. Visual information coming from the retina and the LGN reaches the primary visual areas in the occipital lobe. Neurons in these areas respond to very simple stimuli, such as oriented bars and edges. From this point the visual pathway bifurcates into two branches (see figure 4.1). The ventral stream (*what pathway*) carries information about the objects in the visual scene, such as shape or color, and reaches the inferior temporal cortex (IT). The dorsal stream (*where pathway*) carries information about the spatial relations in the scene, and reaches the posterior parietal cortex (PP).

These two pathways independently process the information about (i) the objects (what), and (ii) the positions (where) in a visual scene. As far as the visual scene is composed by only one object there is no ambiguity in perception: the single object processed by IT is just linked to the single object position processed by PP. In a more general situation, however, a visual scene will be composed of several objects at different locations, and each object must be linked to its position with no ambiguity. To illustrate the problem let us imagine the scene of figure 4.1, consisting of a red cube on the left hand side and a blue sphere on the right hand side.

When looking at this figure, the what-pathway of our brain is processing the information about the objects in the scene, a red cube and a blue sphere; meanwhile the where-pathway is processing the information about the spatial distribution, perceiving activity both on the left and the right hand sides of the scene. While this separate processing is useful in the sense that we do not need processing units that respond to spheres and cubes at every possible spatial location, it could result in a serious problem. If there were no means to associate the perceptions of each area, we

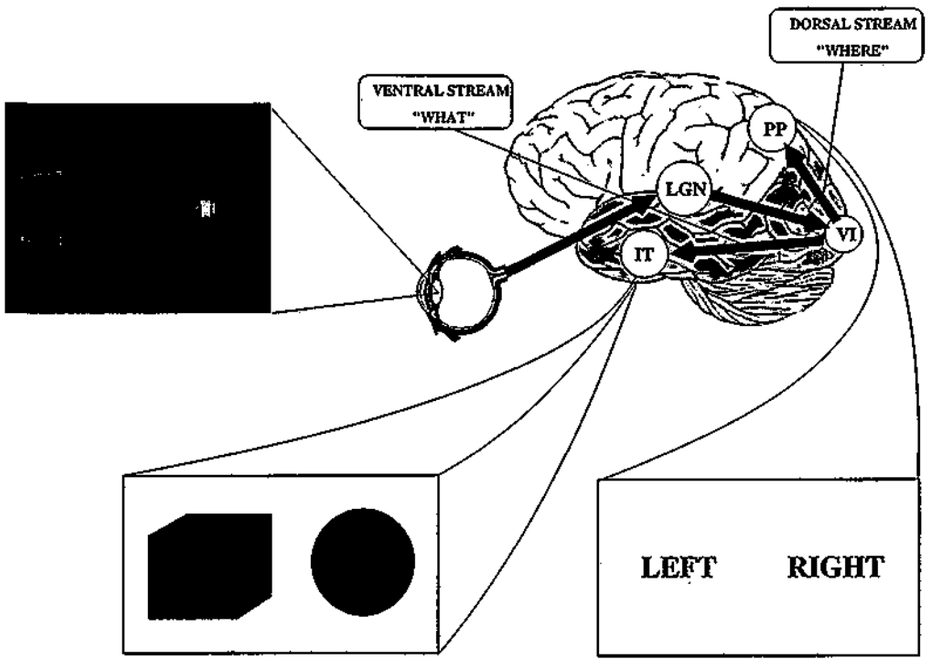

Figure 4.1: Schematics of the flow of visual information in the brain. Information coming from the retina and the LGN reaches the primary visual areas (V1) in the occipital lobe. From there, two different pathways depart. The ventral stream reaches the inferior temporal cortex (IT), and it is involved in the processing of object properties (what). The dorsal stream reaches the posterior parietal cortex (PP), and it is mainly concerned with the processing of spatial information (where).

would have the following perceptual ambiguity:

Are we observing a red cube on the left and a blue sphere on the right; or are we observing a red cube on the right and a blue sphere on the left?

Fortunately most of us can answer this question with no hesitation, so we must assume there are cerebral mechanisms that associate neural activity in IT and PP areas. Here I am discussing the temporal correlation hypothesis [83], and I will try to find a solution in these terms. But before continuing I would like to add that associating objects and positions is not the only binding problem our brain has to deal with. Color, shape, size, orientation, an many more, are features processed by different brain channels that must converge into single object perceptions. Although

the analysis I perform here deals with only two channels, namely the object channel and the position channel, it could be extended to deal with more features.

Since the introduction of the temporal correlation hypothesis [83] and the experimental evidence of correlated activity in the brain [25, 41, 42], there have been many theoretical models that attempt to achieve feature binding by means of activity oscillations in artificial neural networks. Different approaches have dealt with models of orientation selective columns in the cortex [59, 110, 16]; sensory segmentation [84]; image segmentation [127, 107, 55, 56] (see also section 4.5); and clustering [102].

Here I present a simplified model of the mammalian visual system that, based on the same ideas of binding by temporal correlations, achieves synchronization between groups of neurons that respond to the objects and their corresponding positions [67]. It is composed of an input layer that resembles V1, an intermediate layer that resembles V4, and two additional layers that separately process the objects and their positions (see figure 4.2). They resemble, respectively, the inferior temporal (IT) and the posterior parietal (PP) cortices in the mammalian brain. The link between the neurons in IT responding to an object and the neurons in PP responding to its position is given by the temporal correlation of the activity between both neuron populations.

The model departs from a previous model of visual search and attention proposed by G. Deco and J. Zihl [20]. They proposed a model of competition mechanisms in IT and PP, which together with backward connections to earlier visual areas and the assumption of the biased competition hypothesis [24], provides the usual results of visual search experiments. The biased competition hypothesis states that a bias to an attended location in PP is able to balance the competition in IT in favor of the neurons responding to the object at that location (object recognition). Moreover, a bias to the neurons in IT that respond to a searched object can lead the competition in PP in favor of the neurons that respond to its location (visual search). Recurrent connections from IT and PP to earlier visual areas play a key role in this process. They serve as a link that provides the simultaneous activation of the pools in IT and PP that are responding to a particular searched object.

The solution provided by this model of visual search is essentially a correlation

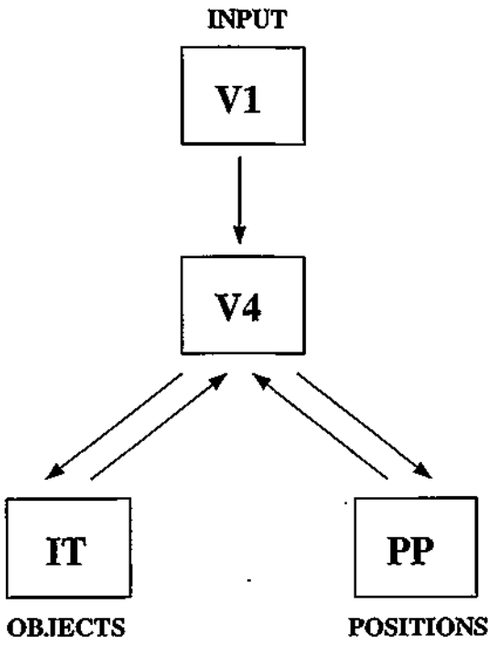

Figure 4.2: Schematics of the network architecture. Arrows indicate excitatory connections between the different layers.

between neurons in IT an PP that are responding to a common stimulus. It is quite easy to adapt the dynamics so that it can be applied to our present purposes. All we need is some mechanism that produces an oscillatory activation of IT and PP neurons. If the response in both the IT and PP layers is an alternation of the competing neurons, the recurrent connections will organize the system so that simultaneous winners in both layers are responding to the same object. The result will be an oscillatory alternation of different neuron groups across the whole network. All the neurons in each group respond to a single object in the input scene.

The oscillatory behavior has been obtained by connecting one inhibitory unit to each of the excitatory units in IT and PP. The inhibition comes with a certain delay, and so each pair excitatory-inhibitory behaves as an oscillator.

The model of Deco and Zihl is based on population equations that describe the mean activity of a group of neurons that are considered a basic processing unit in the brain. Here I will keep this approach on a first stage. However at the end of

the section I will change to a model of spiking neurons that provides results more in accordance with experiments on synchronization.

4.3.1 The mean field approach

I use population equations that describe the mean activity of a group of neurons with common functional and dynamical properties. This groups of neurons, often called pools, are formed by a large and homogeneous population of identical spiking neurons that receive the same external input and are mutually coupled by synapses of uniform strength. The mean activity of such a pool of neurons is formally described in the framework of the mean field theory, see for example [1, 130]. Typically we have the following equation that relates the input current for the pool i to the input currents for other populations:

$$\tau_i^s \frac{dI_i(t)}{dt} = -I_i(t) + \sum_j w_{ji} F(I_j(t)) \tag{4.1}$$

where τ_i^s is a decay constant and the sum on the right hand side extends to all the pools that synaptically influence pool i, with w_{ji} being the synaptic strength of the connection. F is the activation function, that relates the input current to the pool mean activity [122]:

$$F(I) = \frac{1}{T_r - \tau log(1 - \frac{1}{\tau I})} \tag{4.2}$$

where τ is the membrane time constant and T_r is the refractory period. The activation function represents the mean firing rate of the pool, and is calculated as the average spiking frequency of a leaky integrate and fire neuron with threshold $V_{th} = 1/C$, under the assumption that time averages and population averages are equivalent. It is a non negative function defined only for input currents greater than or equal to $I_{min} = 1/\tau$. For input currents lower that I_{min} we assume $F = 0$. It saturates to a maximum value given by the inverse of the refractory period, $F_{max} = 1/T_r$ (see figure 4.3).

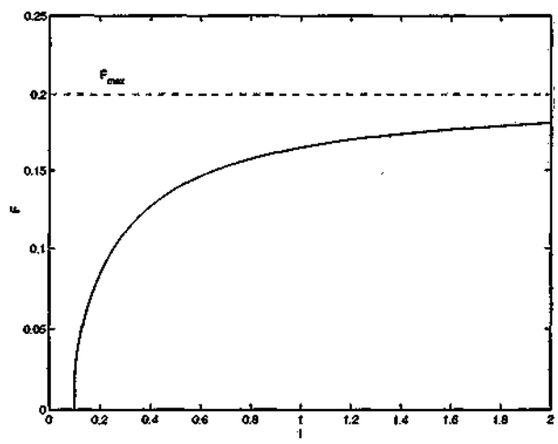

Figure 4.3: Activation function, F, versus input current, I, for the mean field approach. Parameters $\tau = 10$ and $T_r = 5$.

4.3.2 Model architecture

The overall network architecture is shown in figure 4.2. The input layer (V1) responds to active pixels in the input, and the V4 layer responds to simple stimuli (such as letters) at different positions. As shown in figure 4.4, each group of V4 pools converges on a single IT pool (E pools in the figure), and so E pools in IT respond to specific objects independently of their position. The competition in IT is mediated by a common inhibitory pool that receives connections from and sends connections back to all E pools. This common inhibitory pool allows only one E pool to be active at a time.

There is one inhibitory pool (I) connected to every E pool. A delay in the connection from I to E produces the oscillatory behavior on each pair E-I. After an E pool has won the competition it is inhibited and a different pool can win. The final result is an oscillatory alternation of all the E pools that respond to objects in the input.

In figure 4.5 I show the connections reaching the PP layer. Each PP pool responds to activation in a specific location, no matter the object that produces it. Again we have a common inhibitory pool that implements the competition between PP pools, so that only one of them can be active at a time; and local inhibition that generates the oscillations.

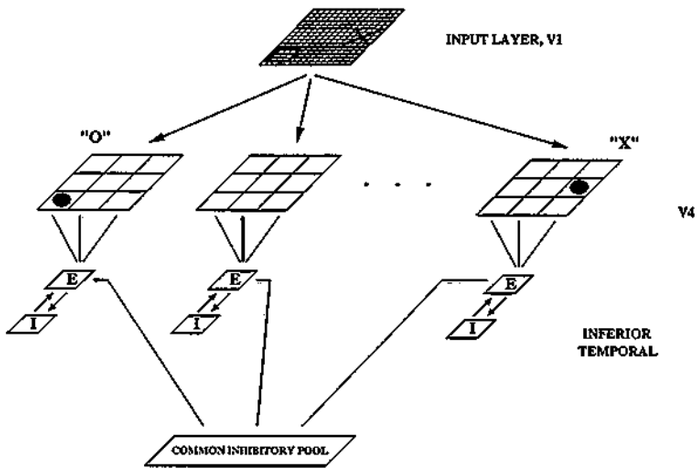

Figure 4.4: Structure of the network showing the connections reaching the IT layer. Non-directed lines represent connections in both ways.

Now we will see the important role that recurrent connections from IT to V4 play. When a pool in IT is dominating, these recurrent connections produce a small increase in the activation of the V4 pools responding to the winning object. This translates into a small bias to the PP pool that responds to the object position, which will then win its own competition. So the pools responding to the object (IT) and its position (PP) win their respective competitions simultaneously.

4.3.3 Equations and parameters

I describe now the neurodynamical equations that regulate the evolution of the whole system. In the recognition layer (IT), the input current for excitatory pools is given by:

$$\tau_s^E \frac{dI_i^E(t)}{dt} = - I_i^E(t) + w^{IE} F(I_i^I(t-\Delta t)) + w^{EE} F(I_i^E(t)) + w^{V_4 E} \sum_j F(I_{ij}^{V_4}(t)) + w^{CE} F(I^C(t)) + I_0 + I_{noise}(\nu) \quad (4.3)$$

where in the superindexes E means excitatory, I means inhibitory, C is the inhibitor

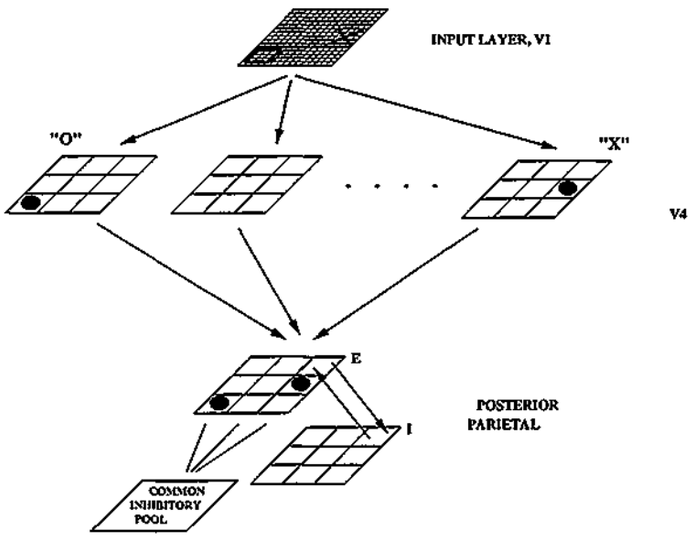

Figure 4.5: Structure of the network showing the connections reaching the PP layer. Non-directed lines represent connections in both ways.

mediating competition in IT and V_4 is the V4 layer; and in the subindexes i refers to "object" and j to "position". The parameters w are the synaptic strengths, and Δt in the connection from inhibitory to excitatory pools is a delay necessary for the appearance of oscillations. I have included a diffuse spontaneous background input current I_0 and a Gaussian noise term $I_{noise}(\nu)$ of amplitude ν. For the inhibitory pools we have:

$$\tau_s^I \frac{dI_i^I(t)}{dt} = -I_i^I(t) + w^{EI} F(I_i^E(t)) + w^{II} F(I_i^I(t)) + I_0 \tag{4.4}$$

And for the common inhibitory pool:

$$\tau_s^C \frac{dI^C(t)}{dt} = -I^C(t) + w^{EC} \sum_i F(I_i^E(t)) + w^{CC} F(I^C(t)) + I_0 + I_{noise}(\nu) \tag{4.5}$$

The parameter values for equations (4.3)-(4.5) are shown in table 4.1.

In the PP layer we have the following equations for the excitatory, inhibitory and common inhibitory pools:

τ_s^E	3.0	w^{V_4E}	0.34
τ_s^C	3.0	w^{EI}	1.5
τ_s^I	30.0	w^{II}	-0.1
I_0	0.025	w^{CC}	-0.1
w^{EE}	0.95	w^{EC}	1.5
w^{IE}	-20.0	Δt	40.0
w^{CE}	-0.5	ν	0.02

Table 4.1: Parameter values for equations (4.3)-(4.5).

$$\tau_s^E \frac{dI_j^E(t)}{dt} = - I_j^E(t) + w^{IE}F(I_j^I(t-\Delta t)) + w^{EE}F(I_j^E(t)) + w^{V_4E}\sum_i F(I_{ij}^{V_4}(t)) + w^{CE}F(I^C(t)) + I_0 + I_{noise}(\nu) \quad (4.6)$$

$$\tau_s^I \frac{dI_j^I(t)}{dt} = -I_j^I(t) + w^{EI}F(I_j^E(t)) + w^{II}F(I_j^I(t)) + I_0 \quad (4.7)$$

$$\tau_s^C \frac{dI^C(t)}{dt} = -I^C(t) + w^{EC}\sum_j F(I_j^E(t)) + w^{CC}F(I^C(t)) + I_0 + I_{noise}(\nu) \quad (4.8)$$

As before, i means object and j means position. The parameters are shown in table 4.2.

τ_s^E	3.0	w^{V_4E}	0.50
τ_s^C	3.0	w^{EI}	1.5
τ_s^I	20.0	w^{II}	-0.1
I_0	0.025	w^{CC}	-0.1
w^{EE}	0.60	w^{EC}	1.0
w^{IE}	-10.0	Δt	40.0
w^{CE}	-0.1	ν	0.02

Table 4.2: Parameter values for equations (4.6)-(4.8).

In the V4 layer, the current for a pool responding to object i and position j is described by the equation:

$$\begin{aligned}\tau_s^{V_4}\frac{dI_{ij}^{V_4}(t)}{dt} = & - I_{ij}^{V_4}(t) + w^{EV_4}F(I_i^E(t)) + \sum_k w_k^{V_1V_4}F(I_k^{V_1}(t)) \\ & + w^{V_4V_4}F(I_{ij}^{V_4}(t)) + I_0 + I_{noise}(\nu) \end{aligned} \tag{4.9}$$

where the E in the superindexes refers to excitatory pools in IT, and the sum in k extends to all the input (V1) pools. Finally, the equations for the input current in the V1 layer are:

$$\tau_s^{V_1}\frac{dI_k^{V_1}(t)}{dt} = -I_k^{V_1}(t) + w^{V_1V_1}F(I_k^{V_1}(t)) + I_0 + I_{noise}(\nu) + I_k^{bias} \tag{4.10}$$

where the bias current I_k^{bias} is used to simulate the activation of the V1 pools due to the stimulus. The parameters for equations (4.9) and (4.10) are given in table 4.3.

$\tau_s^{V_4}$	3.0
w^{EV_4}	0.25
$w^{V_4V_4}$	0.95
$\tau_s^{V_1}$	3.0
$w^{V_1V_1}$	0.95
I_k^{bias}	0.03
ν	0.02

Table 4.3: Parameter values for equations (4.9) and (4.10).

The activation functions for all the pools are given by equation (4.2), with parameters $T_r = 300.0$ and $\tau = 40.0$ for inhibitory pools in both IT and PP; $T_r = 1.0$ and $\tau = 10.0$ for excitatory pools in PP; and $T_r = 1.0$ and $\tau = 20.0$ for the rest of pools. The equations have been numerically solved using the Euler method with a time step of 0.1 ms.

4.3.4 Results

I present the results for a simple case in which a stimulus consisting of two different objects at two different positions is presented to the network, as shown in figures 4.4 and 4.5.

The V4 pools extract the characteristics about the stimulus and send the information to both IT and PP. The two pools in IT responding to the objects start to compete for activation, while the two pools in PP responding to the active locations do the same. Thanks to the local inhibition, the winner pools can only dominate for a few milliseconds, and what we observe is an alternation between winning pools in IT and PP (figure 4.6A-B). This oscillatory behavior backpropagates to V4 through the recurrent connections from IT, and so whenever an IT pool increases its activity we observe an increase in the current of the V4 pool that responds to the same object (figure 4.6C). This generates a small difference in the input to the two PP pools, that balances the competition in favor of the correct position. This mechanism makes possible the synchronization between IT and PP neurons that are responding to the same object. As expected, when an object wins in IT, its position wins in PP as well, and so the association between each object and its position can be done unambiguously.

To quantify the correlation between the IT and the PP layers, I have performed the following analysis. For each of the neuron pools I determine an activation threshold I_{act} and set the state of the pool to be:

$$A = \begin{cases} 1 & \text{if } I \geq I_{act} \\ 0 & \text{otherwise} \end{cases} \tag{4.11}$$

I have taken $I_{act} = 0.05$ for IT, $I_{act} = 0.10$ for PP, and $I_{act} = 0.20$ for V4. As a measure of the correlations I compute, for each pair of pools (i, j), the quantity:

$$C_{ij} = T(i,j)/T(i) \tag{4.12}$$

where $T(i)$ measures how much time the pool i is in the active state, and $T(i,j)$ measures how much time both pools i and j are simultaneously in the active state. The

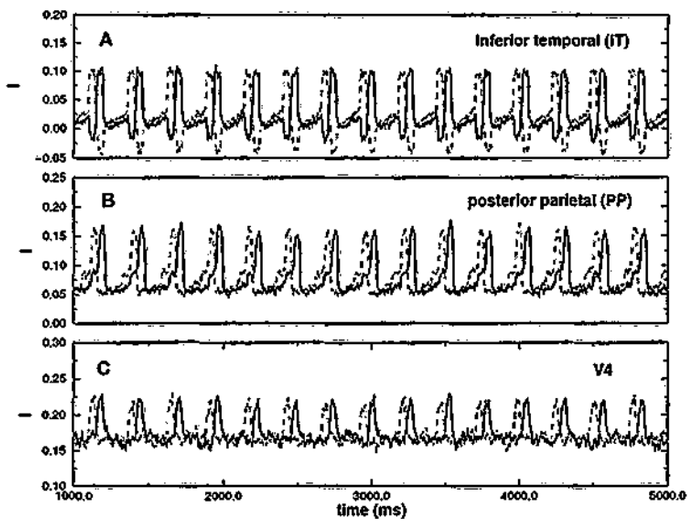

Figure 4.6: Input currents in IT, PP and V4 when two different objects are presented simultaneously to the network. Solid lines: object "X"; dashed lines: object "O". A. IT excitatory pools responding to each object. B. PP excitatory pools responding to each active position. C. V4 active pools. A clear correlation is observed between pools responding to a single object.

quantity C_{ij} is 0 if the active states of the two pools never coincide, and approaches 1 as the activation of pool i tends to overlap with activation of pool j. Results are shown in table 4.4. The correlation between pools that respond to different objects is 0, and autocorrelations are, obviously, 1. The correlations between pools in different layers that respond to a common object are in all the cases higher than 60%. In particular, correlations between IT and PP are higher than 0.9, what is due to the two-way connection between these layers.

4.3.5 Partial conclusions

I have constructed a simplified model of the visual system that separately processes objects and positions, where the link between each object and its position is provided by the temporal correlation of population activities. Although the analysis performed

		Object 1			Object 2		
		V4	IT	PP	V4	IT	PP
Object 1	V4	1.00	0.93	0.81	0.00	0.00	0.00
	IT	0.94	1.00	0.77	0.00	0.00	0.00
	PP	0.70	0.65	1.00	0.00	0.00	0.00
Object 2	V4	0.00	0.00	0.00	1.00	0.94	0.80
	IT	0.00	0.00	0.00	0.91	1.00	0.73
	PP	0.00	0.00	0.00	0.69	0.65	1.00

Table 4.4: Pair correlations between the pools in V4, IT and PP responding to each of the two objects presented as input to the network.

here deals with only two channels, the model could be easily generalized to an arbitrary number of features in the stimulus space. For each dimension in the stimulus space we can have a different processing layer composed of oscillators. Recurrent excitatory connections among these layers would permit the simultaneous activation of the pools in each layer that respond to a single particular object.

The model behavior is based on two main points. First, the representational units in IT and PP are oscillators. This facilitates an alternation of the perceived object, and incorporates the temporal dimension to the processing. Second, there are recurrent excitatory connections from IT to earlier areas (V4) that provide a synchronization between the oscillations in IT and PP. This provides the link between the objects (IT) and the positions (PP), and solves the binding problem. Note that the connections that provide the synchronization across the different layers are purely excitatory.

Although the results shown here provide a solution to the problem, the model presents some discordances with experimental work that I would like to discuss:

- First, if we take a glance at the visual cortex, we observe no alternations of activity at this time scale. Experimental results show that cortical neurons with overlapping receptive fields and different preferences for motion direction can synchronize when stimulated by a single moving bar [42, 62]. But this synchronization can only be measured by analyzing the precise spiking times of

the neurons. Simple firing rate measures show, however, no evidence of temporal correlations.

- Second, a computation based on firing rates may not be compatible with a fast information processing [60]. Considering the processing speed for visual information in the cortex, it is estimated that there are less than $10ms$ for processing at each visual area [116, 117]. This is not enough time for evaluating firing rates.

These two observations suggest that real neurons are doing most of their processing based on spikes rather than firing rates. They can be thought of as *coincidence detectors* that respond to a simultaneous activation of their afferents. With these considerations in mind, I would like to finish this section proposing a simple model of spiking neurons that is more in accordance with the experimental results. However I will turn back to the firing rate model later in section 4.4, where it will be applied to some different phenomena that occur in a much longer time scale. By now let us turn the discussion on models of spiking neurons.

4.3.6 A simple model of spiking neurons

The spike response model (SRM) [37, 38] is a discrete probabilistic model for the generation of spikes, in which for each finite time step t there is a probability for the neuron to fire determined by the difference between the neuron's membrane potential[1] $h(t)$ and the spiking threshold h_0. This spiking probability is given by:

$$P_s(t) = \frac{1}{2}(1 + tanh(\beta(h(t) - h_0))) \tag{4.13}$$

where β is a constant (noise parameter). In figure 4.7 I show the spiking probability versus h for $h_0 = 0.12$ and $\beta = 40$. The occurrence of a spike is always decided by a random process that depends on P_s. However, the model turns into a deterministic model for $\beta = \infty$. In this case the neuron fires with probability 1 whenever its membrane potential $h(t)$ crosses the threshold.

[1] I will refer to $h(t)$ as membrane potential for convenience.

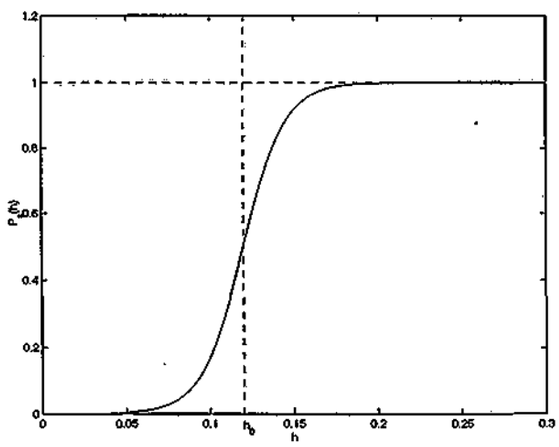

Figure 4.7: Spiking probability P_s versus membrane potential h for the spike response model (SRM) of equation (4.13). The spiking threshold is $h_0 = 0.12$ and the noise parameter is $\beta = 40$.

For each time step the state $S(t)$ of the neuron is determined by the firing probability P_s, by drawing the random variable x from a uniform distribution in the interval $[0, 1]$ and comparing it with $P_s(t)$:

$$S(t) = \begin{cases} 1 & \text{if } x \leq P_s(t) \\ 0 & \text{otherwise} \end{cases} \tag{4.14}$$

The neuron membrane potential is defined as the sum of three contributions:

$$h(t) = h_{syn}(t) + h_{ref}(t) + h_{ext}(t) \tag{4.15}$$

The term h_{syn} represents the synaptic input from other neurons, and is calculated as a sum over all the afferents of terms of the form:

$$h_{syn}(t) = w \sum_{\tau=0}^{\infty} \epsilon(\tau) S(t - \tau - \Delta) \tag{4.16}$$

where w is the synaptic weight, Δ is an axonic delay, and $\epsilon(\tau)$ is a kernel, typically of the form:

$$\epsilon(\tau) = \frac{\tau}{\tau_\epsilon^2} exp(-\tau/\tau_\epsilon) \tag{4.17}$$

with τ_ϵ being a constant. The kernel function $\epsilon(\tau)$ models the process of neurotransmitter release after the occurrence of an action potential, and it has the form of an α-function (section 3.2.3). The term h_{ref} in equation (4.15) takes into account the absolute refractory period after a spike event, during which the neuron can not fire again. It is given by:

$$h_{ref}(t) = \begin{cases} -\infty & \text{if } t_s \leq t \leq t_s + T_{ref} \\ 0 & \text{otherwise} \end{cases} \tag{4.18}$$

where T_{ref} is the absolute refractory period and t_s is the time of the last spike. Finally, the term h_{ext} in equation (4.15) represents an external stimulation of the neuron.

Here I will introduce a simplified version of this model in which the firing probability of the neuron at time step t is given by:

$$P_s(t) = P_{max} tanh(\beta(h(t) - h_0))\Theta(h(t) - h_0) \tag{4.19}$$

where P_{max} is the maximum spiking probability per time step, β is a constant and Θ is the Heaviside step function. I am assuming an absolute spiking threshold h_0. For $h \leq h_0$ no spiking activity is possible, while for $h > h_0$ the firing probability grows with h up to a maximum saturation value P_{max} (figure 4.8). The value of the variable h at time t is given by the sum:

$$h(t) = h_{sp}(t) + h_{ext}(t) + h_{syn}(t) \tag{4.20}$$

where h_{sp} is a spontaneous activity, h_{ext} is a term due to external stimulation, and h_{syn} involves all synaptic contributions to the neuron's activity. As before, the state of the neuron at each time step is given by a random process (cf. equation (4.14)).

Note that in this simplified model we are not taking into account the existence of an absolute refractory period. In principle the model is not free from producing two spikes in a very short (unrealistic) time interval. However the saturation of P_s

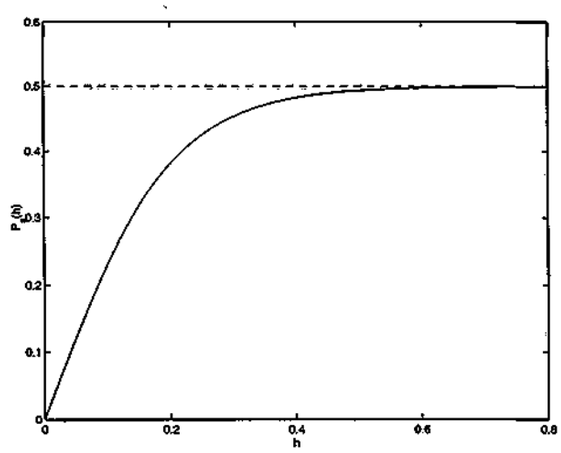

Figure 4.8: Spiking probability P_s versus membrane potential h for the simplified model of equation (4.19). The maximum spiking probability is $P_{max} = 0.5$, the spiking threshold is $h_0 = 0$, and the noise parameter is $\beta = 5$.

guarantees a maximum spiking frequency and so, on average, the minimum inter-spike interval will be on a biological range. The SRM does not limit the maximum value of P_s, so for a strong stimulation in which the membrane potential is far beyond the spiking threshold, we will obtain $P_s \approx 1$ for all the stimulation. To keep the neuron from spiking at every simulation step, the addition of an absolute refractory period results a necessity. In this case the response of the SRM will be a regular spiking pattern at a frequency given by the inverse of the refractory period T_{ref}. In the simplified model, however, a very strong stimulation will force the neuron to spike with a constant firing probability $P_s = P_{max}$, due to saturation. If we select P_{max} so that the maximum frequency is, as before, the inverse of T_{ref}, we obtain that, on average, the responses of the two models are equivalent, but the response of the simplified model is more irregular. Figure 4.9 clarifies this points with an example of response of the SRM and the simplified model to a saturating stimulus.

In the next section I use the simplified version of the SRM to reproduce the previous results for visual binding in a more realistic, spike dependent, manner.

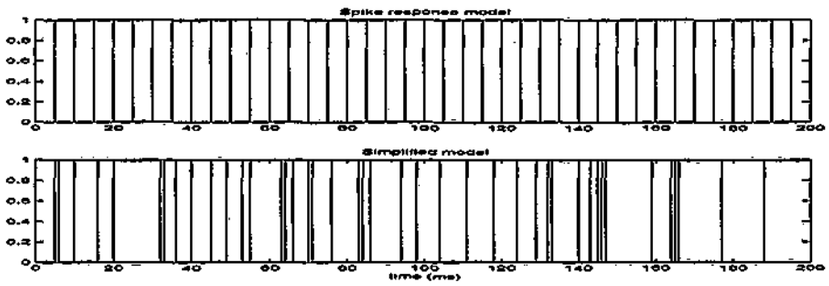

Figure 4.9: Response of the SRM (top) and the simplified model (bottom) to a very strong stimulation.

4.3.7 Back to the binding problem

I have applied the modified SRM to the problem of binding objects and positions in the visual system. My main objective is to show that it is possible to generalize the previous results to spiking models that are closer to experimental observations, both from the point of view of synchronization or spike correlations and from the point of view of processing speed. Also, by using a spiking model that is intrinsically noisy, the obtained results are more robust and less sensitive to parameter variations. The model neuron is described by equations (4.19) and (4.20), with the parameters shown in table 4.5. All the neurons are considered identical, and the synaptic contribution h_{syn} to the membrane potential of a given neuron is assumed to be:

$$h_{syn}(t) = \begin{cases} h_{syn}^{max} & \text{if } t_s \leq t \leq t_s + \tau_{syn} \\ 0 & \text{otherwise} \end{cases} \tag{4.21}$$

where t_s is the last spike of the presynaptic neuron. For the purposes of this section a simple square pulse of amplitude h_{syn}^{max} and duration τ_{syn} will suffice. The network architecture is essentially that of section 4.3.2, but the primary visual area V1 is not explicitly modeled (see figure 4.10). Instead, neurons in V4 that are supposed to be responding to the stimulus receive an external stimulation $h_{ext} = h_{input}$. For the rest of neurons I make $h_{ext} = 0$. All parameter values are shown in table 4.5.

I have performed simulations using a time step of $1ms$, and studied the correlations among different neurons in V4, IT and PP. The results are summarized in figure

P_{max}	0.5
h_{sp}	0.002
h_{input}	0.006
h_{syn}^{max}	0.05
τ_{syn}	6.0
h_0	0.0
β	5.0

Table 4.5: Parameter values for the simplified SRM model.

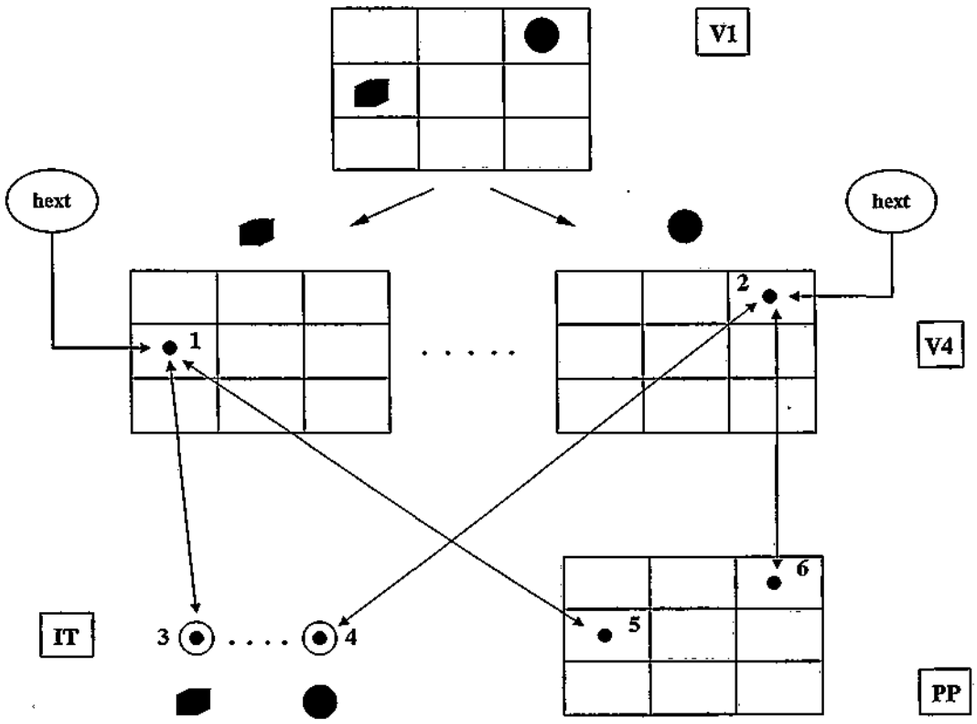

Figure 4.10: Network architecture for the model of spiking neurons. The V1 layer is not explicitly modeled. Instead, an external stimulation h_{ext} is assumed for V4 neurons that respond to the stimuli. All connections are excitatory.

4.11. I have computed spike cross-correlograms between pairs of neurons responding to the same (1-3, 1-5, 3-5) or different (1-4, 1-6, 3-6) stimuli across the network. It is observed that when the two neurons are activated by the same stimulus they

are highly correlated, which is reflected by a high central peak in the correlogram. However cross-correlograms between neurons that are responding to different stimuli are almost flat, showing no spike correlations. This result is clearly in accordance with experimental results [41, 62].

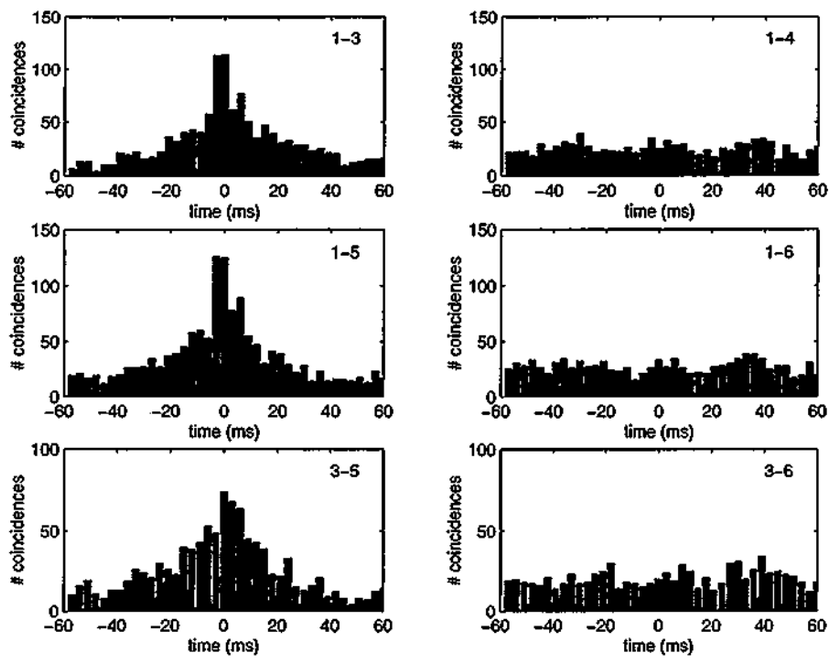

Figure 4.11: Spike cross-correlograms between different neuron pairs for the simplified SRM model, showing correlations (left) between neurons responding to a common stimulus, and absence of correlations (right) between neurons responding to different stimuli. The neuron numbers correspond to those of figure 4.10.

The mechanism that provides spike synchronization in the model is the existence of mutual excitatory connections between different layers. Whenever one neuron fires, the firing probability of the neurons it is connected to highly increases. Thus, it is quite probable that they also fire in the subsequent time steps. This, together with the random activation of the input neurons in V4, produces the effect of synchronized neuronal activity. Here I have not explicitly modeled any mechanism for the desynchronization of neurons that respond to different stimuli. I rely on the stochasticity of spike generation to avoid it. Other models use specific mechanisms that

guarantee this desynchronization through some kind of competition among different neuron assemblies [110, 126]. This was also the case for the model of section 4.3.2. All these cases are examples of models where the processing units are oscillators with a specific frequency. One could rely on the stochasticity of the initial condition to obtain the desynchronization between different oscillators. But if this initial condition is such that the oscillators start in a synchronized state, it is very difficult for the system to escape from such a situation. The present approach does not suffer from this problem. Even if two neurons that activate in response to different objects synchronize their firings at a given time step, it is very unreliable that this occurs often. These coincidences are due to chance and they do not alter the flat shape of the cross-correlogram.

We could summarize the advantages of using a spiking model as follows:

- Synchronization, or spike correlation, is easy to achieve just by excitatory connections. The results obtained by the model are more realistic.
- Computations that are based on spikes are consistent with a fast processing. This point needs, as will be seen, some more consideration.
- If the process of spike generation involves some source of noise, there is no need for explicit mechanisms that achieve desynchronization between neurons that are not related.
- The inclusion of a noisy dynamics also makes the model more robust to parameter variation.

A point that remains unclear after all these analyses is that of the processing time. One of the arguments in favor of a model of spiking neurons was that the computing of firing rates is not compatible with a fast information processing. This led us to look for solutions in which the precise spiking times are relevant. However to test the spike correlations between pairs of neurons we need to compute cross-correlograms during periods of up to 1 second. In other words, we must observe the two neurons during some time interval to be sure of the existence of a statistical dependence

between the spike occurrences of both. And this is not a consequence of the model; experimental studies consider typically time windows of around 1 second, and also a summation of coincidences over several trials is performed in order to have a sufficient amount of entries to calculate the correlograms [62, 42]. It results almost impossible to determine if two neurons are correlated by observing their activity during just a few milliseconds after the stimulus presentation.

We had discarded firing rate models because just a few milliseconds is not enough time to compute the mean rate. Neither it is time enough to calculate correlations. Maybe the solution to this problem could be found going back to population models. If there are many neurons coding each particular feature, the probability that some of them fire quickly after the stimulus can be relatively high. The assumption here is that the cross-correlogram between two neurons across a given time window (say 1 second), is equivalent to a cross-correlogram between two populations, in which the number of entries is obtained not by considering a large time window, but by considering many different neuron pairs.

4.4 Applications to binocular rivalry

In this section I will show an application of the firing rate model of section 4.3 to the study of binocular rivalry[2], a phenomenon that involves alternate perceptions of rival stimuli in a time scale of several seconds. This long time scale makes it reasonable to use a model of firing rates, although it was not appropriate for experiments that involved millisecond precision. Binocular rivalry is observed when the stimuli presented to both eyes are incongruent and can not be fused together into a single coherent percept. In such a situation the brain perceives an alternation of the two images (figure 4.12A), with the mean duration of the dominant perception being a few seconds. For some time it was argued that binocular rivalry arises from a competition between monocular neurons in primary visual cortex [10], but many experimental results in the last years discard this hypothesis. For instance, Leopold and Logothetis [72], in experiments with trained monkeys, reported that only a small percentage of neurons

[2]A complete review on binocular rivalry can be found in [11].

in V1 correlate with the monkey perception. This percentage is higher in V4 and increases as we go further in the visual pathway, reaching a 90% in the inferotemporal cortex and the superior temporal sulcus [113]. Furthermore, when the images presented to both eyes are interchanged with a frequency of 3Hz, no differences are observed with respect to the stationary case [76]. A single image is perceived for several seconds independently of the eye to which it is presented, which is clearly in opposition to a monocular competition model. Also psychophysical studies seem to be inconsistent with this view: the Diaz-Caneja phenomenon [23, 94] shows that the brain organizes the visual stimuli presented to each eye into coherent perceptions taking, if necessary, elements from both monocular channels (figure 4.13). This effect can not be explained if we assume the total suppression of the input from one eye. Also fMRI[3] recordings in humans under binocular rivalry conditions have shown activation in visual areas beyond V1 [77, 118]. A general conclusion from all these works is that the competition leading to binocular rivalry must be placed at high visual areas. The competition between stimulus representations, and not between both eyes, seems to be the last responsible for binocular rivalry, and so it is feasible that its underlying mechanisms are the same that produce other multistable phenomena, such as reversible figures (cf. Necker cube, figure 4.12B).

4.4.1 The model

Here I propose a simple model for binocular rivalry oscillations [69] that is based on concepts exposed in previous sections. It is composed of two neuron pools that compete for dominance in the same fashion as in section 4.3. Inclusion of firing frequency adaptation leads to an oscillatory activation of both pools with the same temporal dynamics as observed in experiments. I will assume that this competition is taking place at some high-level area of the visual path, such as IT. Top-down connections from the modeled IT to earlier visual areas (V4) are able to generate the observed perception-modulated response of some neurons in these areas. The model architecture consists of three layers of neuron pools, as shown in figure 4.14. In IT,

[3]Functional magnetic resonance imaging

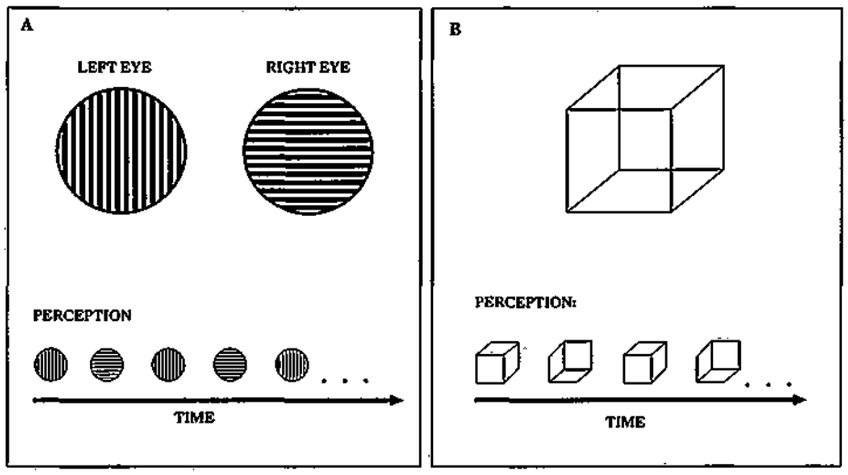

Figure 4.12: A. Binocular rivalry: When two incompatible stimuli are presented one to each eye, the resulting perception is an alternation of them. B. Necker cube illusion: This cube has two possible spatial representations, and both of them are perceived alternatively. It is believed that both effects are produced by the same cerebral mechanisms.

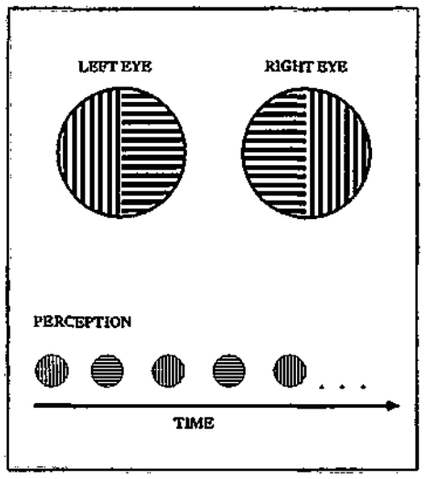

Figure 4.13: The Diaz-Caneja phenomenon. Sometimes during perceptual rivalry the brain mixes information coming from both eyes to form more coherent perceptions. This effect contradicts the theories based on monocular channel competition and places binocular rivalry closer to other visual illusions.

two neuron populations that respond to two different stimuli A and B compete for activation by means of a common inhibitory pool. The input to IT is provided by the V4 layer, where two different kinds of pools are considered. On the one hand *non-modulated* pools serve as a link between the input input layer and IT. They simply send information forward to next processing stages, and its activity is not dependent on what happens in IT. On the other hand, *modulated* pools receive connections both from the input layer and IT. Their activity will be correlated with the activity in IT, and so with the current perception. Finally, the input layer consists of two pools that are forced with an external current that simulates the stimuli.

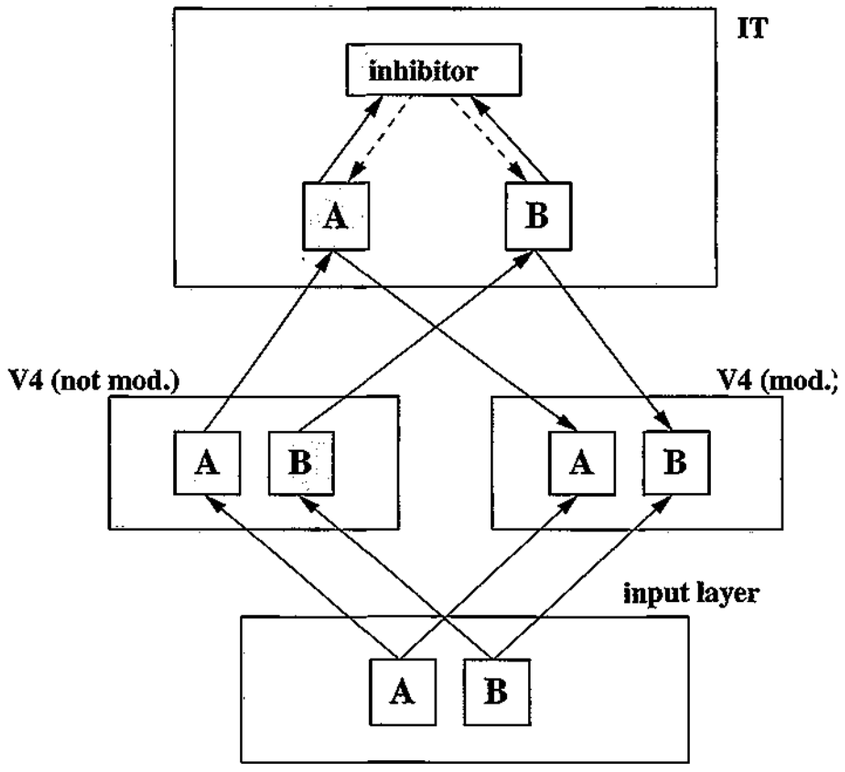

Figure 4.14: Network architecture for the binocular rivalry model. Solid connections are excitatory, dashed connections are inhibitory.

To describe the dynamic behavior of the neuron pools, I use the same kind of population equations of section 4.3.3. The input current for a given pool i is, as

before:

$$\tau^s \frac{dI_i(t)}{dt} = -I_i(t) + \sum_j w_{ij} F(I_j(t)) + I_{noise}(\nu) + I_0 \tag{4.22}$$

where τ^s is a decay constant, $I_{noise}(\nu)$ is a gaussian noise term of amplitude ν, and $I_0 = 0.025$ is a diffuse spontaneous background input current. An extra input current, I_{input}, is added to the pools in the input layer. The sum on the right hand side extends to all the pools that synaptically influence pool i; w_{ij} is the synaptic strength of the connection; and F is the activation function, that relates the input current to the mean pool activity. I use the following activation function, assuming the value 0 for currents smaller than an activation threshold $I_{min} = 1/\tau$:

$$F(I_j(t)) = \frac{1}{T - (\tau + a_j(t)) \log(1 - \frac{1}{\tau I_j(t)})} \tag{4.23}$$

This is essentially the same activation function of equation 4.2, but here I have included frequency adaptation dynamics through the parameter $a(t)$. Frequency adaptation is produced as a consequence of the repetitive firing of a neuron, due to calcium-dependent potassium currents. The result is that, when stimulated with a continuous current pulse, the neuron can not sustain a high firing rate and it decays toward an equilibrium value. To take this adaptation into account, I model a dependency of the pool mean firing rate on an adaptation parameter $a(t)$. I follow an approach similar to that proposed in [131]. The adaptation parameter $a(t)$ increases with input current according to the following differential equation:

$$\tau_a \frac{da_j(t)}{dt} = -a_j(t) + \alpha I_j(t) \tag{4.24}$$

where I have used the values $\tau_a = 400.0$ and $\alpha = 95.0$. As $a(t)$ increases the firing rate for a constant input current decreases. For sustained currents we will observe an increase of a with the subsequent decrease of I, until an equilibrium is reached (see figure 4.15).

I have used a unique model for all the pools, with parameters given in table

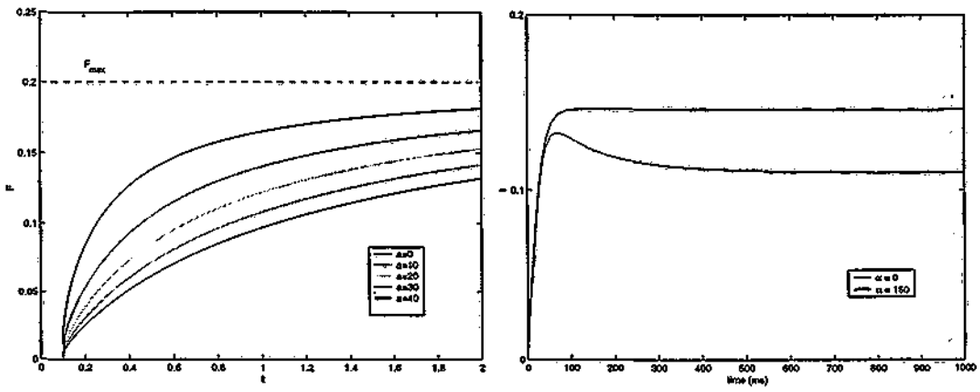

Figure 4.15: Firing rate adaptation dynamics. Left, frequency-current curves for different values of the adaptation parameter a. Right, solution of equations (4.22-4.24) when the pool is being stimulated by a constant current pulse. Blue line corresponds to a simulation with no adaptation; red line corresponds to a simulation in which adaptation is fully effective.

4.6. The input neurons receive an additional current. I_{input} that simulates the external stimulation. The values for the synaptic weights among the different layers are $w^{I-V_{4not}} = 0.85$ and $w^{I-V_{4mod}} = 0.2$ for connections between the input layer and V4; $w^{V_{4not}-IT} = 0.7$ and $w^{IT-V_{4mod}} = 0.2$ for the connections between V4 and IT; and $w^{IT-INH} = 1.8$ and $w^{INH-IT} = -1.2$ for the connections between IT pools and the inhibitor. Self-connection weights are $w^{EXC} = 0.95$ for excitatory pools and $w^{INH} = -0.1$ for the inhibitor. The equations were solved using the Euler method with a time step of $1ms$.

τ^s	6.0
ν	0.01
I_0	0.025
I_{input}	0.05
T	1.0
τ	20.0

Table 4.6: Parameter values for the model of binocular rivalry.

4.4.2 Results and discussion

The dynamics of the model provides the following behavior. When the input pools are excited, the activity propagates through the network and reaches IT. There the two populations responding to the *conflictive* stimuli start competing for perceptual dominance through the common inhibitory pool. Eventually one of them will win the competition and will dominate over the other. However the frequency adaptation mechanism will produce fatigue and weakness in the winning pool and, after a few simulation steps, the other pool will take the lead. This process continues while the stimulus is present, producing an oscillatory activation of the two competing pools that resembles the perceptual alternation measured in experiments (see figure 4.16A).

In experimental works, the measured duration of each perception (*phase duration*) is of the order of some seconds, and typically follows a gamma distribution [72, 76]. As a comparison I have computed the histogram of relative phase durations[4] (figure 4.16C). It is well fitted by a gamma function, $f(x) = \lambda^r/\Gamma(r)x^{r-1}exp(-\lambda x)$, with parameters $r = 4.60$ and $\lambda = 4.70$. This is on the same range as experimental measures.

Most of the physiological experiments related to binocular rivalry have also reported that some neurons in early visual areas modulate their activity according to the perception. Here I propose that this modulation can be due to feedback connections that come from higher visual areas where the competition takes place. Including connections from IT to some V4 populations in the model produces the related modulation (figure 4.16B). The rest of V4 neurons show no dependence with the winning perception. So the model I postulate includes two kinds of neurons in V4. The first type is composed by neurons which act as input for IT, and their activity is uncorrelated with the dominant representation. The second type is composed by neurons which receive top-down connections from IT, and their activity is modulated. This group of neurons could serve as a synchronizing link to other regions such as posterior parietal cortex (PP), which is known to process object positions. Such a schema would allow to have correlated activity between neurons in IT responding to an object

[4]The relative phase duration is the quotient between the phase duration and the mean.

and neurons in PP responding to its position, and would provide a way to solve the problem of binding by means of temporal correlations (cf. section 4.3).

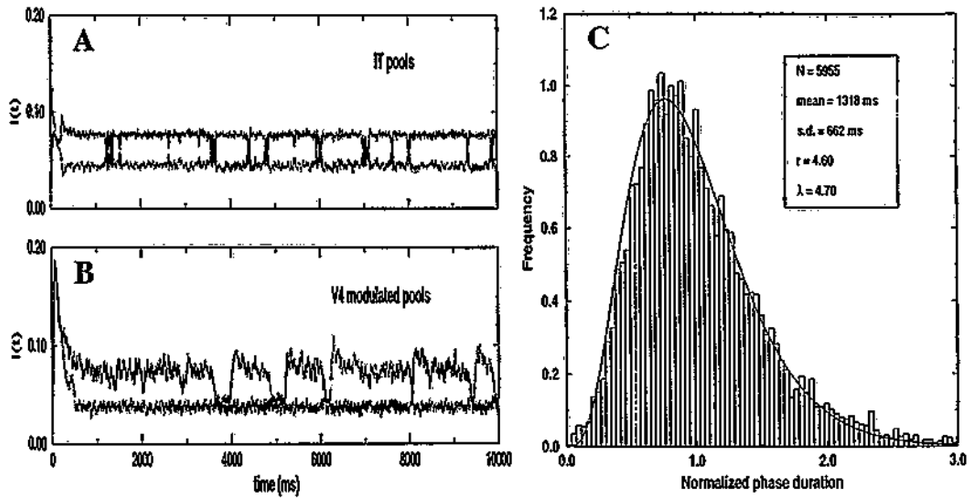

Figure 4.16: (a) Input current for IT pools when both stimuli are presented. The two pools compete for dominance and an alternation of the winning perception is observed. (b) Input current for V4 modulated pools. Note the correlation with pools in IT, achieved through the top-down connections. (c) Distribution of relative phase durations (dominant phase durations as a fraction of the mean phase duration). It has been fitted with a gamma function ($f(x) = \lambda^r/\Gamma(r)x^{r-1}exp(-\lambda x)$) with parameters $r = 4.60$ and $\lambda = 4.70$.

The assumption that competition for perceptual dominance is occurring in IT is based on two facts: First, Sheinberg and Logothetis [113] found that 90% of the neurons in IT are correlated with the perception. Second, current theories assume that the competition that leads to binocular rivalry takes place at the stimulus level, and IT is known to respond to complex stimuli [75, 57]. However this competition could be occurring in other areas or even could be a competition between cerebral hemispheres for visual awareness [87]. In any case the only assumption of the model is the existence of competition mechanisms between different stimulus representations, together with frequency accommodation that allows winner alternation. Where this competition takes place in the brain is, up to this day, an unanswered question.

Finally, I made no assumption on the monocular or binocular nature of the input

neurons. The only requirement for the occurrence of perceptual rivalry is that the competing stimuli be sufficiently different so that they can not be fused together into a single percept. This, in terms of the model, means that there are representational units in IT for each of the stimuli, but there is no one that responds to a combination of both. Under these circumstances we observe an alternative activation of IT pools responding to each of the stimuli. In this sense, the model could also be extended to situations of monocular rivalry or reversible figures. As stated in [76], binocular rivalry is just an easy way to obtain the sufficient discordance between the two alternative representations.

4.5 Image segmentation

As a last application of oscillations and spike synchronization, I want to show an example of a neural network model in which spike synchronization is used to solve a real practical problem: image segmentation. With this approach I would like to remark that this research work is not just dealing with theoretical conjectures about the brain functioning. The ideas extracted from biology can in fact be applied to real problems. Here I will show a first approach to what could be a biologically inspired segmentation mechanism that deals with binary images.

A binary image is an image whose pixel intensities can take only two possible values 0 and 1, usually corresponding to black and white (figure 4.17). In spite of being too simple, they are used in many applications since they are very easy to process. They are useful for example when all the information needed about a particular object can be obtained from its silhouette, or when a simple thresholding of a gray level image can separate the regions of interest from the background. In this section we will deal with binary images in which the background is represented by the value 0 and the objects by the value 1. The images will be composed of an arbitrary number of objects and the objective is to segment each of them, that is, to group together all the pixels that belong to a single object and separate pixels that belong to different objects. This is known as connected components labeling.

In the field of digital image processing, many segmentation algorithms have been

Figure 4.17: An example of binary image.

proposed [15, 99]. Different approaches include thresholding, gradient-based methods, edge detection and region growing. With respect to binary images and connected component labeling, the most classical is the Rosenfeld-Pfaltz algorithm [106]. The main deficiency of this algorithm is the computing time, that can be unacceptably large for large images. More recent labeling algorithms try to gain in speed by using both parallel and divide and conquer techniques.

The approach I will follow here is somehow related to the problem of binding discussed in previous sections. Imagine a neural network composed of as many neurons as pixels in the binary image. The input to a neuron will be I_{ext} if the corresponding pixel is *white* and 0 otherwise. All the neurons that are connected to a *white* pixel will display spiking activity, while the others will be at rest. Then the problem of image segmentation can be viewed as a problem of binding among all the neurons that are responding to connected white regions in the binary image.

In this framework, many research work has dealt with networks of biological oscillators applied to image segmentation. Wang and Terman have proposed a network based on local excitatory connections and global inhibition [127, 126]; and recently

their model has been applied to segmentation of gray level aerial and medical images [17]. Knoblauch and Palm [55, 56] have investigated scene segmentation in a more detailed model of the visual system using spiking neurons. There are also models that exploit the ability of pulse-coupled oscillators to self-organize into clusters to achieve image segmentation [102, 107].

The approach I follow here is related to this last kind of models. I use a network of integrate and fire oscillators that are based on the model of Peskin [98, 88] for the cardiac pacemaker cells. However I consider only local connections, and set an initial condition that guarantees the achievement of global synchronization in just a few oscillations. Also inhibitory connections are included in a final version of the model to generate desynchronization between different neuron groups when dealing with several objects.

4.5.1 The Peskin oscillator

In 1975 Charles S. Peskin [98] proposed a very simple model for the synchronization of heart pacemaker cells. The heart pacemaker is a group of around 10000 cells, called sinoatrial node, that synchronize their electrical activities to generate a single rhythmic pulse. Peskin modeled each cell as an integrate and fire oscillator whose state is described by the variable x (membrane potential) that evolves according to the following differential equation:

$$\frac{dx}{dt} = -\gamma x + S_0 \tag{4.25}$$

The cell state x grows exponentially toward the limiting value S_0/γ, and whenever it reaches a threshold $l < S_0/\gamma$ it fires and is reseted to 0. When one oscillator fires, the potential of all oscillators to which it is connected[5] is increased by a finite amount ϵ, the coupling strength. This kind of coupling is known as pulse-coupling, and Peskin oscillators are usually referred to as pulse-coupled oscillators. With this simple model, Peskin proposed the following two conjectures:

[5]In the original work the connection scheme is all to all.

- Conjecture 1: *For arbitrary initial conditions, a system composed of such oscillators and with global (all to all) coupling will approach a state in which all the oscillators are firing synchronously.*

- Conjecture 2: *This remains true even when the oscillators are not quite identical.*

Peskin gave a proof for conjecture 1 for the case of two oscillators and small coupling strength ϵ. More recently Mirollo and Strogatz [88] proved that conjecture 1 is true for an arbitrary number of oscillators with global coupling (each oscillator is connected to all the others) and for almost all initial conditions. They also showed that the form of the $x - t$ curve does not matter as far as it strictly ascends toward the firing threshold with a negative acceleration, that is, it is an ascending concave function. The synchronization of two Peskin oscillators can be intuitively understood with the aid of figure 4.18. Imagine the oscillators R and S shown in the figure. In figure 4.18A the oscillator R has reached the threshold and is about to fire. The phase difference between both oscillators is ϕ. When oscillator R fires, the potential of oscillator S is pushed up by ϵ, which results on an increase Δt_1 in its phase (figure 4.18B). When oscillator S fires (figures 4.18C-D), it is oscillator R that is pushed up, and now the same ϵ produces an increase in phase Δt_2. So after the two oscillators have fired, the new phase difference between them is:

$$\phi' = \phi - (\Delta t_1 - \Delta t_2) \tag{4.26}$$

For this particular example, due to the form of the $x - t$ curve, we have that $\Delta t_1 - \Delta t_2 > 0$, so the phase difference between oscillators R and S will decrease toward 0, leading to a synchronized state. In fact this is true for all initial conditions except one. If the initial condition is such that $\Delta t_1 = \Delta t_2$, then the two oscillators will remain desynchronized forever. However this equilibrium is unstable and any small perturbation will push the system to a synchronized state.

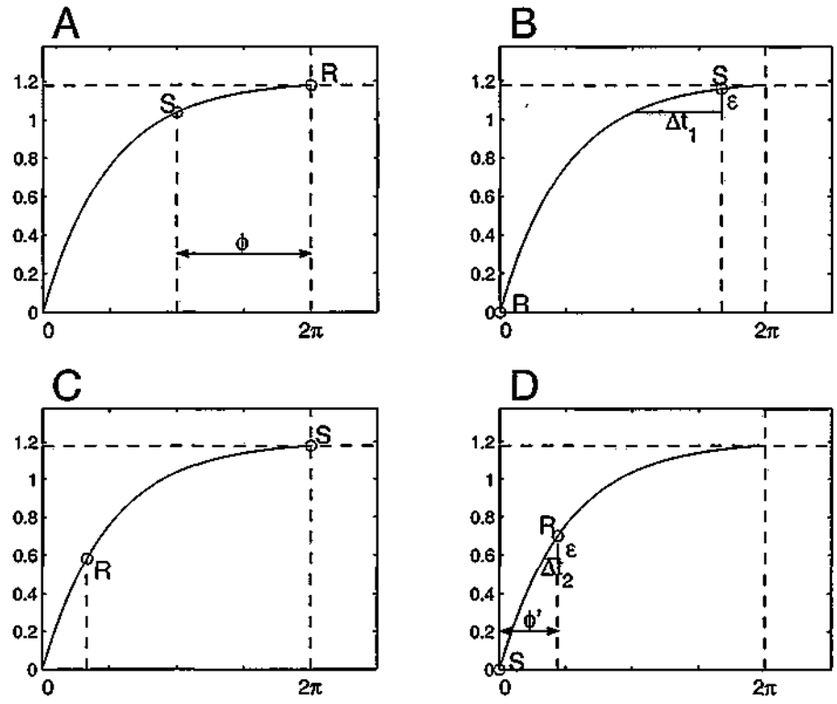

Figure 4.18: Synchronization of two Peskin oscillators. After the first spike of the two oscillators, the phase difference between them decreases form ϕ to ϕ'. Repetition of this process will lead to a synchronized state.

4.5.2 A network of spiking oscillators for binary image segmentation

Due to the facility of Peskin oscillators to reach a global synchronized state, I use them as the basic elements of the neural network. For each pixel in the binary image I consider one oscillator (figure 4.19A-B), which is described by the equation:

$$\frac{dV}{dt} = -\gamma V + I_{ext} \tag{4.27}$$

where $\gamma = 0.1$ and the external current is $I_{ext} = 0.12$ if the oscillator is connected to a white pixel and $I_{ext} = 0$ if it is connected to a black pixel. The spiking threshold is $V_{th} = 0.199$, and the reset potential is $V_{reset} = 0$. With this disposition only

neurons that are connected to a white pixel in the image display spiking activity (see figure 4.19B). The rest of neurons will stay at the equilibrium potential $V_{eq} = 0$. I will consider here only local coupling, instead of the global coupling considered by [98, 88]. Each neuron is connected only to the neurons in some neighborhood around it, with a constant coupling strength $\epsilon = 0.002$. Here I have considered nearest neighbor coupling (figure 4.19C).

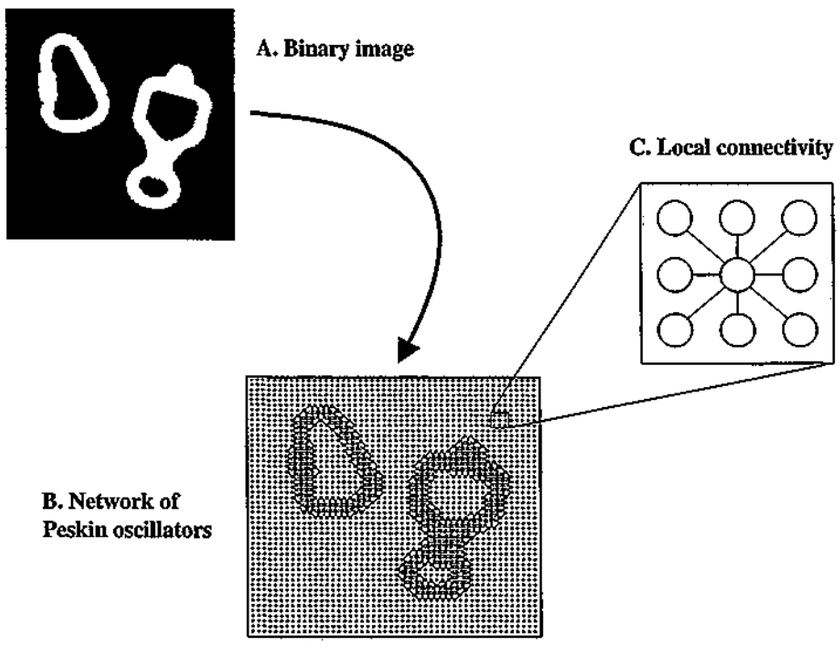

Figure 4.19: Network of Peskin oscillators for binary image segmentation. A. The binary image serves as input to the network. The resolution of the original image is reduced to 40×40 to match the network dimensions. B. Network of 40×40 oscillators, connected one to one to the image pixels. Only those connected to a white pixel (shown as red circles) will display oscillatory activity. C. Connection scheme. Each oscillator is connected to its 8 nearest neighbors.

The reason for considering only local coupling is two-fold. On the one hand a global connection scheme seems not to be biologically plausible. In general, the neuron's axonal and dendritic trees tend to spread out into a limited area around the cell, and so most synaptic contacts are local. On the other hand, a full network connection scheme will produce indiscriminate synchronization of all the neurons

responding to active pixels in the image. In this sense a local coupling scheme seems to be better since it will provide synchronization only among neuron groups that are responding to single connected components in the binary image.

The subject of global synchrony in oscillator networks with only local coupling has been studied by Wang [125]. To achieve synchronization, he had to introduce a weight normalization condition that compensates the weaker coupling for oscillators in the network borders. For this purpose he allowed dynamic modification of connection weights on a fast time scale [83]. König and Schillen [59] also considered the problem, and found a solution based on delayed coupling.

The demonstration given by Mirollo and Strogatz [88] on the global synchronization of networks of Peskin oscillators assumed global coupling. Whenever one oscillator fires, the potential of any other oscillator is increased by the coupling strength. I have not tried to prove if their result remains valid for the case of only local coupling. In this context, Hely [47] has simulated networks of Peskin oscillators with partial connectivity. He found that the time needed by the network to reach a synchronized state increases as the connectivity decreases, and that for connectivities smaller than approximately 60% the network fails to reach the synchronized state for the simulation times he considered. To overcome this problem Hely introduced a chain-reaction condition[6].

In any case, and to prevent from *strange* initial conditions that could lead to non-synchronous solutions, I have opted here by setting a network initial state that guarantees global synchronization after a few oscillations. In the network, each neuron starts at a random initial value between 0 and V_{max}^{ini} (figure 4.20A). The potential V_{max}^{ini} is chosen so that the time it takes for a neuron to evolve from $V = 0$ to $V = V_{max}^{ini}$ is small compared to the spiking period. This simple setting guarantees that when the first neurons fire the others are close to the firing threshold, so a small increase in V represents a great increase in t (the neurons approach the leaders). However when the last neurons fire, the leaders are in the steepest zone of the $V - t$ curve, so they experiment a very small increase in t. The final result is that after all the neurons have

[6]This condition implies that a neuron that reaches the threshold as a consequence of a synaptic impulse can fire in the same time step, and also can bring other neurons above the threshold. The time step is not advanced until there are no more neurons that reach the threshold.

fired the phase difference between the first and last neurons has decreased[7] (figure 4.20B). This kind of initial setting has the extra advantage that global synchronization appears within just a few cycles, which will be compatible with a fast processing.

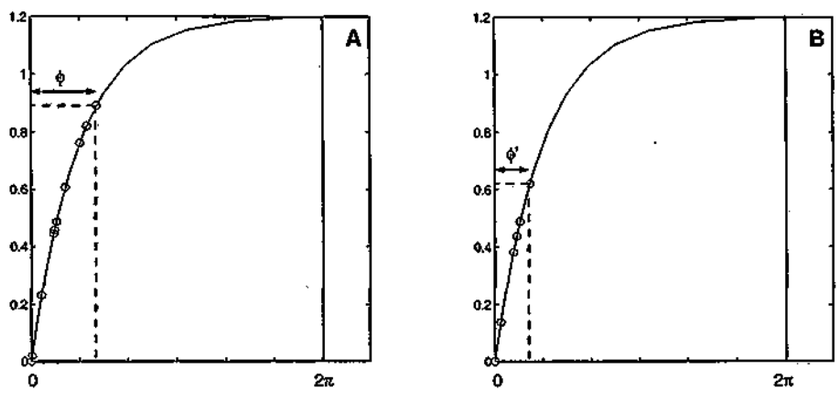

Figure 4.20: A. Initial condition for the network. All the oscillators start with a random potential uniformly distributed between 0 and $V_{max}^{ini} = 0.9$. The phase difference between the first and the last oscillators is marked as ϕ. B. After the first spike of all the network oscillators, the phase difference has decreased to ϕ'.

As a test example of the network performance, let us consider the binary image of figure 4.17. It consists of a 200 × 200 pixel black and white image with two connected components. For computational reasons, the image resolution is reduced to 40 × 40 pixels to serve as input for the network of 40 × 40 oscillators (see figure 4.19). The differential equations that describe the oscillators' activity have been solved using a Runge-Kutta (2-3) method with variable time step. The activity of neurons responding to both the left (A) and right (B) objects in the input image is shown in figure 4.21. The activity of the other neurons is not shown as they do not oscillate. As expected, within a few oscillations all the neurons responding to each of the image components reach a synchronized state. This provides the segmentation of the binary image into its two connected components. For the sake of clarity I also show in figure 4.21C the spiking times of all the 1600 neurons in the network, where red points refer to the left component, and blue points refer to the right component.

[7]Note that this may not be true for an arbitrary initial condition, for which the difference between the first and the last neurons may not be clear.

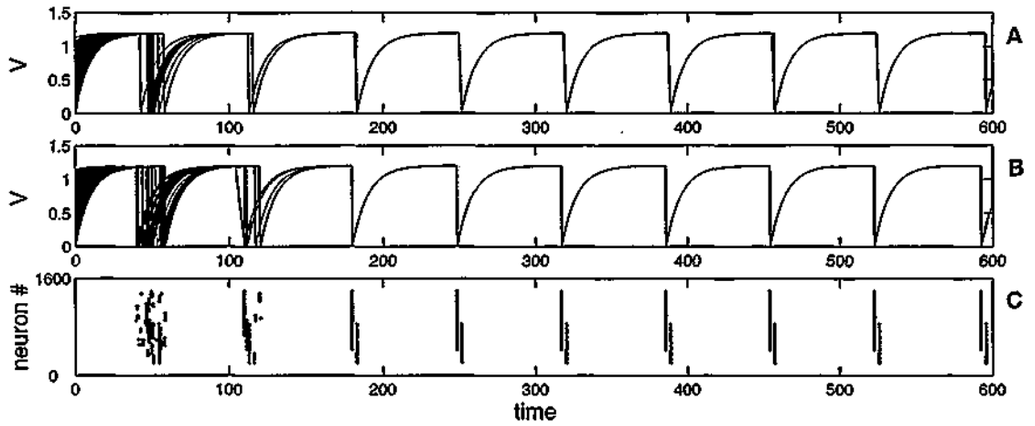

Figure 4.21: Network activity in response to the input image of figure 4.17. A. The activity of all the oscillators responding to the object on the left of the image synchronizes after a few oscillations. B. Idem for the oscillators responding to the object on the right. C. Spike raster of all the 1600 oscillators showing intra-group synchronization and inter-group desynchronization.

The different trials performed show that, using just local connections, the network reaches synchronization in a few periods without the necessity of a dynamical weight adjustment. The reason may be due to the use of pulse coupling instead of continuous coupling, and also to an initial condition with all the oscillators starting close to their resting state. The border effect seems not to affect the network synchronization, even though border oscillators receive fewer coupling pulses. In other applications, however, a dynamical adjustment of connection weights may be useful. When dealing with a continuous input, for example gray level images, different oscillator groups may be spatially contiguous, and so a kind of coupling just based on connectedness may not be sufficient.

Up to this point I have introduced a mechanism that guarantees synchronization among all the neurons that respond to a connected region in the binary image. However, to get a satisfactory segmentation it must also be guaranteed that the different neuron groups will not synchronize, so that all the neurons that fire in a very short time interval are responding to a single connected region. Our neural network is not provided with any mechanism that ensures this inter-group desynchronization, and so

starting from a random initial condition, it is not free from reaching a state in which all the neurons (responding either to the left or the right object) are synchronized (see figure 4.22A). This effect can be specially dramatic when the binary image is composed of several connected components (figure 4.22B).

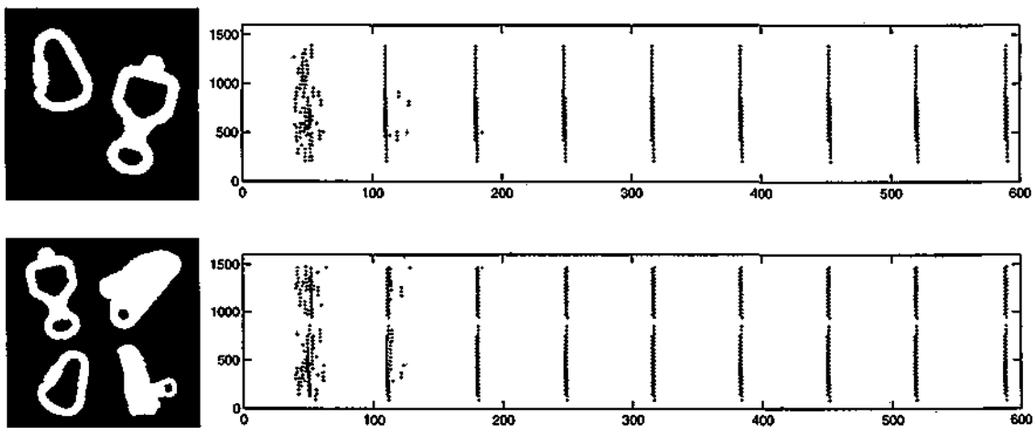

Figure 4.22: A. The same experimental conditions as in figure 4.21, but a different initial condition, may lead to a globally synchronized solution due to the lack of desynchronization mechanisms. B. When the number of connected components in the input image increases, this effect is more evident.

To avoid this unpleasant situation, Wang and Terman have proposed the use of global inhibition [126]. Their Locally Excitatory Globally Inhibitory Oscillator Network (LEGION) rapidly achieves both synchronization within groups of oscillators that are stimulated by connected regions and desynchronization among different groups. I have adopted their solution, including a global inhibitory mechanism in the network. When a neuron fires, the potential of its eight nearest neighbors is increased by ϵ; but also the potential of any other neuron in the network is decreased by a finite amount σ. Assuming the condition $\sigma << \epsilon$, whenever a neuron fires its neighbors get "closer" to it , while the rest of neurons remain almost "flashed" on their current state. The next neurons to fire will be the neighbors, and neurons belonging to a different group will "wait" until all the neurons in the first group have fired. For the simulations I took $\epsilon = 0.025$ and $\sigma = 0.0001$, and tested the network with the 4-object binary image of figure 4.22. The increased value of ϵ leads to a faster

intra-group synchronization, and the inhibitory coupling prevents from inter-group correlations (results shown in figure 4.23).

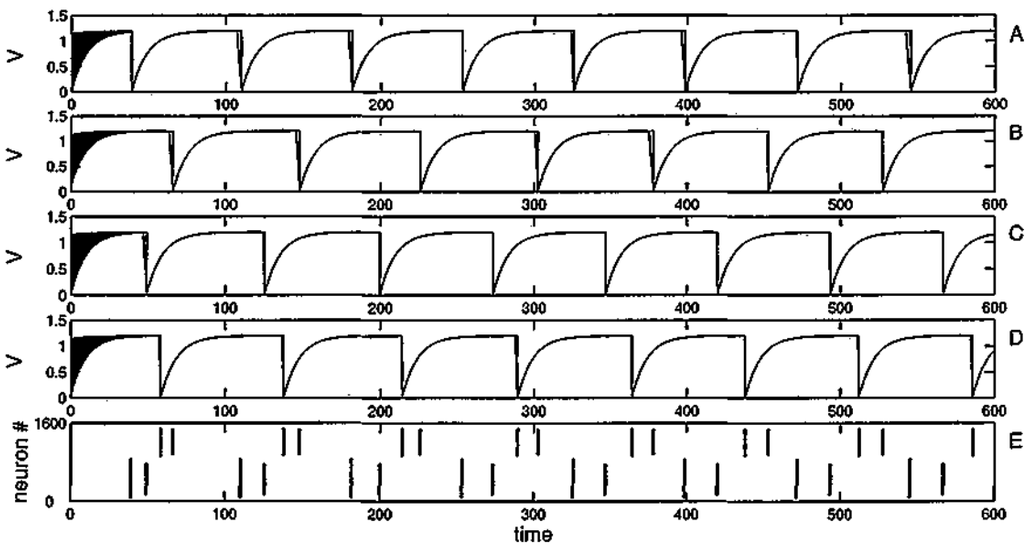

Figure 4.23: Response of the model to a binary image with four connected components. A-D: Activity of all the oscillators responding to each of the four objects. E: Spike raster showing the firing times of all network oscillators. Four different clusters are formed, each one responding to one of the connected components in the input.

4.5.3 Final considerations

The network of pulse-coupled oscillators presented here provides fast synchronization of connected oscillators and desynchronization among groups of oscillators that are not connected. This property makes it interesting for the segmentation of binary images. The key elements are local excitatory coupling together with a close-to-rest initial condition to guarantee fast intra-group synchronization; and global inhibitory coupling to guarantee inter-group desynchronization. The use of local excitation and global inhibition in oscillator networks applied to image segmentation has been previously proposed by [126]. The main difference of the present approach is the use of pulse coupling, that appears to be free of "border" problems, and does not require

from any weight normalization condition.

The role of inhibitory connections in networks of pulse-coupled oscillators has been studied by Ernst et al. [31] and Coombes and Lord [18] among others, who also considered connection delays. They have observed that with excitatory pulses and delayed interaction, networks of globally coupled oscillators showed spontaneous formation of synchronized clusters. However these clusters are unstable and tend to desynchronize. Surprisingly, inhibitory couplings formed stable clusters. Recently Rhouma and Frigui [102] have exploited this spontaneous formation of synchronized groups in problems of clustering and image segmentation. The main deficiency of these approaches is the assumption of global coupling which, apart from being biologically implausible, requires to set the connection weights in function of the input.

Here I opted for a local coupling scheme, and excitatory connections seemed to suffice for the appearance of synchronization. In contrast it is the inhibition which provides the phase separation among the different groups of synchronized oscillators. The reason for this discrepancy may reside on the absence of delays.

Local coupling has been investigated mainly in networks of oscillators described by differential equations that are continuously coupled in time. This leads to complex solutions in which some specific conditions (cf. equal weight condition [125]) may conduct to global synchronization. Networks that use pulse-coupling, however, seem to be insensitive to differences in the coupling strength for different oscillators. In the network here proposed, oscillators located at a group's border receive less effective coupling, but this does not prevent the group from synchronizing. There is so no need for dynamically rearranging connection weights.

However when dealing with more complex inputs, such as gray level images, a dynamic weight adjustment may prove advantageous. As pointed out before, in this case a connection scheme that is based only on connectedness is not useful. A common approach consists of setting the connection weights between two oscillators as a function of the similarity between the inputs to both oscillators. Another possibility would imply different network layers sensitive to different characteristics (ie. gray level ranges). My opinion is closer to this last approach, since it is not clear which kind of neural mechanisms could provide the fast weight rearrangement required by

the former.

Another point to take into consideration is the processing speed. The original theorem of Mirollo and Strogatz [88] guarantees the convergence of the pulse-coupled oscillators to a synchronized state, but says nothing about the convergence time, that could be unacceptably large for practical purposes. The initial condition I use here leads to synchronization in just a few periods, and makes the system interesting for practical applications. In particular, for binary image segmentation, the classical algorithms behave quite bad for large images [78]. The approach presented here is intrinsically parallel, and so no qualitative dependence of the computing time on the image size or the number of connected components is expected. This fact makes the system interesting for applications in computer vision and robotics. In this line some of the concepts discussed in this section have been applied to the visual system of an autonomous robot guided by a TV camera [64, 66]. The goal of this research project is to develop a control system for artificial agents that exploits ideas taken from biology. However these issues are out of the scope of this thesis.

4.6 Conclusions of the chapter

In this chapter we have come closer to the phenomenon of neural synchronization and have seen some applications to different situations. One of the main issues concerning synchronization in the brain is the binding problem. The current state of the experiments tells that a synchronization-based solution is consistent with biology, but it may not be the only possibility. Some other current ideas deal with attentional mechanisms [101], or even propose that there is no binding problem at all, for the brain can encode the information required for perception with no combinatorial explosion [40, 104].

From a practical point of view synchronization can be useful for some applications, such as clustering or image segmentation. In the last section of the chapter we saw the implementation of a neural network that achieves binary image segmentation based on spike synchronization. Oscillations may also be applied to the study of psychophysical phenomena, such as binocular rivalry.

From the different problems that I considered here, the following conclusions may be extracted:

- Synchronization in the brain must not be understood from the point of view of the theory of coupled oscillators. Synchronization between two neurons means just a correlation between the spiking times of them.

- Synchronization in ensembles of coupled oscillators is a complex subject of study, and leads to many approaches to the problem of neural synchronization that are context dependent and quite sensitive to parameters.

- To achieve spike correlations between two neurons in a neural network, only excitatory connections are needed. I have shown that a network of spiking neurons with excitatory connections is sufficient to provide the kind of correlations observed in experiments.

- No explicit mechanisms are needed to provide desynchronization among neurons as far as there is some source of noise in the model. Inclusion of noisy mechanisms of spike generation also provides more robustness to parameter settings.

- Processing times required by biology are more consistent with a spike based computation. Firing rate approaches may be useful for problems that involve different temporal dynamics.

- Synchronization based mechanisms may be useful for practical problems such as image segmentation. Its intrinsically parallel architecture may provide faster segmentation than other sequential approaches.

Chapter 5

Optimal internal representations

At the end of the first chapter the following question was raised: *Which kind of coding is being performed by the brain?* Up to now the main point discussed has been how the brain processes and transmits information, but no effort has been made to understand the kind of information it transmits. In the previous chapters I have been concerned mainly with information transmission in the brain. I have overviewed the two main hypotheses regarding neural coding, namely rate coding and spike coding. I have also discussed the temporal correlation hypothesis for the binding problem, a solution that seems consistent with the experimental evidences. Then I have studied the kind of network topologies that best match the biological constraints, under the assumption that oscillations are essential for information processing in the brain. Finally, I have shown some applications of neural networks with oscillatory activity to practical problems. All these points respond to the same background questions. Is information being carried by single spikes? Do oscillations play any role in information processing?

The other essential question that still has not been addressed is concerned with what in fact is being transmitted. At a higher level of description, and disregarding whether the brain uses spikes, rates or oscillations, we should ask for the cerebral mechanisms that lead to the development of optimal internal representations that provide a good description of the external world. This last chapter deals with this kind of issues. Much of the ideas here presented are work in progress, but I considered

it interesting to include them in this thesis, because I believe the brain can not be understood without addressing this kind of problems.

As an example let us consider the simple cells in primary visual cortex (V1). It has been shown that the receptive fields of these neurons seem to be tuned so that natural images can be represented using the fewest number of neurons [32]. Given the precision with which we can see the world, we must conclude that V1 simple cells provide a good representation of the visual world that (i) contains all the information we need to interact with the environment, and (ii) expresses it in a more convenient form. If we could understand the kind of goals these cells are pursuing, maybe we could extract first principles that provide good coding strategies for more general problems.

In the context of unsupervised learning, different approaches have been proposed for the development of optimal internal representations:

- *Redundancy reduction:* A commonly proposed approach is a mapping to a new space that conserves all the information but eliminates redundancy by expressing the input data in a more compact form [5].

- *Independent component analysis (ICA):* It is quite related to the previous point, and consists on expressing the input in a different basis such that the representational units are as much independent as possible.

- *Sparseness and overcompleteness:* Codes based on sparse (only a few units are active at a time) and overcomplete (the number of outputs is greater than the dimensionality of the input) representations have also been proposed. This kind of codes can be used to explain the response properties of simple cells in V1 based on the statistics of natural images.

The approach I will follow here is somehow related to ICA. I will look for a code that maximizes the statistical independence among the coding units. However I do not assume any knowledge about the input space and try to find a method that simultaneously performs maximization of the transmitted information and minimization of the statistical dependencies. As a proof of concept I apply the method to a classic problem in the unsupervised learning literature [34].

5.1 A simple problem of cause extraction

The generative view in machine learning takes inputs as random samples drawn from some particular, possibly hierarchical, distribution. Hence, an input scene composed of several objects might be more efficiently described using a different generator for each object rather than just one generator for the whole input (independence of objects). The goal in a multiple cause learning model is, therefore, to discover a vocabulary of *independent causes*, or generators, such that each input can be completely accounted for by the cooperative action of a few of these generators.

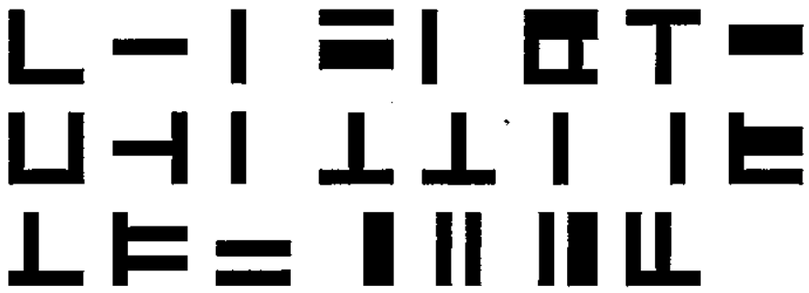

Figure 5.1: Subset of the input patterns. All of them are generated as a random combination of 5 vertical and 5 horizontal bars that appear independently with a probability $p = 0.15$.

As a first approach to the problem of cause extraction, I will consider here a problem introduced by Földiák [34]. It consists of a set of input patterns formed by a combination of horizontal and vertical bars that appear independently of each other with some probability p (figure 5.1). The goal is to code the input using the most compact form that allows reconstruction. It seems that a coding representation based on the bars is optimal, because it extracts the nature of the input. Originally, Földiák used a neural network with a combination of Hebbian and anti-Hebbian mechanisms that were able to reduce statistical dependency between representational units, while preserving information. This problem has been also addressed by other authors [109, 19] as a paradigm for multiple cause unsupervised learning. Recently, O'Reilly [97] has used a generalized recirculation algorithm in combination with inhibitory competition

and Hebbian learning for a similar problem, where it has shown to perform quite well using only a few training patterns.

Here I will address the problem from the point of view of ICA, using a neural network whose units respond to specific pixels in the input. I assume the network's objective is to provide an optimal codification of the input (figure 5.2), which means that it should be possible to reconstruct the input (X) from the information contained in the network units (Y), and at the same time useless and redundant components present in the data are eliminated. Assuming all the information about the input is important, as for this particular example, the problem reduces to finding the most compact representation of the whole input space.

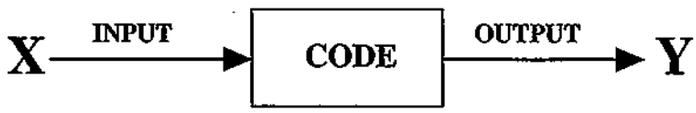

Figure 5.2: Given an input space X, the objective of the code is to provide a good representation Y that conserves all the information while minimizing the statistical dependence between the representational units.

This implies, on the one hand, that the network must be able to discriminate among all the input patterns. This, in mathematical terms, means that the mutual information between input and output is maximal, which for a discrete input space and in the absence of noise reduces to the following condition:

$$H(Y) = H(X), \tag{5.1}$$

where $H(X)$ and $H(Y)$ are the input and output entropies respectively. On the other hand, the network must be able to eliminate all the redundancy that is present in the input, finding the minimum dimension space that satisfies the information preserving constraints. This, as Barlow [5] pointed out, is equivalent to finding an internal representation in which the neurons respond to causes that are as independent as possible. The optimal solution would be to find a *factorial* code, in which the sum of individual entropies equals the output entropy:

$$S(Y) \equiv \sum_{i=1}^{n} H(Y_i) = H(Y), \tag{5.2}$$

where the sum extends to all the hidden neurons in the network. We will search for neural codes that are as discriminant and factorial as possible, which means $H(Y)$ maximization and $S(Y)$ minimization.

In this context, many approaches leading to redundancy elimination have been proposed. Barlow [5] gave a proof of equation 5.2, and applied $S(Y)$ minimization to the problem of coding keyboard characters on 7 binary outputs that occur as independently of each other as possible.

Although previous approaches are able to find good solutions to the problem of cause extraction, they generally depart from assumptions that should not be known a priori. For example, Barlow assumes that a code is known, and reduces the problem to re-ordering the alphabet to find the minimum sum of bit entropies; and in [34, 109, 19] the number of coding units is forced to be equal to the number of hidden causes, which highly reduces the problem complexity.

Here I propose a different approach that is able to find a discriminant and factorial (DF) code whenever such a DF code exists [68]. A new measure based on a proper combination of $H(Y)$ and $S(Y)$ will be introduced in the next section and applied to the problem.

5.2 New measure of independence and discriminability

The two previous conditions required for a good codification of the input space, namely discriminability (maximum $H(Y)$) and factoriality (minimum $S(Y)$), will be combined now into a single condition. I will define a new measure on the output space, $M(Y)$, as the quotient between the squared output entropy and the sum of individual output entropies:

$$M(Y) = \frac{H(Y)^2}{S(Y)} = \frac{H(Y)^2}{\sum_{i=1}^{n} H(Y_i)} \tag{5.3}$$

This quantity is maximal when the network is performing a DF codification of the input. In this case $M(Y)$ takes precisely the value $H(X)$. I will prove three properties that guarantee these results under the conditions of no noise and discrete input space:

1. *The quantity $M(Y)$ is upper bounded by the input entropy $H(X)$.*

   Proof: from the two conditions $H(Y) \leq H(X)$ (no noise and discrete input space) and $H(Y) \leq S(Y)$ (statistical dependence), the result $M(Y) \leq H(X)$ is straightforward.

2. *If the code is factorial and discriminant, then $M(Y) = H(X)$.*

   Proof: we have that $H(Y) = H(X)$ (discriminant code) and $H(Y) = S(Y)$ (factorial code). A simple substitution in the definition of M leads to $M(Y) = H(X)$.

3. *If $M(Y) = H(X)$, then the code is factorial and discriminant.*

   Proof: since $H(Y) \leq S(Y)$ (statistical dependence), we have $M(Y) \leq H(Y)$ and so $H(X) \leq H(Y)$; but also $H(Y) \leq H(X)$ (no noise and discrete input space), so necessarily $H(X) = H(Y)$ and the code is discriminant. Using this last identity, we can write $M(Y) = H(X) = H(X)H(Y)/S(Y)$, so $H(Y) = S(Y)$ and the code is factorial.

These three properties guarantee that, if a factorial and discriminant code exists, we can always find it by maximizing $M(Y)$.

5.3 Results

To test the new measure I will apply it to the previously described problem. The goal is to discriminate among different stimuli composed of vertical and horizontal bars

that appear randomly with a specific probability p. Here I will use an input space of 5×5 pixels and a probability $p = 0.15$ (figure 5.1 shows some of the input patterns). Note that all of them are constructed from a set of only 10 generators. Learning these generators would lead to an optimal coding.

To tackle the problem, a neural network with $N = 20$ units is used. Each unit is connected to the input layer with weights that are either 0 or 1. In other words, the receptive field of a given neuron is defined by a 5×5 binary matrix that determines the region in the input space it responds to. Let us remark that the number of neurons in the network exceeds the number of hidden causes. We expect that the network self-organizes in order to use the minimum number of neurons to explain the input. This is in contrast to other algorithms, such as backpropagation, that tend to use all the available resources.

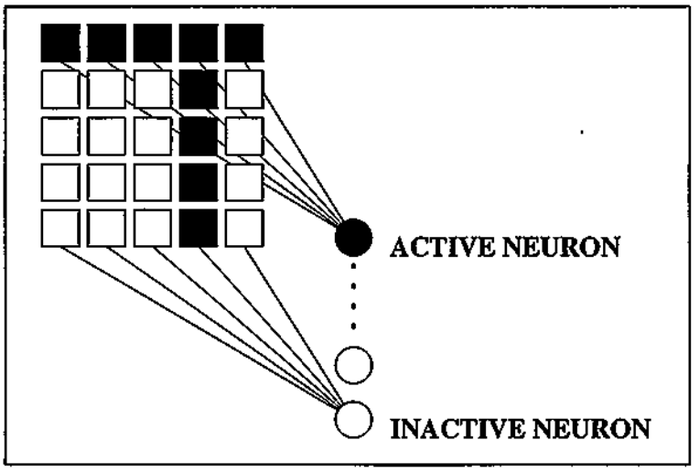

Figure 5.3: Neural network structure. Each of the hidden units responds to a subregion of the input space (its receptive field) determined by a 5×5 binary matrix. The figure shows the receptive fields (only connections with value 1 are drawn) and the corresponding states of two neurons for a given input pattern.

The neuron dynamics is not relevant for our present analysis, since the main interest is focused on finding the receptive fields that best account for the input structure. So I will simply assume that the neuron is active if its receptive field is stimulated, and silent otherwise. In figure 5.3 I show a scheme of the network

structure.

Different receptive field configurations will produce different codes. The receptive field space was searched for the code that best satisfies the discriminability and factoriality criteria, i.e. maximizes $M(Y)$. The search was performed using genetic algorithms with the standard PGAPack libraries [73]; results are shown in figures 5.4 and 5.5. Figures 5.4A and 5.4B show the evolution of $H(Y)$, $M(Y)$ and $S(Y)$ as the genetic algorithm performs maximization of $H(Y)$ and $M(Y)$ respectively. In the first case, a fast convergence of $H(Y)$ to its maximum allowed value ($H(X) = 4.14$) is observed. However $S(Y)$ does not decrease, which is a clear indicator of the lack of independence between neurons. In the second case, $H(Y)$ converges more slowly ($H(X) = 4.18$), but the small difference between $H(Y)$ and $S(Y)$ indicates that the network is performing an almost factorial codification.

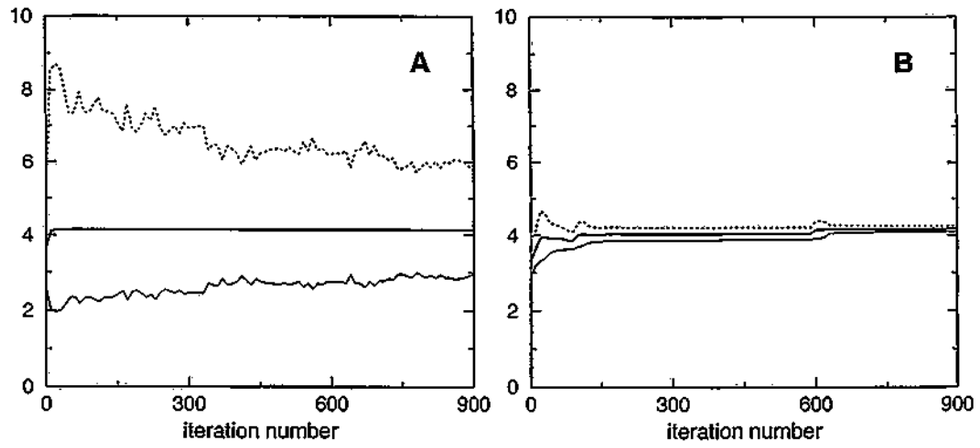

Figure 5.4: $H(Y)$ (solid thick), $M(Y)$ (solid), and $S(Y)$ (dotted) versus iteration number of the genetic algorithm for $H(Y)$ maximization (A) and $M(Y)$ maximization (B). In both cases we used a neural network with $N = 20$ hidden units.

Maximization of $H(Y)$ leads to a code that is able to represent all the input patterns, but it is quite far from being factorial (final receptive fields are shown in figure 5.5A). This problem can be overcome by forcing the network to have $N = 10$ neurons (results not shown). In this case there is only one discriminant solution, that implies knowledge of the input generators. When maximizing $M(Y)$, however, the

network uses exactly 10 neurons (figure 5.5B) whose receptive fields resemble each of the hidden causes. The other 10 neurons are not necessary and the network makes no use of them.

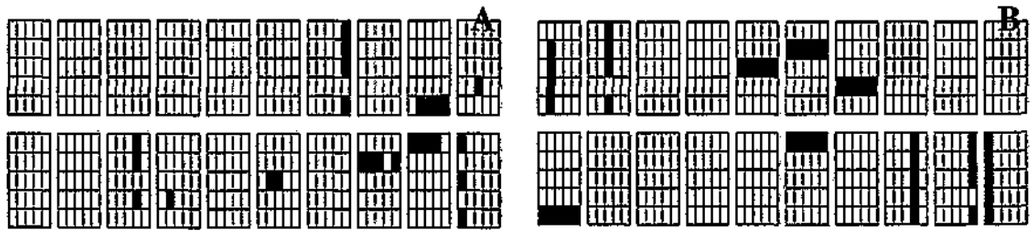

Figure 5.5: A. Receptive fields after maximization of $H(Y)$. B. Receptive fields after maximization of $M(Y)$. The gray level indicates the probability of activation of a neuron with such a receptive field. Neurons with a dark receptive field are stimulated more often than neurons with a brighter one.

5.4 Discussion

I have introduced a new quantity, $M(Y)$, that measures the degree of discriminability and factoriality of a code. In the absence of noise, this quantity turns out to be equal to the input entropy ($M(Y) = H(X)$) for a code that is both discriminant and factorial, whereas $M(Y) < H(X)$ for any other code. So, whenever a DF code exists for a given input space, maximization of $M(Y)$ will find it with no need of extra assumptions. This approach improves some previous results [5, 34, 109, 19, 97] in which some additional information about the input structure is assumed. Other research approaches related to learning factorial representations [48, 71, 95] and nonlinear dimensionality reduction [108, 115] emphasize different aspects of the problem.

I would like to remark that the work shown here must not be seen as a solution, but just as the first stage on the development of the problem. A full theoretical framework for optimal representations extraction should address at least all of the following issues, which are part of ongoing and future work:

- Noise: The absence of noise at the input led us to the discriminability condition 5.1, that greatly simplifies the calculations. When noise is present some different

expression in terms of the mutual information between the output and the input could be derived. Some preliminary experiments have shown sensitivity of the results to noise.

- Non factorial input spaces: A main assumption of the model is that a factorial code always exists for the problem under consideration. However this is not the case for most practical problems. When a totally factorial code does not exist, maximization of M does not guarantee even a discriminant code. A common solution in this cases is to reduce the search space to all the codes that are discriminant and find that with the smallest $S(Y)$ (the most factorial among the discriminant codes). This is the approach of classical ICA [8]. Our approach differs from it in that the search is not restricted to discriminant codes. The algorithm must therefore perform the search simultaneously in terms of discriminability and factoriality. However, for non factorial input spaces a different measure must be derived.

- Local computation: The approach followed here involves computationally expensive entropy calculations that make it difficult to apply to most real problems. Some approximation to $M(Y)$ involving only local computations seems to be essential. From a biological point of view, it is not plausible that the neurons explore the whole space to search for the optimal code. They are performing an optimal coding based mainly on local connections.

- Task orientation: The optimality of the representation must not be seen as an absolute property. Which internal representation is best to achieve an objective must depend on the objective, and this should be taken into account when constructing the model.

Finally, I will add that some recent approaches [6, 96] point to the fact that maybe redundancy reduction is not always the best strategy. Redundancy reduction ideas come from the field of information theory, where the objective is to transmit information at the lowest cost. From this point of view, a compact code results interesting. In a biological context, however, redundancy could be useful to learn

the statistical regularities of the environment [6]. All these concerns should also be taken into account when trying to understand the kind of processing that the brain performs.

Chapter 6

Conclusions

This thesis has dealt with many aspects concerning information processing in neural systems, from neural network topologies to the extraction of optimal representations. The different issues were sometimes motivated by particular facts, but all of them converge into a more global problem: which strategies are used by the brain to perform so well in the complex perceptual tasks it is involved. They just emphasize different aspects of the problem, and a good theory of the brain must unavoidably address all of them.

Nowadays we are still too far from such a theory, and I just hope this work has added some hints to the search. I have inquired about neural network topologies, motivated by the discovery of the small-word graphs, a kind of graphs placed somewhere between order and randomness. The response properties of neural networks with biologically plausible neuron models in their nodes were studied in terms of the topology. These properties showed to be highly topology dependent. In particular, I have shown that small-word network topologies may be a good choice for neural networks that pursue oscillatory activation and fast response to external stimuli.

A general conclusion to be extracted from this study is that topologies must be taken into consideration when designing neural networks, at least at the same level as neuron dynamics. A good choice of the network architecture may be more important than a very specific neuron dynamics. The study presented here dealt with excitatory connections. Open work involves studying the role of inhibitory connections. In

natural systems, these inhibitory connections could provide a means for dynamically rearranging the network topology.

I have studied oscillations and spike synchronization in neural systems, and applied them to different problems: binding, binocular rivalry and image segmentation. Synchronization in the brain has often been modeled from the point of view of continuously coupled oscillators. However this kind of approaches might not be adequate to understand spike correlations between neurons. A simple model in which the spike generation is assumed to be a random process with time varying probability has been introduced. It seems to be more suitable to describe the spike correlations observed in experiments, and suggests that: (i) spike correlations are a direct consequence of excitatory connections between neurons; and (ii) the intrinsically noisy processes of spike generation prevent from "non-desired" correlations.

Oscillations of neural activity on a much slower time scale may be adequate for describing the phenomenon of binocular rivalry. A simple model of competition with firing rate adaptation was proposed. It is able to generate an oscillatory alternation of two neuron populations that compete for dominance, and the calculated histogram of phase durations is in full accordance with experimental results.

The problem of binary image segmentation was addressed from a synchronization based point of view. A network of pulse coupled oscillators with local excitatory connections is able to quickly achieve global synchronization for a wide range of initial conditions. When using a binary image as input to the network, groups of oscillators responding to each connected component in the image engage in synchronized oscillations. A mechanism of global inhibition guarantees desynchronization between different groups. This approach is more robust than similar approaches based on continuously coupled oscillators and converges within just a few oscillations. Its intrinsically parallel structure leads to expect small dependence of segmentation time on the image size or the number of connected components. Future work includes dealing with gray level images by using different layers specific for different intensities, with interlayer connections that account for connectedness.

Finally, turning to more abstract problems also related to the brain behavior, I have tackled the problem of finding optimal representations of an input space. I

considered discrete and factorial input spaces in the absence of noise, and introduced a quantity whose maximization leads to factorial and discriminant codes. This is an open research line whose future objectives involve mainly dealing with noise and task oriented problems.

Appendix A

Introducción

A.0.1 El problema de la percepción

Uno de los problemas más difíciles a los que se enfrenta el cerebro es la percepción del entorno. Constantemente estamos percibiendo e identificando miles de imágenes, sonidos y olores, y lo hacemos aparentemente sin esfuerzo. El análisis de una imagen, o el reconocimiento de una cara, son problemas fáciles para nuestro cerebro. La verdadera dimensión del problema aparece cuando se intenta construir máquinas capaces de ver, oir u oler con la misma precisión y fiabilidad con que lo hace el cerebro, y con la misma velocidad. Imaginemos una de las situaciones típicas a las que se enfrenta nuestro cerebro: estamos buscando a un amigo entre mucha gente. En este proceso, millones de bits de información están llegando a nuestro cerebro procedentes de la retina. El cerebro tiene la delicada tarea de organizar toda esta información lo más rápidamente posible para darnos una respuesta: nuestro amigo volverá a llegar tarde. Para transformar la representación "fotográfica" del mundo que se forma en la retina en la representación cortical más abstracta, el cerebro ha de enfrentarse a los siguientes problemas:

- *Representación.* El cerebro debe codificar internamente la realidad exterior. El código ha de ser eficiente y debe conservar toda la información relevante acerca del entorno.
- *Segmentación.* La información ha de ser separada en sus distintas componentes.

- *Reconocimiento.* El cerebro ha de ser capaz de reconocer los distintos estímulos que recibe. El reconocimiento de objetos es un problema generalmente muy difícil debido a la variabilidad con que los objetos aparecen en el mundo.

Para añadir un grado más de dificultad al problema, el cerebro suele estar limitado en el tiempo. Típicamente, el reconocimiento de objetos comunes conlleva varias decenas de milisegundos, mucho menos que el requerido por la mejor de las máquinas.

En esta tesis, se abordarán distintos temas relacionados con el procesamiento de la información que realiza el cerebro. Algunas de las preguntas que se plantean a lo largo de los distintos capítulos son:

- Cómo procesa el cerebro la información acerca del entorno.
- Cómo soluciona el cerebro el problema del "binding".
- Qué tipo de codificación es el más conveniente para obtener una adecuada representación interna del mundo exterior.

A.0.2 La solución del cerebro

En relación a la primera pregunta, veamos cómo se organiza el cerebro. Los siguientes principios organizativos de la corteza cerebral son esenciales:

- *Estructura por capas y jerárquica.* La corteza visual está organizada en diferentes capas que responden a estímulos cada vez más complejos.
- *Procesamiento paralelo.* El cerebro procesa la información a través de distintos canales que codifican distintas características de los estímulos.
- *Conexiones laterales y recurrentes.* Casi todas las conexiones entre diferentes áreas corticales son recíprocas, y además existen muchas conexiones laterales entre neuronas en un área dada.
- *Aprendizaje.* Las neuronas son capaces de modificar sus conexiones para adaptarse a distintas situaciones.

Dados estos aspectos de la organización cortical, podemos observar que el cerebro hace uso de dos estrategias muy importantes. Por un lado, descompone la información en elementos más simples que son más fáciles de procesar, y gradualmente reconstruye la información a través de una jerarquía de áreas. Esta es una estrategia del tipo *divide y vencerás*. Por otro lado, distribuye la información en paralelo utilizando diferentes poblaciones de neuronas que codifican características distintas. Esto proporciona una representación combinatoria que precisa de menos unidades para codificar, y además permite un procesamiento más rápido.

A.0.3 El problema del "binding"

Suponiendo que el cerebro procesa la información en paralelo, surge el problema de cómo asociar las diferentes características que están siendo procesadas por áreas distintas. Se han propuesto soluciones para este problema desde distintos puntos de vista. Existen enfoques basados en mecanismos de atención [101], enfoques basados en sincronización a nivel de disparos [43], e incluso hay investigadores que opinan que el "binding" no es un problema real para el cerebro [104]. En esta tesis se supone la validez de la hipótesis de la correlación temporal [83, 43], según la cual todas las neuronas que responden a las diferentes características de un estímulo común se sincronizan con una precisión de milisegundos.

A.0.4 Entropía, información, representaciones óptimas y códigos factoriales

Aunque pudiéramos llegar a conocer las respuestas a las dos primeras preguntas que se plantearon al comienzo, aún tendríamos que resolver numerosos problemas relacionados con la útltima, es decir, con el desarrollo de representaciones óptimas. Como regla general, la teoría de la información ha sido usada para intentar comprender el tipo de procesamiento que realizan las neuronas. La maximización de la información mútua entre la entrada y la salida se ha propuesto en numerosas ocasiones como uno de los objetivos. En cualquier caso no debe ser el único, puesto que una simple copia de la entrada maximiza la información mútua, y sin embargo esto no contribuye demasiado

al procesamiento de la información. En el contexto del aprendizaje no supervisado, ha habido muchos intentos por desarrollar sistemas artificiales que desarrollen representaciones internas óptimas básandose en la minimización de la redundancia [5], el análisis de componentes independientes [8], o el uso de representaciones dispersas y "sobrecompletas" [96]. Algunos de estos planteamientos han dado lugar a primeros principios que permiten explicar, por ejemplo, los campos receptivos de las neuronas de V1 a partir de la estadística de las imágenes naturales [95].

A.0.5 Objetivos de la tesis

Los objetivos concretos de esta tesis se describen en los siguientes puntos.

I. Estudio de las topologías de redes neuronales en relación a oscilaciones y velocidad de respuesta

El estudio está motivado por los siguientes aspectos:

- La mayoría de los sistemas neuronales presentan tanto oscilaciones de actividad como respuestas muy rápidas.
- Otros modelos se han centrado principalmente en el estudio de la dinámica, tanto neuronal como sináptica, sin prestar atención a la topología de la red. Normalmente sólo se consideran topologías totalmente ordenadas o totalmente desordenadas.
- Recientemente se ha demostrado que muchos fenómenos reales descritos mediante grafos no pueden ser bien descritos por topologías ordenadas o aleatorias. Un nuevo tipo de topologías, denominadas "small-world" [128, 129], parece ser más apropiado para describir estos fenómenos. Esté podría ser el caso para las redes neuronales.

El estudio se desarrolla a través de las siguientes etapas:

- Estudio de la respuesta de una red neuronal en función de la topología para modelos neuronales con excitabilidad de tipo 1.

- Estudio de la respuesta de una red neuronal en función de la topología para modelos neuronales con excitabilidad de tipo 2.
- Comparación de los resultados para los dos tipos de excitabilidad.

El estudio ha conducido a los siguientes resultados:

- En relación a la excitabilidad de tipo 1:
  - Las redes ordenadas proporcionan oscilaciones de actividad, pero la respuesta es muy lenta.
  - Las redes aleatorias responden de forma muy rápida, pero no son capaces de producir oscilaciones de actividad.
  - Las redes "small-world" proporcionan tanto oscilaciones de actividad como respuesta rápida.
- En relación a la excitabilidad de tipo 2:
  - La respuesta es en general lenta, excepto para topologías aleatorias.
  - Hay un alto grado de sincronización independientemente de la topología.
  - La frecuencia de disparo de las neuronas depende mucho de la topología.

II. Estudio de las oscilaciones y la sincronización en la actividad neuronal, y aplicaciones a "binding", rivalidad binocular y segmentación

El estudio está motivado por los siguientes aspectos:

- En muchos sistemas neuronales se han observado oscilaciones de la actividad.
- Existen evidencias experimentales consistentes con la idea de que el cerebro podría usar la sincronización para asociar neuronas respondiendo a diferentes características de un mismo estímulo [25, 41, 42].

- Existen evidencias experimentales de una implicación directa de las oscilaciones en el procesamiento de la información en el sistema olfativo de los insectos [70, 81, 82].

- Los sistemas biológicos funcionan mucho mejor que los artificiales en problemas reales como la visión. Enfoques basados en la biología podrían conducir a mejoras en algunas aplicaciones reales.

El estudio se desarrolla a través de las siguientes etapas:

- Construcción de un modelo simplificado del sistema visual, con las siguientes características:

  - Hay distintos canales para procesar distintas características.
  - Las unidades son poblaciones de neuronas descritas por ecuaciones de campo medio.
  - La asociación de las distintas características se realiza mediante correlación temporal.

- Extensión del modelo anterior a un modelo de neuronas que disparan, de modo que:

  - Se puedan reproducir las correlaciones entre neuronas medidas experimentalmente.
  - Los tiempos involucrados sean más consistentes con la velocidad de procesamiento en el cerebro.

- Extensión del modelo inicial al estudio de la rivalidad binocular.

- Desarrollo de un mecanismo de segmentación basado en una red de neuronas de integración y disparo, y aplicación del mismo a la segmentación de imágenes binarias.

El estudio ha conducido a los siguientes resultados:

- Un modelo probabilístico de neurona que reproduce los experimentos de sincronización en la corteza cerebral. Las simulaciones sugieren que las correlaciones entre neuronas pueden ser debidas simplemente a conexiones excitadoras, y que las decorrelaciones pueden deberse a la naturaleza, ruidosa, de la generación de disparos.

- Un modelo de rivalidad binocular basado en competición entre poblaciones de neuronas con adaptación de la frecuencia de disparo. Los resultados en cuanto a la duración de la fase dominante están en pleno acuerdo con los experimentos.

- Una red de osciladores acoplados por impulsos que segmenta imágenes binarias. Se basa en conexiones excitadoras a nivel local e inhibición a nivel global. El uso de osciladores acoplados por impulsos aporta una convergencia más rápida y una mayor robustez que en otros modelos basados en acoplamiento continuo.

III. Estudio de la extracción de causas escondidas y el desarrollo de representaciones internas óptimas

El estudio está motivado por los siguientes aspectos:

- El cerebro utiliza representaciones internas que responden a la estadística del espacio de entrada [32].

- Generalmente, un espacio de entrada se describe mejor en base a un conjunto de generadores o causas escondidas.

El estudio se desarrolla a través de las siguientes etapas:

- Análisis de las propiedades deseables en un código: discriminabilidad y factorialidad.

- Desarrollo de una medida para la calidad de un código que combine las dos propiedades anteriores.

- Aplicación de la medida a un problema de ejemplo.

El estudio ha conducido a los siguientes resultados:

- Una nueva medida que tiene en cuenta la discriminabilidad y la factorialidad del código. Para espacios de entrada factoriales y discretos, la maximización de esta medida conduce a códigos óptimos (en ausencia de ruido).

Appendix B

Conclusiones

A lo largo de esta tesis se han tratado diversos aspectos relacionados con el procesamiento de la información en los sistemas neuronales, desde la topología de una red neuronal hasta la extracción de representaciones internas óptimas. Los distintos temas desarrollados han sido, en algunos casos, motivados por hechos específicos, pero todos ellos apuntan hacia un problema global: el estudio del tipo de estrategias que utiliza el cerebro para abordar las complejas tareas en las que está implicado. Cada uno recalca un aspecto distinto del problema, y cualquier teoría del cerebro debería inevitablemente abordar todos ellos. Hoy en día estamos aún muy lejos de dicha teoría, y espero que este trabajo haya aportado nuevas pistas para ayudar en su búsqueda.

Motivado por el reciente descubrimiento de los grafos "small-world", a caballo entre el orden y el azar, he investigado los efectos de la topología en la respuesta de una red neuronal. En redes neuronales con modelos de neuronas biológicamente plausibles en sus nodos, estas propiedades han mostrado ser áltamente dependientes de la topología. En concreto, he mostrado que las topologías de tipo "small-world" podrían ser una buena elección en redes neuronales que persiguen una activación oscilatoria y una respuesta rápida ante los estímulos externos.

Una conclusión general a extraer de este estudio es que las topologías deberían ser tenidas en cuenta a la hora de diseñar redes neuronales, por lo menos al mismo nivel que la dinámica neuronal. Una elección adecuada de la arquitectura de la

red neuronal podría ser más importante incluso que una dinámica neuronal muy específica. El estudio aquí presentado utiliza únicamente conexiones excitadoras. Otras líneas abiertas de investigación incluyen el estudio del papel desempeñado por las conexiones inhibidoras. En los sistemas biológicos, estas conexiones inhibidoras podrían proporcionar una manera de reajustar dinámicamente la topología de la red neuronal.

He estudiado las oscilaciones y la sincronización entre disparos en sistemas neuronales, buscando aplicaciones a diferentes problemas: "binding", rivalidad binocular y segmentación de imágenes. Los procesos de sincronización en el cerebro han sido frecuentemente estudiados desde el punto de vista de osciladores con acoplamiento continuo. Sin embargo, este tipo de enfoque podría no ser adecuado para describir las correlaciones entre las neuronas. He introducido un modelo en el que la generación de un disparo se considera un proceso aleatorio con probabilidad variable en el tiempo. Este modelo parece ser más apropiado para describir las correlaciones entre disparos observadas en los experimentos, y sugiere que (i) las correlaciones son una consecuencia directa de las conexiones excitadoras entre las neuronas; y (ii) los procesos, intrínsecamente ruidosos, involucrados en la generación de los disparos son suficientes para evitar correlaciones "no deseadas".

Oscilaciones de la actividad neuronal en una escala de tiempo mucho más lenta, podrían ser apropiadas para describir fenómenos como la rivalidad binocular. En este contexto, he propuesto un modelo de competición entre poblaciones neuronales con adaptación de la frecuencia de disparo. El modelo es capaz de producir una alternancia entre dos poblaciones neuronales que compiten, y el histograma de fases obtenido coincide con los resultados experimentales.

El problema de la segmentación de imágenes binarias se ha abordado desde un punto de vista basado en la sincronización. Una red de osciladores acoplados por impulsos, con conexiones locales excitadoras, es capaz de alcanzar rápidamente un estado de sincronización gobal para un amplio rango de condiciones iniciales. Cuando se usa una imagen binaria como entrada, se forman distintos grupos de osciladores sincronizados que responden a cada una de las componentes conexas en la imagen. Un mecanismo de inhibición global garantiza la desincronización entre distintos grupos.

Este enfoque es más robusto que otros basados en osciladores con acoplamiento continuo, y converge en tan sólo unas cuantas oscilaciones. La estructura intrínsecamente paralela de la construcción lleva a esperar escasa dependencia del tiempo de segmentación con el tamaño de la imagen o el número de componentes conexas. Entre los objetivos futuros se incluye el análisis de imágenes con distintos niveles de gris usando distintas capas específicas para diferentes intensidades.

Finalmente, atendiendo a problemas más abstractos relacionados con el comportamiento cerebral, he abordado el problema de hallar las representaciones óptimas para describir un espacio de entrada. Considerando espacios de entrada discretos y factoriales en ausencia de ruido, he introducido una medida cuya maximización lleva a códigos factoriales y discriminantes. Esta es una línea de investigación abierta, cuyos objetivos futuros incluyen el estudio de problemas ruidosos y dependientes de la tarea.

Bibliography

[1] L. F. Abbott. *Firing rate models for neural populations.* In: Neural Networks: From Biology to High-Energy Physics (O. Benhar, C. Bosio, P. Del Giudice and E. Tabet, eds.), pp. 179-196. ETS Editrice, Pisa (1991).

[2] L. Adamic. *The small world web.* Lect. Notes Comput. Sci. **1696**, 443-452, Springer, New York (1999).

[3] E. D. Adrian. *The impulses produced by sensory nerve endings.* J. Physiol. **61**, 49-72 (1926).

[4] H. B. Barlow. *Single units and cognition: a neurone doctrine for perceptual psychology.* Perception **1**, 371-394 (1972).

[5] H. B. Barlow, T. P. Kaushal and G. J. Mitchison. *Finding minimum entropy codes.* Neural Comp. **1**, 412-423 (1989).

[6] H. B. Barlow. *Redundancy reduction revisited.* Network: Comput.Neural Syst. **12**, 241-253 (2001).

[7] A. Barrat and M. Weigt. *On the properties of small-world network models.* Eur. Phys. J. B **13**, 547-560 (2000).

[8] A. J. Bell and T. J. Sejnowski. *An information-maximization approach to blind separation and blind deconvolution.* Neural Comp. **7**, 1129-1159 (1995).

[9] W. Bialek, F. Rieke, R. de Ruyter van Stevenick and D. Warland. *Reading a neural code.* Science **252**, 1854-1857 (1991).

[10] R. Blake. *A neural theory of binocular rivalry.* Psychol. Rev. **96**, 145-167 (1989).

[11] R. Blake and N. Logothetis. *Visual competition.* Nature Rev. Neurosci. **3**, 1-11 (2002).

[12] B. Bollobás. *Random graphs.* Academic Press, New York (1985).

[13] V. Bondarenko and T. R. Chay. *Desynchronization and synchronization processes in a randomly coupled ensemble of neurons.* Phys. Rev. E **58**, 8036-8039 (1998).

[14] P. C. Bush and R. J. Douglas. *Synchronization of bursting action potential discharge in a model network of neocortical neurons.* Neural Comp. **3**, 19-30 (1991).

[15] K. R. Castleman. *Digital image processing.* Prentice Hall, Upper Saddle River, NJ, pp. 447-485 (1996).

[16] T. Chawanya, T. Aoyagi, I. Nishikawa, K. Okuda and Y. Kuramoto. *A model for feature linking via collective oscillations in the primary visual cortex.* Biol. Cybern. **68**, 483-490 (1993).

[17] K. Chen and D. L. Wang. *A dynamically coupled neural oscillator network for image segmentation.* Neural Networks **15**, 423-439 (2002).

[18] S. Coombes and G. J. Lord. *Desynchronization of pulse-coupled integrate-and-fire neurons.* Phys. Rev. E **55**, R2104-R2107 (1997).

[19] P. Dayan and R. S. Zemel. *Competition and multiple cause models.* Neural Comp. **7**, 565-579 (1995).

[20] G. Deco and J. Zihl. *Top-down selective visual attention: a neurodynamical approach.* Vis. Cog. **8**, 118-139 (2001).

[21] J. DeFelipe. *Microcircuits in the brain.* Lect. Notes Comput. Sci. **1240**, 1-14 (1997).

[22] A. Destexhe, Z. F. Mainen and T. Sejnowski. *An efficient method for computing synaptic conductances based on a kinetic model of receptor binding.* Neur. Computat. **6**, 14-18 (1994).

[23] E. Diaz-Caneja. *Sur l'alternance binoculaire.* Ann. D'Oculistique **165**, 721-731 (1928).

[24] J. Duncan and G. Humphreys. *Visual search and stimulus similarity.* Psychol. Rev. **96**, 433-458 (1989).

[25] R. Eckhorn, R. Bauer, W. Jordan, M. Brosch, W. Kruse, M. Munk and H. J. Reitboeck. *Coherent oscillations: a mechanism of feature linking in the visual cortex?* Biol. Cybern. **60**, 121-130 (1988).

[26] A. K. Engel, P. König, A. K. Kreiter and W. Singer. *Synchronization of oscillatory neuronal responses between striate and extrastriate visual cortical areas of the cat.* Proc. Natl. Acad. Sci. USA **88**, 6048-6052 (1991).

[27] A. K. Engel, P. König, A. K. Kreiter and W. Singer. *Interhemispheric synchronization of oscillatory neuronal responses in cat visual cortex.* Science **252**, 1177-1179 (1991).

[28] A. K. Engel, P. König and W. Singer. *Direct physiological evidence for scene segmentation by temporal coding.* Proc. Natl. Acad. Sci. USA **88**, 9136-9140 (1991).

[29] P. Erdös and A. Rényi. *On random graphs.* Publicationes Mathematicae **6**, 290-297 (1959).

[30] G. B. Ermentrout and N. Kopell. *Frequency plateaus in a chain of weakly coupled oscillators, I.* Siam J. Math. Anal. **15**, 215-237 (1984).

[31] U. Ernst, K. Pawelzik and T. Geisel. *Synchronization induced by temporal delays in pulse-coupled oscillators.* Phys. Rev. Lett. **74**, 1570-1573 (1995).

[32] D. J. Field. *Relations between the statistics of natural images and the response properties of cortical cells.* J. Opt. Soc. Am. A **4**, 2379-2394 (1987).

[33] R. FitzHugh. *Impulses and physiological states in theoretical models of nerve membrane.* Biophys. J. **1**, 445-446 (1961).

[34] P. Földiák. *Forming sparse representations by local anti-Hebbian learning.* Biol. Cybern. **64**, 165-170 (1990).

[35] T. Fukai and S. Kanemura. *Noise-tolerant stimulus discrimination by synchronization with depressing synapses.* Biol. Cybern. **85**, 107-116 (2001).

[36] H. Gang, T. Ditzinger, C. Z. Ning and H. Haken. *Stochastic resonance without external periodic force.* Phys. Rev. Lett. **71**, 807-810 (1993).

[37] W. Gerstner and J. L. van Hemmen. *Associative memory in a network of spiking neurons.* Network **3**, 139-164 (1992).

[38] W. Gerstner and J. L. van Hemmen. *Coherence and incoherence in a globally coupled ensemble of pulse-emitting units.* Phys. Rev. Lett. **71**, 312-315 (1993).

[39] G. M. Ghose and R. D. Freeman. *Oscillatory discharge in the visual system: does it have a functional role?* J. Neurophysiol. **68**, 1558-1574 (1992).

[40] G. M. Ghose and J. Maunsell. *Specialized representations in the visual cortex: a role for binding?* Neuron **24**, 79-85 (1999).

[41] C. M. Gray, P. König, A. K. Engel and W. Singer. *Oscillatory responses in cat visual cortex exhibit inter-columnar synchronization which reflects global stimulus properties.* Nature **338**, 334-337 (1989).

[42] C. M. Gray. *Synchronous oscillations in neuronal systems: mechanisms and functions.* J. Comp. Neurosci. **1**, 11-38 (1994).

[43] C. M. Gray. *The temporal correlation hypothesis of visual feature integration: still alive and well.* Neuron **24**, 31-47 (1999).

[44] J. Gross and J. Yellen. *Graph theory and its applications.* CRC Press, Boca Raton (1999).

[45] J. Guare. *Six degrees of separation: a play.* Vintage, New York (1990).

[46] D. Hansel and H. Sompolinsky. *Synchronization and computation in a chaotic neural network.* Phys. Rev. Lett. **68** (5), 718-721 (1992).

[47] T. A. Hely. *Computational Models of Developing Neural Systems.* Ph.D. Thesis, Dept. of Cognitive Science, University of Edinburgh, pp. 138-170 (1999).

[48] G. E. Hinton, P. Dayan, B. J. Frey and R. Neal. *The wake-sleep algorithm for unsupervised neural networks.* Science **268**, 1158-1161 (1995).

[49] A. L. Hodgkin. *The local electric changes associated with repetitive action in a nonmedulated axon.* J. Physiol. **107**, 165-181 (1948).

[50] A. L. Hodgkin and A. F. Huxley. *A quantitative description of membrane current and its application to conduction and excitation in nerve.* J. Physiol. **117**, 500-544 (1952).

[51] R. Huerta, M. Bazhenov and M. I. Rabinovich. *Clusters of synchronization and bistability in lattices of chaotic neurons.* Europhys. Lett. **43**, 719-724 (1998).

[52] T. E. Hull, W. H. Enright, B. F. Fellen and R. E. Sedgwick. *Comparing numerical methods of ordinary differential equations.* SIAM J. Num. Anal **9**, 603-637 (1972).

[53] E. M. Izhikevich. *Class 1 neural excitability, conventional synapses, weakly connected networks, and mathematical foundations of pulse-coupled models.* IEEE Trans. Neural Networks **10**, 499-507 (1999).

[54] H. Jeong, B. Tombor, R. Albert, Z. N. Oltavi and A. L. Barabási. *The large-scale organization of metabolic networks.* Nature **407**, 651-654 (2000).

[55] A. Knoblauch and G. Palm. *Scene segmentation by spike synchronization in reciprocally connected visual areas. I. Local effects of cortical feedback.* Biol. Cybern. **87**, 151-167 (2002).

[56] A. Knoblauch and G. Palm. *Scene segmentation by spike synchronization in reciprocally connected visual areas. II. Global assemblies and synchronization on a larger scale in space and time.* Biol. Cybern. **87**, 168-184 (2002).

[57] E. Kobatake and K. Tanaka. *Neuronal selectivities to complex object features in the ventral visual pathway of the macaque cerebral cortex.* J. Neurophysiol. **71**, 856-867 (1995).

[58] C. Koch. *Biophysics of computation. Information processing in single neurons.* Oxford University Press, New York (1999).

[59] P. König and T. B. Schillen. *Stimulus-dependent assembly formation of oscillatory responses: I. Synchronization.* Neural Comp. **3**, 155-166 (1991).

[60] P. König, A. K. Engel and W. Singer. *Integrator or coincidence detector? The role of the cortical neuron revisited.* Trends. Neurosci. **19**, 130-137 (1996).

[61] N. Kopell, W. Zhang and G. B. Ermentrout. *Multiple coupling in chains of oscillators.* Siam J. Math. Anal. **21**, 935-953 (1990).

[62] A. K. Kreiter and W. Singer. *Stimulus-dependent synchronization of neuronal responses in the visual cortex of the awake macaque monkey.* J. Neurosci. **16**, 2381-2396 (1996).

[63] L. F. Lago-Fernández, R. Huerta, F. Corbacho and J. A. Sigüenza. *Fast response and temporal coherent oscillations in small-world networks.* Phys. Rev. Lett. **84**, 2758-2761 (2000).

[64] L. F. Lago-Fernández, M. A. Sánchez-Montañés, S. López-Buedo and F. J. Corbacho. *A biologically inspired autonomous robot that learns approach-avoidance behaviors.* In: Proceedings of the Fourth International Conference on Autonomous Agents (C. Sierra, M. Gini and J. S. Rosenschein, eds.), pp. 27-28. ACM Press, New York (2000).

[65] L. F. Lago-Fernández, R. Huerta and F. Corbacho. *Connection topology dependence of synchronization of neural assemblies on class 1 and 2 excitability.* Neural Networks **14**, 687-696 (2001).

[66] L. F. Lago-Fernández, M. A. Sánchez-Montañés and F. Corbacho. *A biologically inspired visual system for an autonomous robot.* Neurocomputing **38-40**, 1385-1391 (2001).

[67] L. F. Lago-Fernández and G. Deco. *Simultaneous parallel processing of object and position by temporal correlation.* Lect. Notes Comput. Sci. **2085**, 64-71 (2001).

[68] L. F. Lago-Fernández and F. Corbacho. *Optimal extraction of hidden causes.* Lect. Notes Comput. Sci. **2415**, 631-636 (2002).

[69] L. F. Lago-Fernández and G. Deco. *A model of binocular rivalry based on competition in IT.* Neurocomputing **44-46**, 503-507 (2002).

[70] G. Laurent and H. Davidowitz. *Encoding of olfactory information with oscillating neural assemblies.* Science **265**, 1872-1875 (1994).

[71] D. D. Lee and H. S. Seung. *Learning the parts of objects by non-negative matrix factorization.* Nature **401**, 788-91 (1999).

[72] D. A. Leopold and N. K. Logothetis. *Activity changes in early visual cortex reflects monkeys' percepts during binocular rivalry.* Nature **379**, 549-553 (1996).

[73] D. Levine. *Users guide to the PGAPack parallel genetic algorithm library.* Available at: *www-fp.mcs.anl.gov/CCST/research/reports_pre1998/comp_bio/stalk/pgapack.html* (1996).

[74] M. S. Livingstone. *Oscillatory firing and interneuronal correlations in squirrel monkey striate cortex.* J. Neurophysiol. **75**, 2467-2485 (1996).

[75] N. K. Logothetis, J. Pauls and T. Poggio. *Shape representation in the inferior temporal cortex of monkeys.* Curr. Biol. **5**, 552-563 (1995).

[76] N. K. Logothetis, D. A. Leopold and D. L. Sheinberg. *What is rivalling during binocular rivalry?* Nature **380**, 621-624 (1996).

[77] E. D. Lumer, K. J. Friston and G. Rees. *Neural correlates of perceptual rivalry in the human brain.* Sience **280**, 1930-1934 (1998).

[78] R. Lumia, L. Shapiro and O. Zuniga. *A new connected components algorithm for virtual memory computers.* Comput. Vis. Graph. Image Process. **22**, 287-300 (1983).

[79] W. W. Lytton and T. J. Sejnowski. *Simulations of cortical pyramidal neurons synchronized by inhibitory interneurons.* J. Neurophysiol. **66**, 1059-1079 (1991).

[80] W. Maass. *Lower bounds for the computational power of spiking neurons.* Neural Comput. **8**, 1-40 (1996).

[81] K. MacLeod and G. Laurent. *Distinct mechanisms for synchronization and temporal patterning of odor-encoding neural assemblies.* Science **274**, 976-979 (1996).

[82] K. MacLeod, A. Bäcker and G. Laurent. *Who reads temporal information contained across synchronized and oscillatory spike trains?* Nature **395**, 693-698 (1998).

[83] C. von der Malsburg. *The correlation theory of brain function.* Internal Report 81-2, Max-Planck-Institute for Biophysical Chemistry, Göttingen, Germany (1981). Reprinted in: Models of neural networks II (E. Domany, J. L. van Hemmen and K. Schulten, eds.), pp. 95-119. Springer, Berlin (1994).

[84] C. von der Malsburg and J. Buhmann. *Sensory segmentation with coupled neural oscillators.* Biol. Cybern. **67**, 233-242 (1992).

[85] J. H. R. Maunsell and W. T. Newsome. *Visual processing in monkey extrastriate cortex.* Ann. Rev. of Neurosci. **10**, 363-401 (1987).

[86] S. Milgram. *The small world problem.* Psychol. Today **2**, 60-67 (1967).

[87] S. M. Miller, G. B. Liu, T. T. Ngo, G. Hooper, S. Riek, R. G. Carson and J. D. Pettigrew. *Interhemispheric switching mediates perceptual rivalry.* Curr. Biol. **10**, R383-R392 (2000).

[88] R. E. Mirollo and S. H. Strogatz. *Synchronization of pulse-coupled biological oscillators.* Siam J. Appl. Math. **50**, 1645-1662 (1990).

[89] R. Monasson. *Diffusion, localization and dispersion relations on small-world lattices.* Eur. Phys. J. B **12**, 555-567 (1999).

[90] J. S. Nagumo, S. Arimoto and S. Yoshizawa. *An active pulse transmission line simulating nerve axon.* Proc. IRE **50**, 2061-2070 (1962).

[91] M. E. J. Newman and D. J. Watts. *Scaling and percolation in the small-world network model.* Phys. Rev. E **60**, 7332-7342 (1999).

[92] M. E. J. Newman. *Models of the small-world: a review.* J. Stat. Phys. **101**, 819-841 (2000).

[93] M. E. J. Newman. *The structure of scientific collaboration networks.* Proc. Natl. Acad. Sci. USA **98**, 404-409 (2001).

[94] T. T. Ngo, S. M. Miller, G. B. Liu and J. D. Pettigrew. *Binocular rivalry and perceptual coherence.* Curr. Biol. **10** R134-R136 (2000).

[95] B. A. Olshausen and D. J. Field. *Emergence of simple-cell receptive field properties by learning a sparse code for natural images.* Nature **381**, 607-609 (1996).

[96] B. A. Olshausen. *Principles of image representation in visual cortex.* In: The Visual Neurosciences (L. M. Chalupa and J. S. Werner, eds.). MIT Press (in press).

[97] R. C. O'Reilly. *Generalization in interactive networks: the benefits of inhibitory competition and Hebbian learning.* Neural Comp. **13**, 1199-1241 (2001).

[98] C. S. Peskin. *Mathematical aspects of heart physiology.* Courant Institute of Mathematical Sciences, New York University, New York, pp. 268-278 (1975).

[99] I. Pitas. *Digital image processing, algorithms and applications.* John Wiley, New York, pp. 275-321 (2000).

[100] W. Rall. *Distinguishing theoretical synaptic potentials computed for different soma-dendritic distributions of synaptic input.* J. Neurophysiol. **30**, 1138-1168 (1967).

[101] J. H. Reynolds and R. Desimone. *The role of neural mechanisms of attention in solving the binding problem.* Neuron **24**, 19-29 (1999).

[102] M. B. H. Rhouma and H. Frigui. *Self-organization of biological oscillators with application to clustering.* IEEE Trans. Patt. Analysis Mach. Intell. **23**, 180-195 (2001).

[103] F. Rieke, D. Warland, R. de Ruyter van Steveninck and W. Bialek. *Spikes - Exploring the neural code.* MIT Press, Cambridge, MA (1996).

[104] M. Riesenhuber and T. Poggio. *Are cortical models really bound by the "binding problem"?* Neuron **24**, 87-93 (1999).

[105] J. Rinzel and B. Ermentrout. *Analysis of neural excitability and oscillations.* In: Methods in neuronal modeling, from ions to networks (C. Koch and I. Segev, eds.), pp. 251-291. MIT Press, Cambridge MA (1999).

[106] A. Rosenfeld and D. Pfaltz. *Sequential operations in digital picture processing.* J. Ass. Comp. Mach. **13** (4), 471-494 (1966).

[107] P. Rowcliffe, J. Feng and H. Buxton. *Clustering within integrate-and-fire neurons for image segmentation.* Lect. Notes Comput. Sci. **2415**, 69-74 (2002).

[108] S. T. Roweiss and L. K. Saul. *Nonlinear dimensionality reduction by locally linear embedding.* Science **290**, 2323-2326 (2000).

[109] E. Saund. *A multiple cause mixture model for unsupervised learning.* Neural Comp. **7**, 51-71 (1995).

[110] T. B. Schillen and P. König. *Stimulus-dependent assembly formation of oscillatory responses: II. Desynchronization.* Neural Comp. **3**, 167-178 (1991).

[111] M. N. Shadlen and W. T. Newsome. *The variable discharge of cortical neurons: implications for connectivity, computation, and information coding.* J. Neurosci. **18**, 3870-3896 (1998).

[112] M. N. Shadlen and A. Movshon. *Synchrony unbound: a critical evaluation of the temporal binding hypothesis.* Neuron **24**, 67-77 (1999).

[113] D. L. Sheinberg and N. K. Logothetis. *The role of temporal cortical areas in perceptual organization.* Proc. Natl. Acad. Sci. USA **94**, 3408-3413 (1997).

[114] W. Singer. *Neuronal synchrony: a versatile code for the definition of relations?* Neuron **24**, 49-65 (1999).

[115] J. B. Tenenbaum, V. de Silva and J. C. Langford. *A global geometric framework for nonlinear dimensionality reduction.* Science **290**, 2319-2323 (2000).

[116] S. Thorpe and M. Imbert. *Biological constraints on connectionist models.* In: Connectionism in perspective (R. Pfeifer, Z. Schreter and F. Fogelman-Soulie, eds.), pp. 63-92. Elsevier, Amsterdam (1989).

[117] S. Thorpe, F. Fize and C. Marlot. *Speed of processing in the human visual system.* Nature **381**, 520-522 (1996).

[118] F. Tong, K. Nakayama, J. T. Vaughan and N. Kanwisher. *Binocular rivalry and visual awareness in human extrastriate cortex.* Neuron **21**, 753-759 (1998).

[119] M. J. Tovee and E. T. Rolls. *Oscillatory activity is not evident in the primate temporal visual cortex with static stimuli.* Neuroreport **3**, 369-372 (1992).

[120] R. D. Traub. *Simulation of intrinsic bursting in CA3 hippocampal neurons.* Neurosci. **7**, 1233-1242 (1982).

[121] L. Ungerleider and M. Mishkin. *Two cortical visual systems.* In: Analysis of visual behavior (D. J. Ingle, M. A. Goodale and R. J. W. Mansfield, eds.), pp. 549-586. Cambridge, MA (1982).

[122] M. Usher and E. Niebur. *Modelling the temporal dynamics of IT neurons in visual search: a mechanism for top-down selective attention.* J. Cog. Neurosci. 8, 311-327 (1996).

[123] W. M. Usrey and R. C. Reid. *Synchronous activity in the visual system.* Annu. Rev. Physiol. **61**, 435-456 (1999).

[124] R. VanRullen and S. Thorpe. *Ultra-rapid visual categorization of natural scenes: order of spiking in ganglion cells as a code.* Perception **27** (1998).

[125] D. L. Wang. *Emergent synchrony in locally coupled neural oscillators.* IEEE Trans. Neural Networks, **6**, 941-948 (1995).

[126] D. L. Wang and D. Terman. *Locally excitatory globally inhibitory oscillator networks.* IEEE Trans. Neural Networks, **6**, 283-286 (1995).

[127] D. L. Wang and D. Terman. *Image segmentation based on oscillatory correlation.* Neural Comp. **9**, 805-836 (1997).

[128] D. J. Watts and S. H. Strogatz. *Collective dynamics of small-world networks.* Nature **393**, 440-442 (1998).

[129] D. J. Watts. *Small worlds. The dynamics of networks between order and randomness.* Princeton University Press, Princeton (1999).

[130] H. R. Wilson and J. D. Cowan. *Excitatory and inhibitory interactions in localized populations of model neurons.* Biophys. J. **12**, 1-24 (1972).

[131] H. R. Wilson. *Spikes, decisions and actions: dynamical foundations of neuroscience.* Oxford University Press, Oxford (1999).

[132] A. T. Winfree. *The geometry of biological time.* Springer, New York (1980).

[133] M. P. Young, K. Tanaka and S. Yamane. *On oscillating neuronal responses in the visual cortex of the monkey.* J. Neurophysiol. **67**, 1464-1474 (1992).

Reunido el tribunal que suscribe en el día
de la fecha presente Tesis
doctoral titulada "Sobre algunos
Madrid, 1 de julio de 2003

FDO: JUAN ALBERTO SIGÜENZA PIZARRO

FDO: GUSTAVO DECO

FDO: EDUARDO SANCHEZ VILA

FDO: JAVIER DE FELIPE ORDOQUIA

FDO: FCO. DE BORJA RODRIGUEZ ORTIZ